

OCCURRENCE AND *IN VITRO* TOXICITY OF UNREGULATED DISINFECTION BY-
PRODUCTS IN TWO SASKATCHEWAN DRINKING WATER TREATMENT PLANTS

A Thesis Submitted to the
College of Graduate and Postdoctoral Studies
In Partial Fulfillment of the Requirements
For the Degree of Master of Science
In the Toxicology Program
University of Saskatchewan
Saskatoon

By

CHRISTENA LEIGH WATTS

PERMISSION TO USE

In presenting this thesis in partial fulfillment of the requirements for a Master of Science degree from the University of Saskatchewan, I agree that the libraries of this university may make it freely available for inspection. I further agree that permission to copy this thesis in any manner, in whole or in part, for scholarly purposes may be granted by the professors who supervised my thesis work or, in their absence by the Head of the Department or the Dean of the College in which my thesis work was done. It is understood that any copying, publication, or use of this thesis or parts thereof for financial gain shall not be allowed without my written permission. It is also understood that due recognition shall be given to me and to the University of Saskatchewan in any scholarly use which may be made of any material in my thesis.

Requests for permission to copy or to make use of material in this thesis in whole or in part should be addressed to:

Dean
College of Graduate and Postdoctoral Studies
University of Saskatchewan
116 Thorvaldson Building, 110 Science Place
Saskatoon, Saskatchewan S7N 5C9
Canada

Chair of the Toxicology Graduate Program
Toxicology Centre
University of Saskatchewan
44 Campus Drive
Saskatoon, Saskatchewan S7N 5B3
Canada

ABSTRACT

Halogenated disinfection by-products (DBPs) are a diverse class of compounds formed during the treatment of drinking water through reactions between natural organic matter (NOM), inorganic precursors such as bromide, and applied disinfectants. Health Canada regulates a handful of DBPs, but there are over 700 unregulated DBPs that have been described and many of these are more toxic than the regulated DBPs. Here, a data-independent precursor isolation and characteristic fragment (DIPIC-Frag) method operated on a Q ExactiveTM Hybrid Quadrupole-OrbitrapTM Mass Spectrometer equipped with a UHPLC system was adapted for the detection of brominated and iodinated DBPs (Br-DBPs and I-DBPs) in chlorinated water. Extraction and analytical conditions were optimized, chemometric strategies were applied, and a library of 553 Br-DBPs and 112 I-DBPs was established with structures predicted for the most abundant compounds. As the method exhibited good precision (~15% RSD), it was then used to study trends of formation and temporal trends of unregulated Br-DBPs in a year-long study that sampled raw, clearwell, and finished waters. While most Br-DBPs increased through the treatment process, cluster I Br-DBPs decreased between the clearwell and finished stages, a pattern significantly related to their chemical properties of low O/C and Br/C ratios. Correlation matrices were used to determine if quality parameters of the source waters (e.g. NOM, turbidity, river level, temperature, bromine (Br)) could explain monthly variations of Br-DBPs, but few significant relationships were found. Unexpectedly, total Br increased from 0.013-0.038 mg/L in raw water to 0.04-0.12 mg/L in finished water, which indicated introduction of Br during disinfection. Concentrations of Br in clearwell and finished water were significantly correlated to detection of 34/54 Br-DBPs at $\alpha=0.05$ and 14/54 Br-DBPs at $\alpha=0.001$. As few studies have evaluated toxicity of DBPs in mixtures, the next goal of this thesis was to explore temporal changes in whole mixture toxicity and to determine if raw water parameters could predict toxicity of finished water. By use of a 72 h CHO-K1 cytotoxicity assay and an Nrf2/ARE oxidative stress assay, results indicated cytotoxicity was greatest in finished water collected in November and March while oxidative stress was greatest in June and November, both of which could be related to seasonal trends in unregulated Br-DBPs. These toxic endpoints were correlated ($R^2 = 0.53$, $p = 7.4 \times 10^{-3}$) and three classes of Br-DBPs (Br₂, BrCl, S-DBPs) demonstrated significant correlations to both. The greatest predictors of mixture toxicity were

concentration of Br and applied doses of chlorine at related stages. These were equally correlated to both cytotoxicity ($R^2 = 0.43$, $p = 0.002$) and oxidative stress ($R^2 = 0.67$, $p = 0.001$). This study is the first to explore temporal trends in whole mixture toxicity of DBPs. It is also the first to suggest that the concentration of Br may be a predictor of the occurrence of unregulated Br-DBPs as well as whole mixture toxicity.

ACKNOWLEDGEMENTS

I would like to thank my supervisor Dr. Paul Jones as well as Dr. John Giesy for the opportunity to work on this research project. I gained valuable skills in analytical chemistry as well as cell culture, and in overcoming challenges of this project was able to develop on a personal level. To Dr. Les Dickson, a member of my committee, and Dr. Lynn Weber, graduate chair, thank you for your time and support. To Dan Conrad, Andy Busse, and Jim Hevdebo, thank you for your collaboration and input. Importantly, I want to say thank you to Dr. Hui Peng for always being available to answer questions and for the crucial contributions you made to the mass spectrometric analyses of this project. I must also thank the NSERC Collaborative Research and Training Experience (CREATE) Program in Water Security for providing my scholarship and for offering specialized workshops to develop professional skills. Lastly, I want to thank the friends I made at the Toxicology Centre during my time in Saskatoon. Surrounding myself with successful and supportive colleagues helped me to push this project to completion and strive for greater goals in life.

TABLE OF CONTENTS

PERMISSION TO USE	i
ABSTRACT	ii
ACKNOWLEDGEMENTS	iv
LIST OF TABLES	ix
LIST OF FIGURES	xi
LIST OF ABBREVIATIONS	xviii
NOTE TO READERS	xxi
CHAPTER 1: GENERAL INTRODUCTION	1
1.1 Preface	2
1.2 History and Regulation of DBPs	2
1.3 Formation of Disinfection By-Products in Drinking Water	5
1.4 Physical and Chemical Factors that Influence Formation of DBPs	7
1.5 Toxicity of DBPs	10
1.6 Analytical Techniques for Detection of DBPs	13
1.7 Current Challenges in DBP Research	14
1.8 Research Objectives	15
CHAPTER 2: DETECTION AND COMPARATIVE ANALYSIS OF BROMINATED AND IODINATED DISINFECTION BY-PRODUCTS IN DRINKING WATER	18
ABSTRACT	19
2.1 Introduction	20
2.2 Materials and Methods	21
2.2.1 Chemicals and Reagents	21
2.2.2 Collection of Drinking Water	21
2.2.3 Optimization of the DIPIC-Frag Method for DBP Screening	22
2.2.3.1 Sample Pretreatment	22
2.2.3.2 LC-Q Exactive Data Acquisition	23

2.2.3.3 Quality Control and Assurance	24
2.2.3.4 Data Treatment and Statistical Analyses	24
2.3 Results and Discussion	24
2.3.1 Optimization of DIPIC-Frag Method for DBP Screening	24
2.3.2 Library of Br-DBPs in Chlorinated Water	27
2.3.3 Library of I-DBPs in Chlorinated Water	31
2.3.4 Minor Effects of Quenching Reagents on the Profile of DBPs	32
2.3.5 Comparative Analysis of DBPs	33
2.3.6 Proposed Chemical Structures of High Abundance DBPs	35
2.4 Conclusions	39
2.5 Supporting Information	40
2.6 Acknowledgements	41

CHAPTER 3: MONTHLY VARIATIONS OF UNREGULATED BROMINATED DISINFECTION BY-PRODUCTS ARE PRIMARILY ASSOCIATED WITH TOTAL BROMINE IN CHLORINATED WATER	42
ABSTRACT	43
3.1 Introduction	44
3.2 Materials and Methods	45
3.2.1 Chemicals and Reagents	45
3.2.2 Collection of Water	46
3.2.3 Sample Extraction	46
3.2.4 Quality Assurance and Control	46
3.2.5 Characterization of Br-DBPs by UHRMS	47
3.2.6 Characterization of Natural Organic Matter by UHRMS	47
3.2.7 Data Analyses	48
3.3 Results and Discussion	49
3.3.1 Occurrences of Unregulated Br-DBPs	49

3.3.2 Fates of Br-DBPs are related to Chemical Properties.....	51
3.3.3 Monthly Variations of Br-DBPs are not correlated to NOM.....	53
3.3.4 Monthly Variations of Br-DBPs are Primarily Correlated to Total Bromine.....	55
3.3.5 Implications.....	61
3.4 Acknowledgements.....	61
3.5 Supporting Information.....	62
 CHAPTER 4: PREDICTING <i>IN VITRO</i> TOXICITY OF MIXTURES OF DISINFECTION BY- PRODUCTS BY INVESTIGATING SEASONAL CHANGES IN WATER QUALITY	63
ABSTRACT.....	64
4.1 Introduction.....	65
4.2 Materials and Methods.....	66
4.2.1 Chemicals and Reagents	67
4.2.2 Collection of Water Samples	67
4.2.3 Chemical Analysis for Br-DBPs.....	68
4.2.4 72 h CHO-K1 Cytotoxicity Assay	68
4.2.5 16 h Nrf2/ARE Oxidative Stress Assay with MCF7 Cell Line	69
4.2.6 Correlation Analysis for Predicting Toxicity of DBP Mixtures	70
4.3 Results and Discussion	71
4.3.1 Trends in the Occurrences of Unregulated Br-DBPs.....	71
4.3.2 Monthly Trends in Cytotoxicity of Mixtures of DBPs	71
4.3.3 Monthly Trends in Oxidative Stress	73
4.3.4 Predicting Toxicity of DBP Mixtures	78
4.3.4.1 Oxidative Stress and Cytotoxicity of DBP Mixtures are related	78
4.3.4.2 Classes of Br-DBPs Contribute to Whole Mixture Toxicity to Varying Degrees	79
4.3.4.3 Toxicities of Mixtures of DBPs are Primarily Associated with Total Br and Chlorine Dose	82

4.4 Conclusions.....	86
4.5 Supporting Information.....	87
4.6 Acknowledgements.....	101
 CHAPTER 5: GENERAL DISCUSSION	89
5.1 Project Rationale and Summary.....	90
5.1.1 Application of the DIPIC-Frag Method for Untargeted Detection of Br-DBPs.....	90
5.1.2 Unregulated Br-DBPs in Saskatchewan Drinking Water Treatment Plants	91
5.1.3 Toxicity of Unregulated Br-DBP Mixtures	94
5.1.4 Predicting the Occurrence of Br-DBPs and Toxicity of DBP Mixtures.....	95
5.2 Limitations	97
5.3 Future Research Considerations	98
5.4 Conclusion	99
 APPENDICES	101
APPENDIX A: CHAPTER 2 SUPPORTING INFORMATION.....	102
APPENDIX B: CHAPTER 3 SUPPORTING INFORMATION	128
APPENDIX C: CHAPTER 4 SUPPORTING INFORMATION	143
 REFERENCES	153

LIST OF TABLES

Table 1.1. Disinfection by-products for which Health Canada regulations exist. Adapted from http://www.hc-sc.gc.ca/ewh-semt/pubs/water-eau/sum_guide-res_recom/index-eng.php#t2	4
Table 4.1. 72 h CHO-K1 cytotoxicity of water samples collected at three stages of treatment (raw, clearwell, finished) and at six time points over a year. LC ₅₀ values (mean ± se) were predicted by a Weibull dose-response model with the lower limit fixed at zero (see Fig. C.2)	72
Table 4.2. Fold induction of the Nrf2/ARE oxidative stress pathway by extracts of raw, clearwell, and finished water at three concentration factors (3.75 x, 7.5 x, and 15 x) compared to the negative control. Samples were collected at 6 monthly time points (April 2016 – March 2017)	75
Table 4.3. Correlations between detected classes of Br-DBPs and measured toxicities of concentrated extracts of clearwell and finished water	81
Table A.1. Formulae of compounds, <i>m/z</i> values, peak abundances, and predicted chemical structures of the 50 most abundant Br-DBPs. The relative position of halogen or phenol/hydroxyl groups on the alkyl chain or aromatic ring could not be accurately determined for some DBPs. The exact structures of some chemicals were determined according to previous studies. Considering the potential existence of multiple adducts for a given detected ion, only the formula was shown for detected ions. <i>m/z</i> values were shown for most abundant isotopic peak or monoisotopic peak. Several Br-DBPs were predicted as isomers with same formulae	108
Table A.2. Formulae for compounds, <i>m/z</i> values, peak abundances and predicted chemical structures of the top 10 I-DBPs. The relative position of halogen or phenol/hydroxyl groups on the alkyl chain or aromatic ring could not be accurately determined	114

Table A.3. Comparison of water quality parameters and details for treatment processes for the two sampling dates and sampling points used in method development. Information obtained through personal communication with the Manager of Laboratory & Research at the water treatment plant (Conrad, 2017)	116
Table A.4. Concentrations of free and total chlorine in water collected August 17, 2017 as determined by an Orion AQUAfast™ AQ4000 colorimeter (Thermo Scientific)	117
Table B.1. Raw water parameters, total bromine determinations, and applied doses of chlorine as reported for the eleven sampling dates of this study (2016-2017)	130
Table B.2. Detection frequencies of Br-DBPs at each stage of treatment, as well as median, minimum, and maximum ion abundances detected at the clearwell and finished stages	131
Table B.3. R^2 and p -values (ANOVA) of linear models calculated based on ion abundances of sulfonated DBPs (found in the red square of Fig. 3.1A) at the clearwell and finished stages of treatment (n=22)	133
Table B.4. ID# and predicted molecular formulae of Br-DBPs in correlation matrix found in Fig. 3.1A	134
Table B.5. ID# and predicted molecular formulae of Br-DBPs in correlation matrix found in Fig. B.1	135

LIST OF FIGURES

Fig. 1.1. Parameters of water quality and properties of the water treatment process that can influence speciation of disinfection by-products	8
Fig. 2.1. Typical workflow of the DIPIC-Frag method used to identify brominated and iodinated by-products in chlorinated water: (A) Hybrid conditions were combined to maximize the mass spectrometry library; (B) Bromine and iodine fragment peaks from each DIA window were used to produce the library; (C) Multiple libraries were constructed for the different operational conditions; (D) A scoring system was used to align precursor ions and predict compound formulae; (E) The final non-redundant library was constructed by matching compound formulae and retention times to merge libraries	26
Fig. 2.2. Heat map of log-transformed peak abundances of (A) Br-DBPs and (B) I-DBPs detected by use of three solid phase extraction cartridges (WAX, HLB, C18) and two sample pretreatment conditions (no pH adjustment or pH 2). Samples were collected in October (water chlorinated at raw intake) or April (water chlorinated post-coagulation and clarification) and triplicate samples were analyzed for each condition	28
Fig. 2.3. Ion abundance (red) of (A) Br-DBPs and (B) I-DBPs and their cumulative contribution (blue) to total DBPs detected. Structures of several of the most abundant DBPs are shown for comparison	30
Fig. 2.4. Frequency distributions of method precision for (A) Br-DBPs and (B) I-DBPs shown as a violin plot for the C18_pH2, HLB_pH2, and WAX sample pretreatment methods. Precision was calculated as relative standard deviation of each DBP to the mean value of abundances. Width of the violin indicates frequency at that precision	34
Fig. 2.5. Prediction of four typical Br-DBPs using high-resolution MS ² spectra. The red formulae indicate the expected loss. Positions of bromine, chlorine, carboxylic acid or hydroxyl groups in compounds could not be exactly predicted	37

Fig. 2.6. MS² spectra for the detected class of high abundance sulfonic acid DBPs. The position of bromine, sulfonic acid, carboxylic acid or hydroxyl groups in compounds from panel B-D could not be exactly predicted38

Fig. 3.1. (A) Spearman's correlation matrix based on ion abundances of 54 Br-DBPs detected in clearwell and finished water at 11 monthly time points (n=11). Representative compounds are indicated and a full list can be found in Table B.4. Examples are shown for (B) a strong positive correlation found between two trihalo-HCDs analogues and (C) a negative correlation found between C₇H₇O₆Br and C₇H₄O₃ClBr. Red points represent ion abundances detected in clearwell water and blue points represent ion abundance detected in finished water, with 95% confidence intervals indicated in grey51

Fig. 3.2. (A) Three trends identified for Br-DBPs detected through the drinking water treatment process. Each coloured line represents one of 54 unregulated Br-DBPs. (B) Representative compounds are shown for each of the three clusters defined in (A). Data from eleven months included to illustrate that trends were consistent through the year53

Fig. 3.3. Four temporal trends identified by soft clustering analysis for the detection of 54 unregulated Br-DBPs in finished water over 11 months55

Fig. 3.4. Spearman's correlation matrix indicating significant relationships ($\alpha=0.05$ for top figure, $\alpha=0.01$ for bottom figure) among raw water parameters, concentrations of bromine (Br), applied doses of chlorine, and ion abundances of individual Br-DBPs detected in finished water (n=11)57

Fig. 3.5. Concentrations of total bromine (Br) in samples of water collected over a year at the raw, clearwell, and finished stages of treatment. (A) Results were shown across different months for raw (green), clearwell (red) and finished water (blue). (B) Increasing concentrations of total Br across treatment stages58

Fig. 3.6. (A) Distribution of retention times and m/z values for 54 abundant Br-DBPs, with the significance (p -value) of correlation to concentrations of Br at the clearwell and finished stages of treatment represented by colour. The relationship between $\text{CH}_2\text{O}_3\text{SClBr}$ and Br is shown with (B) one linear model incorporating both clearwell and finished data ($R^2 = 0.59$, $p = 2.8 \times 10^{-5}$), and (C) two linear models that consider clearwell and finished water data separately (Clearwell: $R^2 = 0.51$, $p = 0.013$; Finished: $R^2 = 0.41$, $p = 0.034$). Red points represent data from clearwell and blue points represent data from finished water, with 95% confidence intervals shown in grey.....60

Fig. 4.1. Trends in cytotoxicity (plotted as $1/\text{LC}_{50}$ (mean)) for concentrated extracts of water visualized by (A) stage of treatment and (B) month of sampling. Predicted LC_{50} values can be found in Table 4.172

Fig. 4.2. Fold induction of the Nrf2/ARE oxidative stress pathway (mean \pm sd) in MCF7 cell line after 16 h exposure to 15 x concentrated extracts of water, visualized by (A) stage of treatment and (B) month of sampling. Average fold increase ($n=3$) normalized as percent of negative control response. Results are reported in Table 4.277

Fig. 4.3. Relationship between oxidative stress and cytotoxicity induced by concentrated extracts of clearwell (red) and finished (blue) water. Linear model $R^2 = 0.53$, $F_{1,10} = 11.18$, $p = 7.4 \times 10^{-3}$ 79

Fig. 4.4. Spearman's correlation matrix indicating significant* ($\alpha=0.05$) correlations between measures of toxicity, parameters of water quality, and doses of chlorine ($n=6$)83

Fig. 4.5. Relationships between concentrations of Br and (A) predicted LC_{50} values and (B) oxidative stress induced by concentrated water extracts (15 x) collected at the clearwell (red) and finished stages (blue) of treatment. Linear model for predicted LC_{50} : $R^2 = 0.43$, $F_{1,10} = 7.44$, $p = 0.021$. Linear model for oxidative stress: $R^2 = 0.67$, $F_{1,10} = 20.68$, $p = 0.0011$ 84

Fig. 4.6. Relationships between pre- and post-chlorine doses with (A) predicted LC₅₀ values and (B) oxidative stress induced by concentrated water extracts (15 x) collected at the clearwell (red) and finished stages (blue) of treatment. Linear model for predicted LC₅₀ : $R^2 = 0.43$, $F_{1,10} = 7.44$, $p = 0.021$. Linear model for oxidative stress: $R^2 = 0.68$, $F_{1,10} = 21.0$, $p = 0.001$ 85

Fig. A.1. Typical process employed at the DWTP where samples were collected for this study. In October 2015, samples of raw chlorinated water were collected at (A). In April 2016, the point of chlorination changed to post-clarification (B) and samples were collected after sand filtration (C). In August 2017, the plant had returned to operating with pre-chlorination and the granular activated carbon (GAC) filter was in operation. Samples collected in August 2017 were sampled pre-GAC (C). Adapted from <http://www.buffalopoundwtp.ca/plant/water-treatment-process...> 118

Fig. A.2. Schematic workflow of homologue models incorporated in the DIPIC-Frag method. 1) Br-DBP compound 1 was predicted; due to the characteristic peak and lower mass values, the formula of this compound could be predicted reliably; 2) Br-DBP compound 2 was then predicted based on a homologue model with $-\text{CH}_2$ difference to compound 1; 3) I-DBP compound 3 was then predicted, and the homologue information from compound 1 would increase the score and prediction accuracy of this compound; 4) I-DBP compound 4 was then confidently predicted with homologue information from compound 2 (I-Br) and compound 3 ($-\text{CH}_2$)119

Fig. A.3. Typical chromatograms of Br-DBP peaks (230 ± 2.5 m/z DIA window) using ESI (A) or APCI (B) ionization sources120

Fig. A.4. Typical chromatograms of Br-DBPs peaks under (A) Hypersil GOLD™ C18 column (3 μm ; 2.1 mm \times 50 mm; Thermo Fisher Scientific) and (B) TSKgel Amide-80 column (3 μm ; 4.6 mm \times 150 mm; TOSOH). Most abundant peaks on C18 columns were eluted in the first 3 min with poor separation, indicating poor retention ability of Br-DBPs on C18 columns. Ultrapure water containing 0.1% NH_4OH (A) and acetonitrile containing 0.1% NH_4OH (B) were used as mobile phases. Initially 95% of B was decreased to 90% in 18 min, then decreased to 30% at 26 min, followed by an increase back to 95% of B held for 3 min121

Fig. A.5. Typical chromatograms of Br-DBP peaks (215 ± 2.5 m/z DIA window) using different SPE pretreatment methods. Chromatograms of Br-DBPs using HLB was similar to C18, and thus was not shown here122

Fig. A.6. Distribution of Br-DBPs and I-DBPs detected in chlorinated raw water and conventionally treated water by retention time (min) and m/z values. (A) Br-DBPs; (B) I-DBPs. Size of the dots is proportional to abundances. Colour of dots represents number of bromine or iodine atoms123

Fig. A.7. Typical chromatogram of isomers of two detected Br-DBPs. Red arrows indicate peaks of isomers. Isomers were determined by exact mass and isotopic peaks124

Fig. A.8. Ratios of iodinated DBPs to corresponding brominated DBP analogues. X-axis indicates four different DBPs with predicted compound formulae. Chemical structures are shown for iodinated analogues of each DBPs. Data are expressed as the mean \pm sd (n=3)125

Fig. A.9. Heatmap of 25 Br-DBPs detected in water collected at the preGAC stage of treatment on August 17, 2017. Samples (n=3) were treated with no quenching reagent, an excess of 5 mg/L of ascorbic acid, or an excess of 3.5 mg/L of sodium thiosulfate. Concentrated extracts were analyzed by LC-Q Exactive MS126

Fig. A.10. Chromatograms of bromomethanesulfonic acid from authentic acid (A), actual drinking water (B) and bromochloromethanesulfonic acid from drinking water (C). Retention times of chlorinated and brominated analogues were similar on an Amide-column.....127

Fig. B.1. Spearman's correlation matrix based on ion abundances of 54 Br-DBPs detected in finished water at 11 monthly time points. Red, black, and blue boxes highlight groups of compounds detected with similar monthly trends. Order of compounds and precursor formulae can be found in Table B.5136

Fig. B.2. Linear models of the strong correlations found between detected ion abundances of isomers of $C_7H_3O_3ClBr$ and $C_7H_3O_3Br_2$ at the clearwell (red) and finished (blue) stages of treatment	137
Fig. B.3. (A) Ratio of bromine to carbon (Br/C) and (B) ratio of oxygen to carbon (O/C) in compounds classified by cluster based on their trend through the treatment process (Fig. 3.2A). <i>P</i> -values represent results of T-tests	138
Fig. B.4. (A) Total ion abundance of NOM detected in raw water collected over eleven months, stacked based on composition of chemical formulae. (B) Total ion abundance of NOM detected at raw, clearwell, and finished stages of treatment, collected over eleven months	139
Fig. B.5. Four temporal trends identified by soft clustering analysis for the total ion abundance of NOM detected in raw water	140
Fig. B.6. Van Krevelen plots of compounds of NOM detected in raw water with correlation to the ion abundances of (A) $C_7H_7O_6Br$ and (B) $C_5HO_3Cl_2Br$ as detected in treated water represented by colour and size. The blue box in (A) indicates compounds of NOM containing CHOSN	141
Fig. B.7. Spearman's correlation matrix indicating significant relationships ($\alpha=0.05$) between parameters of raw water and ion abundances of Br-DBPs detected in finished water. Data from seven months included (September 2016 to March 2017)	142
Fig. C.1. Standard dose-response curve of cytotoxicity induced by iodoacetic acid in the 72 h CHO-K1 cytotoxicity assay	145
Fig. C.2. 72 h CHO-K1 cytotoxicity of (A) raw, (B) clearwell, and (C) finished water collected at six time points over a year. Average cell density ($n=3$) at nine concentrations plotted as percent of negative control by a Weibull dose-response model with lower limit fixed at zero. Predicted LC_{50} values (concentration factor \pm se) can be found in Table 4.1	146

Fig. C.3. Relationships between cytotoxicity of (A) raw and (B) clearwell water with cytotoxicity of finished water. Linear models had (A) $R^2 = 0.015$, $p = 0.82$, and (B) $R^2 = 0.28$, $p = 0.28$	147
Fig. C.4. (A) Nrf2/ARE oxidative stress assay and (B) MTT cytotoxicity assay of concentrated water extracts collected at three stages of treatment and at six monthly time points. MCF7 cell line was exposed to concentrated extracts for 16 h (n=3)	148
Fig. C.5. Relationships between fold induction of the Nrf2/ARE oxidative stress pathway by (A) raw and (B) clearwell water with that of finished water. Linear models had (A) $R^2 = 0.13$, $p = 0.49$, and (B) $R^2 = 0.64$, $p = 0.91$	149
Fig. C.6. Significant ($\alpha=0.05$) correlations to toxicity of finished water	150
Fig. C.7. Relationships between concentrations of Br in raw water (A and B) or finished water (C and D) to predicted LC_{50} values (A and C) and induction of oxidative stress at 15 x (B and D) for extracts of finished water	151
Fig. C.8. Relationship between applied doses of chlorine (pre- and post-chlorine) with the change in total Br between related stages of treatment; change from raw to clearwell water (red) and change from clearwell to finished water (blue). Linear model $R^2 = 0.63$, $F_{1,10} = 17.29$, $p = 0.002$)	152

LIST OF ABBREVIATIONS

ANOVA	Analysis of variance
ACN	Acetonitrile
APCI	Atmospheric pressure chemical ionization
APPI	Atmospheric pressure photoionization
BDCM	Bromodichloromethane
Br	Bromine
Br ⁻	Bromide
Br/C	Bromine to carbon ratio
Br-DBP	Brominated disinfection by-product
C	Carbon
C18	Column with a stationary phase comprised of molecules with 18 carbons
CHO	Chinese hamster ovarian cell line
C-DBP	Carbonaceous disinfection by-product
Cl	Chlorine
Cl ₂	Chlorine gas
Cl-DBP	Chlorinated disinfection by-product
cm	Centimeter
CO ₂	Carbon dioxide
DBP	Disinfection by-product
DCM	Dichloromethane
DIA	Data independent acquisition
DBA	Dibromoacetic acid
DCA	Dichloroacetic acid
DBAN	Dibromoacetonitrile
DBCM	Dibromochloromethane
DHAN	Dihaloacetonitrile
DIPIC-Frag	Data-independent precursor isolation and characteristic fragment method
DMEM	Dulbecco modified eagle medium
DMSO	Dimethyl sulfonate
DWTP	Drinking water treatment plant
DOC	Dissolve organic matter
EPA	Environmental protection agency
ESI	Electrospray ionization
FBS	Fetal bovine serum
FDR	False discovery rate
FT-ICR	Fourier transform ion cyclotron resonance
FWHM	Full width at half maximum
g	Grams
GAC	Granular activated carbon
GC	Gas chromatography

H	Hydrogen
HAA	Haloacetic acid
HCD	Hydroxy-cyclopentene-dione
HBSS	Hank's balanced salt solution
HILIC	Hydrophilic interaction chromatography
HIWATE	Health impacts of long-term exposure to disinfection by-products in drinking water in Europe
HLB	Hydrophilic-lipophilic balance cartridge
HOCl	Hypochlorous acid
HOBr	Hypobromous acid
HOI	Hypoiodous acid
HPLC	High-performance liquid chromatography
I ⁻	Iodide
I	Iodine
I-DBP	Iodinated disinfection by-product
ICP-MS	Inductively coupled plasma – mass spectrometry
K _{ow}	n-Octanol/water partition coefficient
kV	Kilovolt
L	Litre
LC	Liquid chromatography
LC ₅₀	Concentration estimated to cause 50% lethality
MAC	Maximum allowable concentration
MBA	Monobromoacetic acid
MCA	Monochloroacetic acid
MCF7	Human breast adenocarcinoma cell line
MDL	Method detection limit
MeOH	Methanol
mg	Milligram
min	Minute
ml	Millilitre
mm	Millimetre
MS	Mass spectrometry
MTT	MTT 3-(4,5-dimethylthiazol-2-yl)-2,5-diphenyltetrazolium bromide
<i>m/z</i>	Mass to charge ratio
n	Number of replicates
N	Nitrogen
N-DBP	Nitrogenous disinfection by-product
NH ₂ Cl	Monochloramine
NH ₄ OH	Ammonium hydroxide
NOM	Natural organic matter
Nrf2/ARE	Nuclear factor erythroid 2-related factor 2/Antioxidant response element
NSF	National Sanitation Foundation
O	Oxygen

O/C	Oxygen to carbon ratio
PBS	Phosphate buffered saline
ppb	Part per billion
ppm	Part per million
preGAC	Pre-granular activated carbon filter
ROS	Reactive oxygen species
rt	Retention time
S	Sulfur
S-DBP	Sulfonated disinfection by-product
SD	Standard deviation
SE	Standard error
SI	Supporting information
SPE	Solid phase extraction
SUVA	Specific absorbance (UV ₂₅₄ /DOC)
TBA	Tribromoacetic acid
TBM	Tribromomethane (bromoform)
TCA	Trichloroacetic acid
TCM	Trichloromethane (chloroform)
THM	Trihalomethane
TOBr	Total organic bromine
TOC	Total organic carbon
TOCl	Total organic chlorine
TOI	Total organic iodine
UHPLC	Ultrahigh-performance liquid chromatography
UHRMS	Ultrahigh resolution mass spectrometry
UV	Ultraviolet
UVT	UV transmittance
WAX	Weak anion exchange
WHO	World Health Organization
°C	Degrees Celsius
µg	Microgram
µl	Microlitre
µm	Micrometre

NOTE TO READERS

This thesis is organized and formatted to follow the University of Saskatchewan College of Graduate Studies and Research guidelines for a manuscript-style thesis. Chapter 1 is a general introduction and includes a literature review on disinfection by-products as well as objectives of this study. Chapters 2, 3, and 4 of this thesis are organized as manuscripts for publication in scientific journals. These chapters are targeted towards the journals *Environmental Science & Technology* or *Water Research*. For consistency, all chapters in this thesis have been similarly formatted. Supporting information associated with each research chapter is presented in the ‘Appendices’ section at the end of this thesis with Appendix A, B, and C corresponding to the chapters 2, 3, and, 4, respectively. Chapter 5 contains a general discussion with overall conclusions. The tables, figures, and references have been reformatted to adhere to the thesis style; references cited in each chapter are combined and listed in the last section of this thesis. As a result of the manuscript-style format there may be repetitions of information.

CHAPTER 1

GENERAL INTRODUCTION

1.1 Preface

Disinfection of drinking water is the process by which pathogenic bacteria and viruses are inactivated by means of chemical or physical technologies such as chlorination, ozonation, or ultraviolet radiation. Disinfection is often hailed as one of the greatest advances in public health because of its significant role in controlling lethal, water-borne diseases such as typhoid and cholera; however, these treatment methods are also responsible for producing a range of chemical by-products some of which are known to cause adverse effects in humans and wildlife (Nathanson, 2015). While risks associated with these disinfection by-products (DBPs) do not outweigh the immediate benefits of disinfection of water, DBPs are still a concern due to their toxic potentials and the nature of their exposure pathways, which are population-wide, through multiple routes on a daily basis (drinking, bathing, cooking), and over lifespans of individuals.

Specifically, concerns have been raised over brominated DBPs (Br-DBPs), because they are consistently more toxic than their chlorinated analogues (Richardson et al., 2007; World Health Organization, 2000). This holds true among various chemical classes as well as in the assessment of various endpoints of toxicity including cytotoxicity and genotoxicity (Li et al., 2016; Plewa et al., 2008; Richardson et al., 2008; Yang and Zhang, 2013; Yang et al., 2014; Zhang et al., 2000). There is a need to identify and characterize Br-DBPs so that any significant risks associated with their occurrence can be mitigated, thus ensuring the public is supplied with safe drinking water. The favoured approach would be to identify the various DBPs so that they can be monitored and so effective treatment processes could be developed to remove the most potent DBPs while still allowing for effective disinfection by use of proven technologies that are cost effective.

1.2 History and Regulation of DBPs

One of the first known attempts to use chlorine to disinfect public water occurred in London, England in 1854 when Dr. John Snow identified contaminated drinking wells as the source of a cholera outbreak (Centers for Disease Control and Prevention, 2014). Plant-scale implementations of chlorination began to arise across Europe through the 1890s, but it wasn't

until 1908 that this method of disinfection was first used in the United States, specifically by the states of New Jersey and Illinois (Water Quality and Health Council, 2015).

DBPs were first identified by Rook in the early 1970s when he discovered that hypochlorous acid and hypobromous acid would react with organic matter naturally present in water to form trihalomethanes (THMs) such as chloroform (Centers for Disease Control and Prevention, 2014). The presence of these compounds in drinking water was confirmed by Bellar *et al.* (1974) and two years later the United States Environmental Protection Agency (US EPA) published survey results showing the presence of THMs in drinking water at a national scale (Richardson et al., 2007). At the same time, studies by the National Cancer Institute reported carcinogenicity of chloroform in laboratory animals (National Cancer Institute, 1976). Together, these reports provided the initial information required to assess risks posed by DBPs.

In 1979 the US EPA began to regulate DBPs in drinking water. They imposed a maximum annual average concentration of 100 µg/L (ppb) of total THMs, which included chloroform, bromodichloromethane (BDCM), dibromochloromethane (DBCM), and bromoform (Richardson et al., 2007). Nearly twenty years later the Stage 1 Disinfectant (D)/DBP rule was issued which lowered the allowable concentration of total THMs to 80 µg/L and added regulations for five haloacetic acids (HAAs), bromate, and chlorite. In 2012, the Stage 2 D/DBP rule came into effect with an added condition that each location in the distribution system must comply with these regulations, due to the potential for concentrations of THMs to increase as water traveled away from the treatment plant to customers (Arbuckle et al., 2002; United States Environmental Protection Agency, 2008).

Currently, Health Canada has set the maximum allowable concentration (MAC) for total THMs (chloroform, BDCM, DBCM, and bromoform) in drinking water at 100 µg /L and the MAC for total haloacetic acids (monochloroacetic acid (MCA), dichloroacetic acid (DCA), trichloroacetic acid (TCA), monobromoacetic acid (MBA), and dibromoacetic acid (DBA)) in drinking water as 80 µg/L or as low as reasonably achievable without compromising disinfection (Health Canada, 2014). As reported by Health Canada, the health basis for each defined MAC along with the primary method of disinfection associated with production of each regulated DBP can be found in Table 1.1. The MAC values for total THMs and total HAAs are expressed as a locational running annual average of quarterly samples. Alternatively, the World Health Organization provides an additive guideline for the trihalomethanes chloroform, BDCM, DBCM,

and bromoform (Equation 1), with corresponding guideline values (GV) being 200, 60, 100, and 100 µg/L, respectively (Health Canada, 2014).

$$\frac{\text{Chloroform}}{\text{Chloroform GV}} + \frac{\text{BDCM}}{\text{BDCM GV}} + \frac{\text{DBCM}}{\text{DBCM GV}} + \frac{\text{Bromoform}}{\text{Bromoform GV}} < 1.0$$

(1)

Table 2.1. Disinfection by-products for which Health Canada regulations exist. Adapted from http://www.hc-sc.gc.ca/ewh-semt/pubs/water-eau/sum_guide-res_recom/index-eng.php#t2

Disinfection By-Product	MAC ¹ (mg/L)	Health Considerations	Notes
Bromate	0.01	Renal cell tumours Probable carcinogen	DBP of ozone; possible contaminant in hypochlorite solution
Chlorate	1	Thyroid gland effects	DBP of chlorine dioxide; possible contaminant of hypochlorite solution
Chlorite	1	Neurobehavioural effects, decreased absolute brain weight, altered liver weights	DBP of chlorine dioxide
Formaldehyde	N/A	N/A	DBP of ozone, but found at levels below which adverse effects occur
Total Haloacetic Acids	0.08 ALARA ²	Liver and other organ cancers Reduced organ weights	DBP of chlorine (primarily)
Total Trihalomethanes	0.1	Liver effects Kidney and colorectal cancer	DBP of chlorine (primarily)
N-Nitroso-dimethylamine (NDMA)	0.00004	Liver cancer Probable carcinogen	DBP of chlorine or chloramines

¹Maximum allowable concentration
²As low as reasonably achievable, without compromising disinfection

Current regulatory guidelines do not encompass all DBPs that have been described, primarily due to the fact that more than 700 compounds have been detected as DBPs and the time and money required to produce sufficient toxicity data on each is substantial (Richardson et al., 2007; Yang and Zhang, 2016). Further challenging regulation of DBPs is the chemical diversity of detected compounds, which makes it possible for multiple toxic pathways to be targeted by the complex mixtures in which DBPs exist. Differences in treatment processes, quality of source water, and seasonal changes contribute to the variety of DBPs that have been detected, and advances in the sensitivity of scientific instrumentation are likely to unveil an even greater number of DBPs in the coming years (Richardson et al., 2007).

1.3 Formation of Disinfection By-Products in Drinking Water

Chlorination is the most commonly used method for disinfection of water because of the simplicity associated with implementation, its efficacy against a wide range of pathogens, and the residual protection it provides throughout a distribution system (Water Resources Management Division and Department of Environment and Labour, 2000). Whether chlorine gas, sodium hypochlorite, or calcium hypochlorite is used as the source of chlorine, reaction with water yields the effective disinfectant hypochlorous acid ($\text{HOCl} \leftrightarrow \text{H}^+ + \text{OCl}^-$ ($\text{pK}_a = 7.5$)). In addition to inactivating pathogens, hypochlorous acid also reacts with natural organic matter (NOM) found in source water to produce chlorinated DBPs (Cl-DBPs) as well as with bromide ions found in source water to form hypobromous acid ($\text{HOBr} \leftrightarrow \text{H}^+ + \text{OBr}^-$ ($\text{pK}_a = 8.7$)) (2). Hypobromous acid is generally more reactive in substitution reactions with NOM than hypochlorous acid and produces a variety of Br-DBPs (Sharma et al., 2014; Uyak and Toroz, 2007). Br-DBPs are particularly prevalent when source water contains large concentrations of both dissolved organic carbon (DOC) and bromide ions (Haag and Hoigné, 1983; Sharma et al., 2014; Watson et al., 2014).



Where: $k = 2.95 \times 10^3 \text{ M}^{-1} \text{ s}^{-1}$ at 25°C

As an alternative to chlorination, some drinking water treatment plants (DWTPs) opt to use chlorine dioxide (ClO₂) or chloramines (monochloramine; NH₂Cl), or might use these in conjunction with chlorination. Chlorine dioxide has the benefit of minimizing production of THMs; however, it produces the by-product chlorite (ClO₂⁻) and can make maintenance of sufficient disinfection through the distribution systems more difficult (Richardson et al., 2003). A report from the Information Collection Rule (ICR) also indicated that treatment plants that employed chlorine dioxide produced greater concentrations of nine bromo-chloro-HAAs than those using chlorine alone (Richardson et al., 2007). Monochloramine (NH₂Cl) used in chloramination is a weaker disinfectant than is chlorine, but it does result in lesser production of THMs, HAAs, and total organic halogen (TOX) (Cowman and Singer, 1996; Sharma et al., 2014). However, chloramination has been associated with greater formation of N-nitrosodimethylamine (NDMA), which is a potent carcinogen, as well as other nitrogenous DBPs (Richardson et al., 2007).

During disinfection by ozonation, the bromide ion, if present, is initially oxidized to BrO⁻/BrOH (3), which is capable of reacting with organic compounds via bromine substitution to produce by-products in a manner similar to chlorination. In contrast to chlorination, ionized BrO⁻ can further react with ozone (O₃), which results in the formation of bromite (BrO₂⁻) (4), regeneration of bromide ion (5), and catalytic decomposition of ozone (Haag and Hoigné, 1983). In addition to previously accepted O transfer reactions between ozone and bromite, which yield bromate ion (BrO₃⁻) (6 and 7), it has been proposed that an additional e⁻ transfer pathway exists that can result in formation of the ozone radical (O₃⁻) (8). Ozone radicals could then react with water to produce the highly reactive hydroxyl radical (·OH).



Relative to the formation of DBPs, there are advantages and disadvantages to use of ozonation instead of chlorination. Compared to chlorination, ozonation can significantly reduce formation of THMs and HAAs, but the carcinogenic by-products bromate and dibromoacetic acid (DBA) are preferentially produced (Jeong et al., 2012; Richardson et al., 2007). When used prior to chlorination and chloramination, ozonation can also increase production of halonitromethanes (Bond et al., 2014).

To effectively reduce concentrations of THMs and HAAs in drinking water, efforts are being directed towards protection of source water from industrial inputs and control of algal blooms which can produce organic compounds that can subsequently form DBPs and require additional chlorination to deal with taste and odor. Advanced treatment technologies can also be implemented to improve the water treatment process, but at extra costs. Membrane filtration prior to disinfection can reduce content of NOM in source water, which not only reduces the amount of DBP precursors, but can also result in shorter chlorine contact times for complete disinfection to occur (Health Canada, 2014). Unfortunately, enhanced removal of NOM from waters rich in bromide can result in greater production of more highly brominated DBPs (Government of Newfoundland and Labrador, 2009; Watson et al., 2014). This is an issue because Br-DBPs are considered to exhibit greater toxic potencies than do analogous Cl-DBPs. Other options to manage DBPs include changing locations where intakes are placed in lakes, pH adjustment of source water, removal of iron and manganese to reduce chlorine demand, biofiltration, or the use of alternative disinfection methods such as ultraviolet radiation or MIOX (mixed oxidant) processes (Government of Newfoundland and Labrador, 2009).

1.4 Physical and Chemical Factors that Influence Formation of DBPs

Multiple physical and chemical factors, primarily quality of source water and method of disinfection, can influence profiles of DBPs formed during disinfection of water (Figure 1.1). For Br-DBPs, the concentration of bromide ion (Br^-) in raw water is also a major driving force for formation during chlorination, ozonation, or chloramination (Sharma et al., 2014; Watson et al., 2014; Yang et al., 2007). Concentrations of Br^- are generally greater in sea water or salinity-impacted waters such as bore water, and speciation of DBPs following chlorination tends to shift towards brominated compounds when water is sourced as groundwater in comparison to surface

water (Kawamoto and Makihata, 2004). Both natural processes and activities of humans can contribute Br⁻ to surface water, which can make it difficult for a water treatment plant experiencing issues with greater formation of Br-DBPs to identify and mitigate problems.

Water Quality + Treatment Process →		Disinfection By-Products
Physicochemical properties: pH, temperature, alkalinity/hardness, salinity	Type of disinfectant: Chlorine, chloramine, chlorine dioxide, ozone, ultraviolet	Trihalomethanes Haloacetic acids Haloacetaldehydes Halonitromethanes Nitrosamines Haloketones Halopicrines MX and analogs Haloacetoneitriles Haloacetates Haloacetamides Cyanogenic halides Haloacetones Unknown DBPs
Organic precursors: Algal organic matter Natural organic matter (fulvic and humic acids)	Treatment time and dose Combination of methods Filtration Coagulation and flocculation	
Inorganic precursors: Br ⁻ , I ⁻ , NO ₂ ⁻ , NH ₃		

Fig. 1.1. Parameters of water quality and properties of the water treatment process that can influence speciation of disinfection by-products.

Aquatic biota such as algae, fungi, and bacteria are known to biosynthesize more than a thousand organo-bromines including some like methyl bromide and bromoform that are identical to compounds produced industrially (Gribble, 2000). There are also possible contributions from degradation of brominated flame retardants, biocides, and dyes; however, many of these compounds have been or are being taken off the market because of mounting evidence of their toxic potential.

During spring and summer months, greater concentrations of THMs, HAAs, and specifically Br-DBPs can be observed at water treatment plants employing chlorination or ozonation (Richardson et al., 2003; Rodriguez and Sérodes, 2001; Zhang et al., 2005). A multivariate analysis found that water temperature was the best predictor of THM seasonal variation, although, other factors such as rainfall, pH, and organic matter also affected the outcome (Rodriguez and Sérodes, 2001). With warmer water temperatures, it is expected that rates of reactions between NOM and disinfectants increase, but greater temperatures of source

water can also contribute to greater productivity of algae which can subsequently increase the amount of DBP precursors entering a DWTP (Richardson et al., 2003). Few studies have investigated the role of algae in the formation of DBPs, but it has been reported that blooms of phytoplankton can contribute as much as 20-50% of total DBPs formed, particularly HAAs (Chen et al., 2008). Greater run-off during spring raises DOC content in source water and can affect leaching/sorption of minerals, while greater alkalinity of source water has been correlated with a shift in speciation of THMs and dihaloacetonitriles (DHANs) towards brominated compounds (Watson et al., 2014).

NOM in source water plays a significant role in formation of DBPs, with both the total amount and the fulvic/humic acid composition being important (Chen et al., 2008; Krasner, 2009; Richardson et al., 2003; Watson et al., 2014). It is generally accepted that the hydrophobic acid fraction of NOM, which is comprised of fulvic and humic acids, is responsible for production of THMs, HAAs, and specifically brominated THMs (Chen et al., 2008; Platikanov et al., 2010). Formation of DBPs is positively correlated to the aromatic carbon content of water, therefore, greater humic composition tends to produce greater concentrations of DBPs. This is supported by work such as that by Singer (1999) and Chellam & Krasner (2001), but it does not hold true in all investigations. For example, it was reported that fulvic acid was more likely to result in formation of THMs, HAAs, and aldehydes when source waters contained large concentrations of Br^- (Richardson *et al.*, 2003).

The ratio of bromide ions to organic matter (Br/DOC) can be a useful parameter to explain rates of formation of Br-DBPs. It is theorized that due to competition between NOM and bromide ion for oxidants, waters with greater Br/DOC ratios might preferentially form DBPs containing more bromine atoms upon chlorination (Watson et al., 2014; Westerhoff et al., 1998). In water containing greater concentrations of Br^- , the concentrations of NOM were directly correlated to detection of fully chlorinated DBPs as well as total THM; however, NOM was negatively correlated with the detection of Br-DBPs such as DBCM, dibromoacetonitrile (DBAN), and bromoform (Watson et al., 2014). Strategies that maximize removal of NOM but that do not remove Br^- , such as coagulation, might create a suitable environment for greater formation of Br-DBPs due to shifts in the ratio of Br/DOC. This is particularly important to consider at DWTPs where source waters have elevated concentrations of Br^- . Implementation of

alternative technologies such as reverse osmosis might be necessary for plants unable to control Br-DBPs (Watson et al., 2014).

1.5 Toxicity of DBPs

Three main approaches have been used to quantify and compare toxic potencies associated with DBPs: epidemiological studies; 2-year rat carcinogenicity studies; and *in vitro* assays. Epidemiological studies and 2-year rat carcinogenicity studies have focussed on regulated DBPs such as THMs and HAAs, while *in vitro* assays have been applied to a much broader range of compounds due to the reduced cost and time required to conduct them. In this thesis, cytotoxicity and oxidative stress were selected as toxic endpoints for evaluation, therefore they receive more in-depth discussion here.

In epidemiological studies of THMs and HAAs, the two main toxic endpoints that have been considered are adverse pregnancy outcomes and cancer. Individual studies have shown evidence of associations between exposure to THMs and adverse outcomes of pregnancies such as fetal growth restriction, stillbirths, and preterm delivery (Costet et al., 2012; Toledano et al., 2005). However, a meta-analysis of all currently available studies on chlorinated THMs and congenital anomalies found little evidence of associations (Nieuwenhuijsen et al., 2009a). A major research initiative called The Health Impacts of Long-Term Exposure to Disinfection By-Products in Drinking Water in Europe (HIWATE) study reported a correlation between exposure to THMs and increased risk for bladder cancer, while results for other types of cancer such as colorectal were inconclusive (Nieuwenhuijsen et al., 2009b). It has also been estimated that increasing concentrations of Br⁻ in source waters by 50 µg/L could potentially lead to 10⁻³ to 10⁻⁴ increase in lifetime risk of bladder cancer due to production of brominated THMs (Regli et al., 2015).

Of the regulated DBPs, all except MBA have undergone a standard 2-year rodent carcinogenicity bioassay and all have shown evidence of carcinogenicity with the exception of MCA (World Health Organization, 2000). The most common site of tumour formation was liver, but BDCM also caused both renal and intestinal tumours, chloroform was linked to renal tumours, bromoform induced intestinal tumours, and studies of bromate have found renal and thyroid tumours (Richardson et al., 2007). Based on these rodent assays, regulated DBPs are

classified as probable or possible human carcinogens. Discrepancies in sites of formation of tumours between rodents and humans are thought to be due to differences in physiology, metabolism, and also route of exposure. Studies on the effects of DBPs on rodents typically evaluate carcinogenicity due to exposure via drinking water or gavage, while exposure through skin or inhalation while showering may be more significant for humans, particularly for volatile DBPs such as THMs.

In vitro assays have been most widely used to assess toxic potencies of DBPs and efforts have been made by The Water Research Foundation to create standardized tests (Plewa and Wagner, 2009; Wagner and Plewa, 2017). They have published methods for a 72 h chronic mammalian cell cytotoxicity assay and a single cell gel electrophoresis (SCGE) assay that assesses genotoxicity after a 4 h period of exposure, both performed with a Chinese hamster ovarian (CHO) AS52 cell line. This cell line expresses a stable chromosome complement, consistent cell doubling time, and a functional p53 protein, also known as tumour suppressor protein (Plewa & Wagner, 2009). For regulated DBPs assessed by the 72 h CHO chronic cytotoxicity assay, the order of decreasing toxicity has been defined as: MBA > DBA > MCA > TCA > TBM (bromoform) > DCA > TCM (chloroform) > BDCM (Wagner and Plewa, 2017). By 2009, these assays had been used to characterize forty-seven DBPs from seven chemical classes ranking them from most toxic to least toxic as: haloacetaldehydes > haloacetamides > halonitromethanes > haloacetonitriles > >2C-haloacids > haloacetic acids > halomethanes (Plewa and Wagner, 2009). By 2017, the number of DBPs assessed by these assays grew to 103 (Wagner and Plewa, 2017). Note that regulated classes of DBPs, haloacetic acids and halomethanes, fall at the less potent end of the toxicity spectrum based on these assays.

While the main application of these standardized tests has been to evaluate individual chemical standards, some studies have expanded their use to include assessment of concentrated extracts of water. For example, as part of the HIWATE study these assays were used to assess the toxicity of European drinking water after concentration by use of XAD resin (Jeong et al., 2012). A positive correlation was found between cytotoxicity and number of DBPs detected in each sample as well as between cytotoxicity and concentrations of specific families such as THMs ($r=0.74$, $p<0.01$), halo-acids ($r=0.75$, $p<0.008$), and Br-DBPs ($r=0.68$, $p<0.022$) (Jeong et al., 2012). These assays were also used to identify strong correlations between concentrations of total organic bromine (TOBr) in raw water prior to chlorination with genotoxicity and

cytotoxicity of corresponding finished water ($r = 0.85$ and $r = 0.92$, respectively) (Yang et al., 2014). In contrast, relationships between these endpoints with total organic chlorine (TOCl) in raw water were weak and inverse ($r = -0.56$ and $r = -0.39$, respectively), which suggested that Br-DBPs are of greater concern than Cl-DBPs (Yang et al., 2014).

Another endpoint often discussed relative to studies of effects of DBPs is oxidative stress, which occurs when reactive oxygen species (ROS) are produced at a rate greater than cellular systems can counteract them. Antioxidants such as glutathione (GSH) and ascorbic acid act to quench ROS before they cause damage to DNA, proteins, or cell membranes (Rahal et al., 2014). Oxidative stress is involved in multiple toxic pathways, therefore, it serves as a good endpoint for comparison of toxicities of chemically diverse DBPs. Support for involvement of ROS in the induction of cytotoxicity and genotoxicity by DBPs comes from several studies, with most research focussed on regulated THMs and HAAs. For example, acute oral dosing of HAAs increased concentrations of two oxidative stress biomarkers, thiobarbituric acid reactive substances (TBARS) and 8-hydroxydeoxyguanosine (8-OH-dG) content of nuclear DNA, in liver of male B6C3F1 mice (Austin et al., 1996). The oxidative stress response was more rapid and prolonged for brominated HAAs with the order of potency reported as DBA = BCA > BDCA > DCA > TCA. MonoHAAs induced significant concentration-dependent expression of β -lactamase reporter under control of the antioxidant response element (ARE) in HepG2 cells, and they were able to alter transcription of multiple oxidative stress response genes, such as thioredoxin reductase 1, in nontransformed human intestinal epithelial cells (Pals et al., 2013). BDCM induced both liver and kidney damage in rodents with effects exacerbated in GSH-depleted rats, which again supports involvement of oxidative stress (Gao et al., 1996; Lilly et al., 1997). Observed oxidative stress, genomic DNA damage, and depletion of ATP are correlated with S_N2 alkylating potential, which is consistent with the observed order of potency of HAAs (iodoacetic acid > bromoacetic acid >> chloroacetic acid) (Dad et al., 2013; Pals et al., 2013).

1.6 Analytical Techniques for Detection of DBPs

The first DBPs were detected using gas chromatography (GC) coupled to mass spectrometry (MS), but routine analysis shifted to GC coupled with an electron capture detector (ECD) because of its sensitivity towards halogenated compounds (Richardson, 2002; Weinberg,

2009). Many of the early DBPs studied were thermally and chemically stable as well as volatile, so GC-ECD was an effective method. In contrast, many newly identified DBPs are polar, non-volatile, or thermally labile making them unsuited for GC separation (Weinberg, 2009). Moreover, novel DBPs often exist at very low concentration in water so sensitive analytical methods are needed for their detection. Many improvements in MS sensitivity and selectivity can be attributed to the development of tandem MS techniques such as triple quadrupole and quadrupole/time-of-flight (Q-ToF), as well as their pairing to liquid chromatography (LC) separation (Farré et al., 2012).

LC-MS has gained popularity because it offers the ability to detect non-volatile and polar DBPs that may have been overlooked in the past with enhanced selectivity (Zwiener and Richardson, 2005). For example, ultra-performance LC (UPLC) paired with electrospray ionization (ESI) – triple quadrupole MS was used to detect and predict formulae for novel classes of DBPs such as trihalo-hydroxy-cyclopentene-diones (trihalo-HCDs), dihalo-4-hydroxybenzaldehydes, and methanesulfonic acids (Pan et al., 2016a; Pan and Zhang, 2013; Zahn et al., 2016). Fourier transform ion cyclotron resonance mass spectrometry (FT-ICR MS) has also been very useful for identification of novel DBPs due to its extreme sensitivity and mass accuracy of <1 ppm (Farré et al., 2012). FT-ICR MS was recently used to predict molecular compositions for 1000 novel chlorine-containing DBPs and 473 novel polar Br-DBPs (Zhang et al., 2014, 2012a, 2012b).

To target novel DBPs, tandem MS methods have been developed that use precursor ion scans to selectively detect halogenated compounds. Chlorine exists as ^{35}Cl and ^{37}Cl and bromine exists as ^{79}Br and ^{81}Br , therefore, by setting the precursor ion scan (PIS) to m/z 35/37 and 79/81 in negative ion mode all ionizable compounds that contain chlorine or bromide, respectively, can be detected (Zhang et al., 2008). To utilize this method, an original water sample should be extracted and concentrated 1000-2000 times in order to eliminate inorganic salts and to concentrate trace DBPs (Zhai and Zhang, 2009). Paired with UPLC, this approach has been used to identify eleven new aromatic halogenated DBPs in drinking water, and the six novel wastewater DBPs bromomaleic acid, 5-bromosalicylic acid, 3,5-dibromo-4-hydroxybenzaldehyde, 3,5-dibromo-4-hydroxybenzoic acid, 2,6-dibromo-4-nitrophenol, and 2,4,6-tribromophenol (Ding et al., 2013; Pan and Zhang, 2013). Following PIS of m/z 35/37 or m/z 79/81, the use of product ion scan at a specific retention time can provide structural

information for a selected ion (Ding et al., 2013; Pan and Zhang, 2013; Zhang et al., 2008). By observing isotopic ratios in mass spectra it can be predicted how many of each halogen the compound is likely to contain. For example, $\text{ClBr}_2\text{CCOOH}$ produces ion clusters with a ratio of 3:7:5:1 while Br_3CCOOH produces the ratio 1:3:3:1 in full scan (Zhai and Zhang, 2009). In precursor ion scans of m/z 79 and 81 these ratios shift to 3:4:1 and 1:2:1, respectively.

1.7 Current Challenges in DBP Research

The main challenges in DBP research relate to: 1) the number of parameters that can influence fates and behaviours of DBPs, as discussed in section 1.4; 2) the enhanced toxicity of some unregulated DBPs compared to regulated THMs and HAAs; and 3) the vast number of compounds identified as DBPs.

Research has shown that many unregulated DBPs including, but not limited to, haloacetaldehydes, halonitromethanes, haloacetamides, and haloacetonitriles exhibit greater toxic potencies than do regulated THMs and HAAs (Kundu et al., 2004; Muellner et al., 2007; Plewa et al., 2008; Richardson et al., 2007). As a class, thirteen haloacetamides were determined to exhibit 142-fold greater toxic potencies and were 12-fold more genotoxic than the five regulated HAAs (Plewa et al., 2008). A comparison of halonitromethanes with halomethane homologs revealed that halonitromethanes are more potent mutagens and at least ten times more cytotoxic (Kundu et al., 2004). The general conclusions are that due to increased reactivity of the nitro-group, nitrogenous DBPs are more toxic than carbonaceous DBPs, and due to bromine being a better leaving group than chlorine, brominated DBPs are more toxic than their chlorinated analogues within a chemical class (Giller et al., 1997; Kundu et al., 2004; Muellner et al., 2007; Pals et al., 2013; Plewa et al., 2008; Richardson et al., 2007). More research is needed to fully characterize toxicity of these unregulated DBPs to determine if regulations should be implemented, but the fact that over 700 compounds have been identified as DBPs makes this a daunting task.

Unfortunately, the number of unregulated DBPs that have been identified is only expected to grow as analytical instruments become increasingly more powerful. Currently, gas and liquid chromatography-mass spectrometry (GC/LC-MS) are the primary methods used to monitor DBPs while Fourier transform ion cyclotron resonance mass spectrometry (FT-ICR MS) has

played an important role in detecting novel DBPs (Fan et al., 2013; Jeong et al., 2015, 2012, Zhang et al., 2014, 2012a). To date, ~700 halogenated DBPs have been identified and validated in laboratory produced chlorinated waters (Yang and Zhang, 2016). In plant-scale chlorinated water, FT-ICR MS was used to detect ~800 Cl-DBPs but limited information was available on the occurrence of Br-DBPs and iodinated DBPs (I-DBPs) in actual samples of drinking water (Gonsior et al., 2014). This was mainly due to complicated interferences and the lesser abundances of Br- and I-DBPs in drinking water compared to Cl-DBPs (Postigo et al., 2016; Zhang et al., 2014). Additionally, the limited scanning speeds of FT-ICR MS make it less compatible with current HPLC techniques which means direct infusion is commonly used. This method can be limited by matrix effects and thereby poses a challenge for comparative analysis of drinking water, especially since internal/external standards are not available for most detected DBPs.

1.8 Research Objectives

There is a need to further understand what unregulated Br-DBPs exist in drinking water as well as what the toxic potentials of these compounds may be. In particular, there are few studies that evaluated the toxicity of complex mixtures of DBPs as they actually occur in drinking water. Initial screening consistently shows that Br-DBPs and I-DBPs are more cytotoxic and genotoxic than their chlorinated analogues; however, it is possible that some Br- and I-DBPs have yet to be identified in drinking water by current analytical methods. Untargeted screening methods, exploration of what processes favour formation of unregulated DBPs, and knowledge of what can influence overall mixture toxicity are required to better assess whether regulatory guidelines should be implemented to protect the public. The research objectives of this thesis are as follows:

Objective 1: Develop a reproducible method for untargeted screening and semi-quantitative comparison of Br-DBPs in samples of drinking water (Chapter 2).

In this study, a novel method used to detect 1593 unique organo-bromines in sediments from the Great Lakes region of Ontario, Canada was modified to detect Br-DBPs and I-DBPs in samples of chlorinated water, collected from DWTPs in Saskatchewan, Canada (Peng et al.,

2015a; Peng et al., 2015b). The method involves a data-independent precursor isolation and characteristic fragment method (DIPIC-Frag) performed by use of liquid chromatography (LC) and ultrahigh-resolution mass spectrometry (UHRMS) operated on a Q Exactive™ Hybrid Quadrupole-Orbitrap™ MS. Due to the chemical diversity of DBPs, multiple extraction and analytical parameters were compared to optimize the method and to establish a library of Br-DBPs and I-DBPs. Structures were predicted for the most abundant compounds.

H₀₋₁: There will be no significant differences in the detection of brominated and iodinated compounds in chlorinated water compared to raw water.

H₀₋₂: There will be no significant differences in the detection of brominated and iodinated compounds in samples of chlorinated water extracted by different methods.

H₀₋₃: There will be no significant differences in the detection of brominated or iodinated compounds in temporally distinct samples of water, extracted by the same method

Objective 2: Identify fates and behaviours of unregulated Br-DBPs in drinking water, and determine if parameters of source water can explain their occurrences (Chapter 3).

The optimized method and established library of Br-DBPs was then used to screen samples of water collected monthly over a year, from various stages during the treatment process, including raw, clearwell, and finished stages of treatment at a second DWTP located in central Saskatchewan. Seasonal trends of unregulated Br-DBPs as well as trends through the treatment process were explored. Samples were analyzed for NOM by direct injection UHRMS and concentration of total bromine (Br) by inductively coupled plasma mass spectrometry (ICP-MS). Correlation analysis was employed to elucidate relationships between source water parameters and detection of Br-DBPs, with significance defined as $\alpha=0.05$.

H₀₋₄: There will be no significant correlations ($\alpha=0.05$) between the occurrences of Br-DBPs at different stages of treatment as well as at different time points.

H₀₋₅: There will be no significant correlations ($\alpha=0.05$) between parameters of raw water or treatment conditions with occurrences of Br-DBPs.

Objective 3: Explore monthly trends in the toxicity of real DBP mixtures by use of *in vitro* assays and identify variables that may predict whole mixture toxicity of DBPs (Chapter 4).

Concentrated extracts of raw, clearwell, and finished water from six months were subjected to *in vitro* assessments of cytotoxicity and oxidative stress. Cytotoxicity was assessed using the 72 h CHO cytotoxicity assay described by Elizabeth D. Wagner and Michael J. Plewa. The CHO AS52 cell line is not commercially available, and efforts to obtain the cell line from Dr. Michael J. Plewa from the University of Illinois at Urbana-Champaign (UIUC) were unsuccessful. In place of that assay, a CHO-K1 cell line (ATCC® CCL-61™) was purchased from Cedarlane (Burlington, ON, CA) and was used. An Nrf2/ARE-luciferase tagged bioassay was used to measure induction of oxidative stress. Nrf-2 (nuclear factor erythroid 2-related factor 2) is a basic leucine transcription factor that is activated by electrophiles and ROS (Itoh et al., 1999). After release from Keap1 and translocation to the nucleus, Nrf2 can bind to antioxidant response elements (AREs) located in the promoter region of antioxidant genes, leading to expression of antioxidant enzymes and target genes (Kansanen et al., 2013; Nguyen et al., 2009). This assay measures a general, downstream response to oxidative stress which is advantageous for assessing combined toxicity of DBP mixtures as individual pathways were not overlooked. This assay has previously been used by our lab to compare induction of oxidative stress by water samples collected from a water treatment plant in June 2015, with initial results indicating that chlorinated water contains greater concentrations of oxidative compounds compared to raw water.

Temporal trends in results from both assays were compared to determine if oxidative stress plays a role in cytotoxicity induced by complex mixtures of DBPs. Correlation analyses were used to identify significant relationships ($\alpha=0.05$) between parameters of water quality, treatment conditions, unregulated Br-DBPs, and observed toxic responses.

H₀₋₆: There will be no significant differences in cytotoxicity or oxidative stress induced by concentrated extracts of water compared to negative controls.

H₀₋₇: There will be no significant differences in the toxicity of water collected at the raw, clearwell, and finished stages of treatment.

H₀₋₈: There will be no significant differences in the toxicity of water collected at different time points over a year.

H₀₋₉: There will be no significant correlations ($\alpha=0.05$) between parameters of raw water, treatment conditions, and observed toxicities of chlorinated water.

CHAPTER 2

DETECTION AND COMPARATIVE ANALYSIS OF BROMINATED AND IODINATED DISINFECTION BY-PRODUCTS IN DRINKING WATER

Christena Watts, Jianxian Sun, Paul D. Jones, John P. Giesy, and Hui Peng

Chapter 2 was submitted to *Water Research* September 2018. Contributions from each author are as follows:

Christena Watts (University of Saskatchewan) collected samples of water, performed chemical extractions, and collaborated to analyze data and prepare the manuscript.

Jianxian Sun (University of Toronto) contributed to data analysis.

Paul D. Jones and John P. Giesy (University of Saskatchewan) secured funding for this research, and provided scientific input and editorial comments on the manuscript.

Hui Peng (University of Toronto) developed, operated, and perform primary data analysis for the DIPIC-Frag to characterize Br-DBPs and I-DBPs. He also assisted with preparation of the manuscript.

ABSTRACT

Many halogenated disinfection by-products (DBPs) that exist in drinking water have not yet been identified, which is especially true for brominated (Br-DBPs) and iodinated DBPs (I-DBPs) that occur at lesser concentrations than chlorinated DBPs. In this study, a recently described, data-independent precursor isolation and characteristic fragment (DIPIC-Frag) method was used to screen Br- and I-DBPs in waters collected from a drinking water treatment plant in Saskatchewan, Canada. Analytical conditions such as ionization source, chromatographic column, and sample pretreatment were optimized and 553 Br-DBPs and 112 I-DBPs were detected. These DBPs exhibited variations in m/z values (170.884 – 497.0278), retention times (2.4-26.2 min) and number of incorporated halogen atoms (1-3). The method exhibited good precision and allowed for comparative analysis between samples. Contrasting profiles of Br-DBPs and I-DBPs were observed, and methoxylated DBPs showed distinct trends from DBPs with greater O/C ratios. While large variation in abundances were observed, the 50 most abundant Br-DBPs contributed 45.3% to the total abundance of Br-DBPs. Structures for these detected DBPs were predicted by retrospectively interpreting MS² spectra, and several greater-abundance DBPs were predicted to be hetero-atomic compounds. Future studies on formation, behaviours and potential toxic effects of these unregulated DBPs are warranted.

KEYWORDS: disinfection by-product; DIPIC-Frag; halogenated methanesulfonic acid; tri-halo-HCD; Orbitrap

2.1 Introduction

Chlorinated disinfection by-products (Cl-DBPs) are produced during treatment of drinking water as a result of oxidation of natural organic matter (NOM) by chlorine disinfectants. During disinfection, chlorine in the form of hypochlorous acid (HOCl) also reacts with bromide (Br⁻) and iodide (I⁻) ions found naturally in source waters to form hypobromous (HOBr) and hypoiodous (HOI) acids. These oxidants further react with NOM as well as previously formed Cl-DBPs to produce a diverse mixture of brominated and iodinated disinfection by-products (Br-DBPs and I-DBPs) (Richardson et al., 1999; Richardson et al., 2007; Yang et al., 2014). Multiple toxicities have been reported for DBPs such as cytotoxicity, genotoxicity and mutagenicity with a general trend emerging across different chemical classes that I-DBPs are more toxic than Br-DBPs which are more toxic than Cl-DBPs (Li et al., 2016; Plewa et al., 2008; Richardson et al., 2008; Richardson et al., 2007; Yang & Zhang, 2013; Yang et al., 2014; Zhang et al., 2000). Epidemiological studies have also documented associations between exposure to DBPs and greater risks of bladder cancer and adverse outcomes of pregnancies (Cantor et al., 1998; Costet et al., 2012; Villanueva et al., 2003). Since humans are exposed to DBPs on a daily basis it is imperative to better understand processes involved in their formation and associated hazards.

Currently, gas/liquid chromatography-mass spectrometry (GC/LC-MS) are the primary methods used to monitor DBPs while Fourier transform ion cyclotron resonance mass spectrometry (FT-ICR MS) has played an important role in detecting novel DBPs (Fan et al., 2013; Jeong et al., 2015, 2012, Zhang et al., 2014, 2012a). To date, ~700 halogenated DBPs have been identified and more continue to be described (Yang and Zhang, 2016). For example, FT-ICR MS was used to detect ~800 Cl-DBPs in drinking water from Sweden (Gonsior et al., 2014). Limited information is available on the occurrence of Br-DBPs and I-DBPs in actual samples of drinking water, mainly due to complicated interferences and the lesser abundances of Br- and I-DBPs in drinking water compared to Cl-DBPs (Postigo et al., 2016; Zhang et al., 2014). In particular, identification of I-DBPs is challenged by the fact that iodine has only one naturally-occurring stable isotope, and thus mass spectrometric confirmation cannot rely on the use of isotopic profiles (Postigo et al., 2016). This limitation affects the specificity of analyses and gives rise to false positive identifications. Additionally, the limited scanning speeds of FT-ICR MS make it incompatible with current HPLC techniques which means direct infusion is

commonly used. This method can be limited by matrix effects and thereby poses a challenge for comparative analysis of drinking water, especially since internal/external standards are not available for most detected DBPs.

An untargeted, data-independent, precursor isolation and characteristic fragment (DIPIC-Frag) method has recently been developed for untargeted screening of brominated and iodinated compounds (Peng et al., 2015; Peng et al., 2016a; Peng et al., 2016b). In contrast to previous mass spectrometry approaches relying on MS¹ spectra, DIPIC-Frag is a “bottom up” method that uses characteristic product ions from MS² spectra to retrospectively align corresponding precursor ions. This method exhibited advantages such as greater sensitivity, expanded dynamic range (i.e. fewer co-eluting interferences) and a lesser false positive rate for untargeted screening of brominated/iodinated compounds in complicated environmental samples (Peng et al., 2016a; Peng et al., 2016b; Peng et al., 2016c). Thus, application of the DIPIC-Frag method to detect and comparatively determine Br-DBPs and I-DBPs in drinking water was deemed to be of interest.

The main objective of this study was to detect Br-DBPs and I-DBPs in chlorinated water collected from a DWTP by use of the DIPIC-Frag method implemented on a Q ExactiveTM Hybrid Quadrupole-OrbitrapTM Mass Spectrometer (MS). Multiple solid phase extraction (SPE) methods and instrumental conditions were compared to enhance chemical coverage. A non-redundant library for Br-DBPs and I-DBPs was established, and chemical structures of the most abundant DBPs were predicted. The effect of quenching reagents on the profile of detected DBPs was investigated.

2.2 Materials and Methods

2.2.1 Chemicals and Reagents

Details are provided in Supporting Information.

2.2.2 Collection of Drinking Water

Samples of water were collected on October 8, 2015, April 15, 2016, and August 17, 2017 from a drinking water treatment plant (DWTP) in Saskatchewan, Canada. Details on the treatment process can be found in Supporting Information and Fig. A.1. Samples collected in October and April underwent untargeted screening for DBPs to establish a mass spectrometry library. Water collected in October was sampled after pre-chlorination which serves as primary disinfection (chlorinated raw water). In April 2016 the point of chlorination was changed to occur post-clarification, therefore, water collected in April was sampled near the end of the treatment process (conventionally treated water).

Samples collected in August 2017 were used to investigate the possibility that residual chlorine could be reacting with previously formed DBPs or experimental materials to produce detected DBPs. On this date the plant was performing pre-chlorination and their granular activated carbon (GAC) filter was in operation, which removes many produced DBPs. Therefore, water was collected after sand filtration, or just prior to GAC filtration (preGAC). At the treatment plant, these samples received either no quenching reagent (n=3), an excess of 3.5 mg/L of sodium thiosulfate (n=3), or an excess of 5 mg/L of ascorbic acid (n=3). Doses of quenching reagents were chosen based on literature references and the average concentration of free chlorine found at the preGAC stage (0.25 mg/L) (Conrad, 2017; Farré et al., 2013; Tikkanen et al., 2001). Trip-blanks of ultrapure water were transported to the DWTP, opened within the plant, then received either no quenching reagent or one of the quenching reagents at the same concentrations as above (n=2). Raw water (n=3) was collected so halogenated compounds present in lake water could be differentiated from DBPs formed during treatment. A blank sample of ultrapure water (blank) and two additional control samples of ultrapure water spiked with sodium hypochlorite (NaOCl) to mimic residual chlorine were included in the experimental design. All samples were collected in 4-L headspace-free, amber glass containers previously rinsed with ultrapure water and methanol. All samples were extracted within 4-h of collection.

2.2.3 Optimization of the DIPIC-Frag Method for DBP Screening

2.2.3.1 Sample Pretreatment

Chlorinated raw water collected October 8, 2015 underwent three different SPE pretreatment methods (C18, HLB, and WAX) which were compared to achieve the best coverage of DBPs. Oasis C18 and HLB cartridges have been widely used for extraction of water samples. A WAX cartridge was also tested since many DBPs have been found to be acidic or phenolic compounds in preliminary experiments. For C18 and HLB methods, cartridges were preconditioned with DCM, methanol and ultrapure water and then 1 L of water (n=3) was extracted at a flow rate of 5-10 mL/min. Cartridges were dried under a gentle flow of nitrogen, and adsorbed compounds were eluted from the cartridges with 5 mL of methanol and 5 mL of DCM. Extracts were dried under a stream of nitrogen and reconstituted in 500 μ L of methanol. For the WAX method, cartridges were preconditioned with methanol containing 0.5% NH_4OH , methanol and ultrapure water and then 1 L of water (n=3) was extracted at a flow rate of 5-10 mL/min. Cartridges were dried under a stream of nitrogen, and adsorbed compounds eluted with 6 mL of methanol containing 0.5% NH_4OH . Extracts were dried under a stream of nitrogen and reconstituted in 500 μ L of methanol. Conventionally treated water collected April 15, 2016 underwent four pretreatment methods: the same HLB and C18 methods as above, as well as two pretreatment methods in which the effect of pH was assessed. For the latter, 1 L of water (n=3) was acidified with hydrochloric acid to pH 2, then extracted using HLB (termed HLB_pH2) or C18 cartridges (termed C18_pH2) following the above protocol.

For the study on quenching reagents, preGAC and raw water samples were extracted in triplicate by the HLB_pH2 method and corresponding trip blanks were extracted in duplicate. Prior to extraction, concentrations of free and total chlorine were measured by an Orion AQUAfast™ AQ4000 colorimeter (Thermo Scientific) (Table A.4). Using the in-house established library of DBPs these samples were screened for the 50 most abundant Br-DBPs and 10 most abundant I-DBPs (Tables A.1 and A.2).

2.2.3.2 LC-Q Exactive Data Acquisition

Aliquots of extracts were analyzed using a Q Exactive™ UHRMS (negative ion mode) equipped with a Dionex™ UltiMate™ 3000 UHPLC system (Thermo Fisher Scientific). To avoid shifts in instrument sensitivity, aliquots of samples from different sampling events

(October and April) were analyzed at the same time. Further analytical details are provided in Supporting Information.

2.2.3.3 Quality Control and Assurance

Details are provided in Supporting Information.

2.2.3.4 Data Treatment and Statistical Analyses

The chemometric strategy used for detection of peaks and matching of peaks among samples, identification of precursor ions, and determination of formulae for compounds is described in Supporting Information. Potential false discovery rates (FDR) have not been statistically evaluated in the current deterministic DIPIC-Frag method and only the predicted formula with the greatest score was selected for addition to the library. While the low molecular weight of most DBPs makes the FDR substantially lower, future studies are warranted to advance the current deterministic DIPIC-Frag method, for statistical FDR control. Some halogenated compounds were also detected in source water, and thus only those compounds showing >3-fold greater abundances in chlorinated water compared to source water were considered to be DBPs produced during chlorination. Normality of the data was assessed using the Kolmogorov-Smirnov test. All data analyses such as Pearson, pairwise correlations, linear regressions, and cluster analyses were performed with an in-house R program (software version 3.1.2; <http://www.R-project.org>; R Foundation for Statistical Computing, Vienna, Austria). For those results that were less than the method detection limit (MDL), half of the MDL was assigned to avoid missing values in the statistical analyses. Statistical significance was defined as $p < 0.05$.

2.3 Results and Discussion

2.3.1 Optimization of DIPIC-Frag Method for DBP Screening

To adapt the DIPIC-Frag method for untargeted screening of Br-DBPs and I-DBPs in water, a chemometric strategy different from those used in previous studies was used for alignment of precursor ions and prediction of compound formulae: i) In contrast to previous studies on sediments and house dust (Peng et al., 2016a; Peng et al., 2016c), bromine fragment peaks in extracts of drinking water were found to be more complicated. Overlap of close peaks was frequently observed especially for DIA windows with greater mass. This presented challenges during deconvolution of the brominated fragment peaks, which also led to misalignment of precursor ions. To avoid this, a peak top triggered method was used, rather than chromatographic elution profiles, to identify relevant precursor ions (see method section in SI); ii) While HOBr and HOI react with NOM at faster rates than does HOCl, Cl-DBPs exhibit the greatest abundances because the concentration of chlorine added during disinfection is typically orders of magnitude greater than concentrations of bromide or iodide in fresh water (Hua et al., 2006; Westerhoff et al., 2004). Thus, to narrow precursor ion candidates, only those candidate precursor ions with greater abundances of predicted chlorinated analogues were included for subsequent data analyses; iii) Previous studies have documented that multiple DBPs are homologues with differences in $-\text{CH}_2$ groups or substitution with alternative halogens (*e.g.*, R-Br versus R-I) (Zhang et al., 2012; Zhang et al., 2014). Based on such prior knowledge, two homologue models were developed (Fig. A.2): a) For the $-\text{CH}_2$ homologue model, DBPs with lesser masses were predicted first because of their lesser rate of false positives (*e.g.*, for an ion $m/z \sim 200$, possible formulae were typically less than three within a 5 ppm mass tolerance; but more than 15 for ion $m/z \sim 600$). The established library was used for prediction of high-mass DBPs with a reduced rate of false positives; b) For the halogen homologue model, formulae of Br-DBPs were reliably predicted by their characteristic isotopic peak ratios and greater abundances. To assign formulae for the I-DBP analogues, the established library of Br-DBPs was then incorporated into the scoring system. In addition, libraries established from previous studies (Gonsior et al., 2014; Lavonen et al., 2013) using FT-ICR MS were also incorporated into the homologue model. By including all this information, a novel scoring algorithm was developed for processing DIPIC-Frag results from extracts of partially or fully treated water (Fig. 2.1).

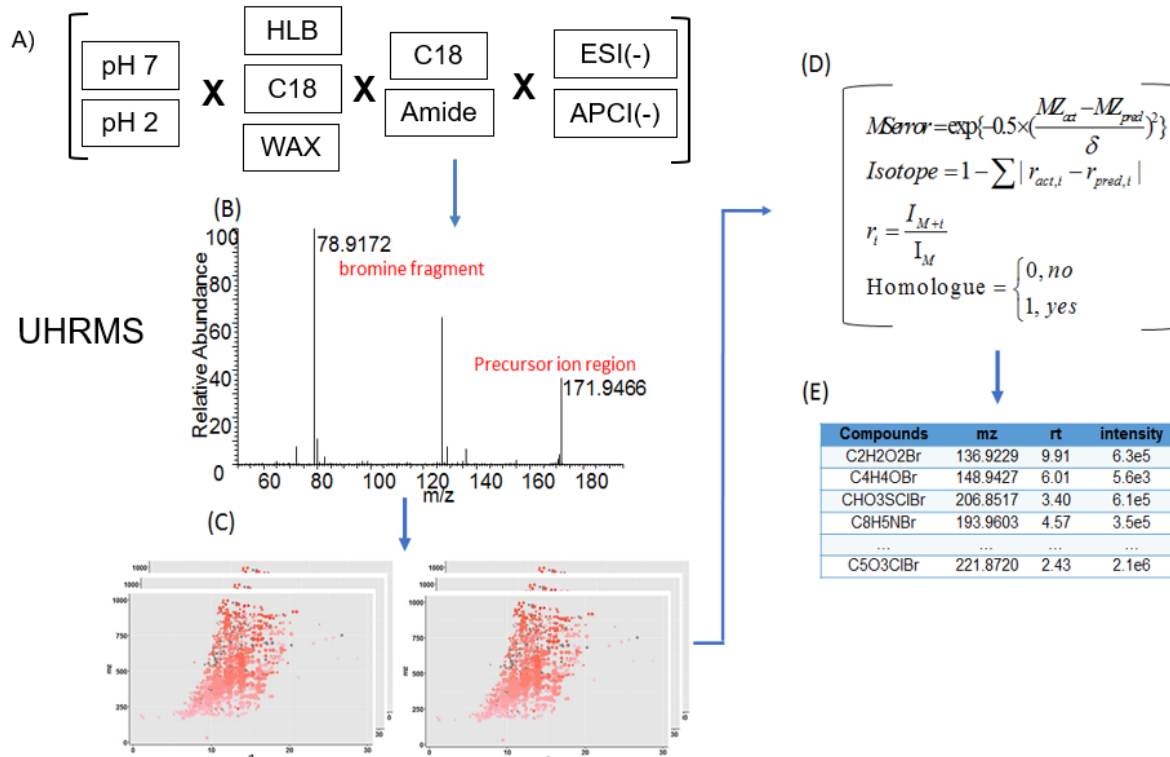


Fig. 2.1. Typical workflow of the DIPIC-Frag method used to identify brominated and iodinated by-products in chlorinated water: (A) Hybrid conditions were combined to maximize the mass spectrometry library; (B) Bromine and iodine fragment peaks from each DIA window were used to produce the library; (C) Multiple libraries were constructed for the different operational conditions; (D) A scoring system was used to align precursor ions and predict compound formulae; (E) The final non-redundant library was constructed by matching compound formulae and retention times to merge libraries.

In previous studies, better chemical coverage of organo-bromines in sediment was achieved using an APCI source (Peng et al., 2015); however, in this study an ESI source (abundance was 1.82×10^5 for Br-DBPs extracted from 230 ± 2.5 DIA window) resulted in 10-fold greater sensitivity than that of the APCI source (abundance was 2.46×10^4 for Br-DBPs extracted from 230 ± 2.5 DIA window) (Fig. A.3). Most DBPs are polar compounds, and previous studies have documented preferential ionization of polar compounds, specifically DBPs, using ESI (Zhang et al., 2008). Thus, an ESI source was used in subsequent experiments.

While a C18 HPLC column was used in previous DIPIC-Frag studies of sediments and dusts (Peng et al., 2016a; Peng et al., 2016c), Br-DBPs exhibited poor retention on the C18 column with most eluting in the first 3 minutes (Fig. A.4A). These results indicated Br-DBPs are more polar than brominated compounds from sediments, which is consistent with the low K_{ow} values of known DBPs (Plewa et al., 2004a; Plewa et al., 2004b; Richardson et al., 2003; Richardson et al., 2008). Several more hydrophilic columns (Amide, T3, HILIC (XBridge™ HILIC, Waters), and C8) were tested. An Amide column with mobile phases of 0.1% NH_4OH in water and 0.1% NH_4OH in acetonitrile gave better separation than other HPLC conditions, with multiple Br-DBPs peaks detected throughout the retention window of 2-15 min (Fig. A.4B).

2.3.2 Library of Br-DBPs in Chlorinated Water

When the bromide fragment from the same DIA window ($215 \pm 2.5 \text{ m/z}$) was extracted for each SPE method, unique chromatograms were observed (Fig. A.5). Numerous unknown Br-DBPs were detected by each method, with some complementary chemical coverage (Fig. 2.2A). The fewest number of Br-DBPs were detected in October samples extracted by HLB and C18 cartridges. With a peak intensity cutoff of 50,000, 226 and 238 Br-DBPs were detected in samples collected in April extracted by C18 or HLB cartridges, respectively. When pH was adjusted to 2 before extraction by C18 (C18_pH2) and HLB (HLB_pH2) cartridges, a greater variety of Br-DBPs were detected (291 and 290 Br-DBPs for C18_pH2 and HLB_pH2, respectively). Better extraction efficiencies for Br-DBPs from water after acidification suggests that some Br-DBPs have low pK_a values and thus, their absorptions on hydrophobic C18/HLB cartridges were improved. Supporting this hypothesis, the greatest number of Br-DBPs (313) was detected in samples of chlorinated raw water extracted by WAX cartridges, which specifically capture acidic compounds (Fig. 2.2A). The pattern of chemicals in chlorinated raw water samples extracted by WAX cartridges was different from that observed when extracted with HLB and C18 cartridges. In particular, polyoxygenated Br-DBPs (*i.e.*, $\text{C}_4\text{H}_5\text{O}_3\text{Br}$, $\text{CH}_2\text{O}_3\text{SClBr}$) were specifically captured by WAX cartridges. Such results could be explained by relatively strong polarities of these polyoxygenated Br-DBPs, which affects efficiency of recovery by HLB and C18 cartridges even after pH adjustment. Considering the similar number of compounds isolated and abundances of Br-DBPs between C18 and HLB cartridges, and the better chemical

coverage of acidification methods, it can be concluded that acidified HLB/C18 and WAX are the preferred methods for analysis of Br-DBPs.

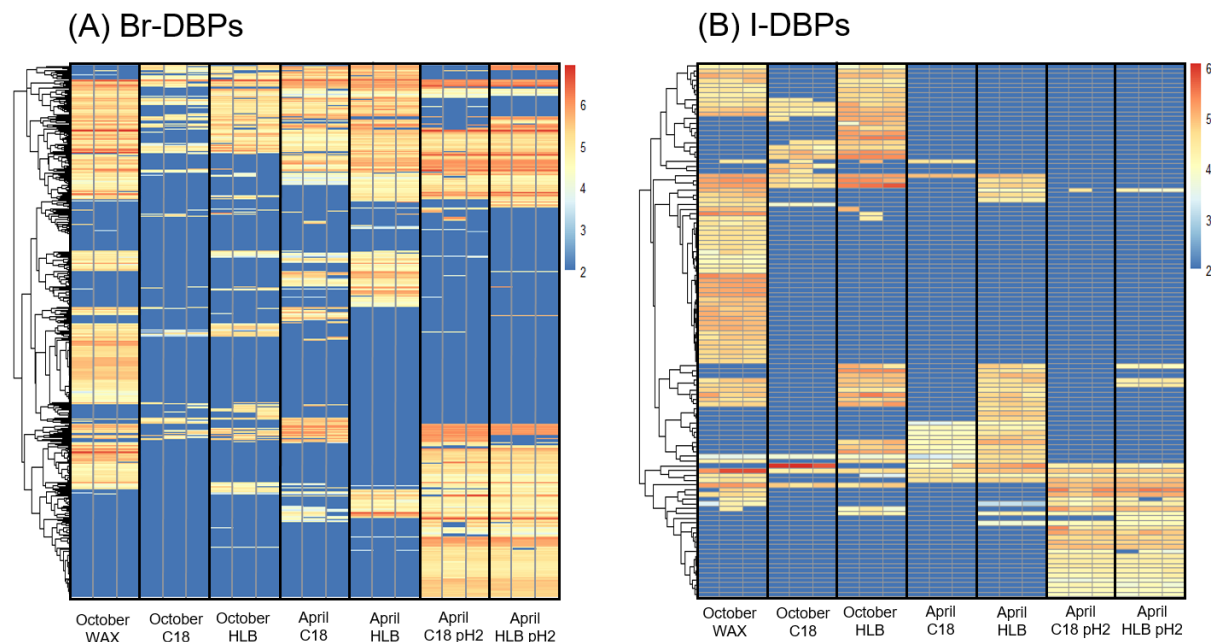


Fig. 2.2. Heat map of log-transformed peak abundances of (A) Br-DBPs and (B) I-DBPs detected by use of three solid phase extraction cartridges (WAX, HLB, C18) and two sample pretreatment conditions (no pH adjustment or pH 2). Samples were collected in October (water chlorinated at raw intake) or April (water chlorinated post-coagulation and clarification) and triplicate samples were analyzed for each condition.

When libraries from all SPE methods were combined using retention times and predicted formulae, a non-redundant library containing 553 Br-DBPs was established. Detected Br-DBPs exhibited variations in m/z (170.884 – 497.0278), retention times (2.4–26.2 min) and number of bromine atoms (1–3) (Fig. A.6A). 447 (81%) of the Br-DBPs contained only one bromine atom (with or without chlorine atoms), which is different from brominated compounds detected in Lake Michigan sediments, many of which contained multiple bromine atoms (Peng et al., 2016a). The relatively small number of halogens incorporated in DBPs is consistent with previous studies (Zhang et al., 2014; Zhang et al., 2000). Abundances of peaks associated with Br-DBPs were distributed from 10^4 to 8.4×10^6 (Fig. 2.3A). It should be noted that discussion of relative chemical abundances is based on an assumption that all chemicals have relatively similar instrumental response factors, which has been widely adopted in previous studies (Peng et al.

2016). Identifications of two of the most abundant Br-DBPs, bromophenol and brominated acetic acid, were successfully confirmed using commercially available, authentic standards. Most of the detected Br-DBPs are unregulated and no commercial standards are available, so future studies are warranted to confirm the structure and potential toxicities of these Br-DBPs using chemically synthesized standards. HAAs were among the most abundant Br-DBPs, but other Br-DBPs were detected with similar or even greater abundances. In particular, a Br-DBP with predicted formula CHSO_3ClBr (8.4×10^6) (Fig. 2.3A) was more abundant than were HAAs (6.8×10^6). The detection of this compound as a DBP is supported by a recent study conducted on European waters, in which CHSO_3ClBr , or bromochloromethanesulfonic acid, as well as six additional halogenated methanesulfonic acids were detected (Zahn et al., 2016).

Due to the compatibility of the DIPIC-Frag method with HPLC, it was possible to differentiate isomers of DBPs that have the same exact m/z value, an objective that could not be achieved by previous direct infusion methods (Gong & Zhang, 2015; Zhang et al., 2014). Multiple isomers were detected for two Br-DBPs ($\text{C}_6\text{H}_5\text{O}_4\text{Br}$, $\text{C}_8\text{H}_5\text{O}_5\text{Br}$) (Fig. A.7). Among the 553 detected Br-DBPs, isomers were detected for 204 (37%) of them. Such results indicate the wide occurrence of isomers of DBPs; however, relative abundances of isomers varied (Fig. A.7). Currently, regulated THMs or HAAs are simple molecules without isomers, and thus identification of isomers of DBPs has not received significant attention in previous studies.

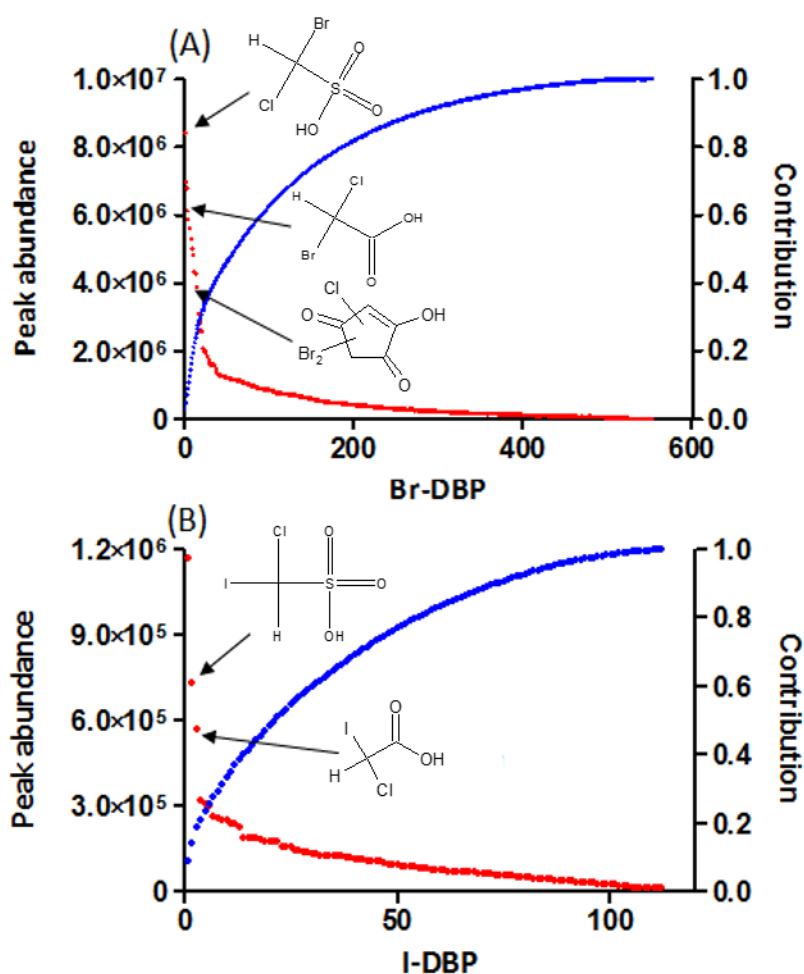


Fig. 2.3. Ion abundance (red) of (A) Br-DBPs and (B) I-DBPs and their cumulative contribution (blue) to total DBPs detected. Structures of several of the most abundant DBPs are shown for comparison.

To the best of our knowledge, these results provide the greatest number of Br-DBPs detected in plant-scale, chlorinated drinking waters. In other studies, a total of 478 Br-DBPs were detected in laboratory produced drinking water samples by FT-ICR MS (Zhang et al., 2014). Similarly, approximately 800 halogenated DBPs, dominated by Cl-DBPs, were observed in treated drinking water by FT-ICR MS (Gonsior et al., 2014). The chemometric strategy of FT-ICR MS is to use accurate mass, isotopic peaks and homologue models to identify DBPs. This approach is fundamentally different from the DIPIC-Frag method. The major advantages of the DIPIC-Frag method are transient scan speeds, compatibility with HPLC separation times, and the use of a DIA scanning mode. Thus, good specificity and sensitivity can be achieved for analysis of actual drinking waters. However, because of the somewhat poorer mass accuracy of Orbitrap

MS (standard derivation of mass error was 2.3 ppm determined in the present study) compared to FT-ICR MS (<1 ppm), the rate of false positives when assigning formulae might be greater for a given precursor ion. Thus, a combination of the DIPIC-Frag and FT-ICR MS methods in future studies may be appropriate. Indeed, as mentioned above, the library produced from FT-ICR MS methods has been incorporated into the DIPIC-Frag method in the present study to decrease the false discovery rate.

2.3.3 Library of I-DBPs in Chlorinated Water

After establishment of the Br-DBP library, untargeted detection of I-DBPs was conducted by using the homologue information from the Br-DBPs. With a peak response cutoff of 10,000, 112 unique I-DBPs were detected in samples of chlorinated water (Fig. 2.2B). Consistent with Br-DBPs, the greatest number of I-DBPs (69) was detected in chlorinated raw water extracted by WAX cartridge. This more than doubled the number of I-DBPs detected in conventionally treated water extracted by acidification methods (28 and 32 for C18_pH2 and HLB_pH2 cartridges, respectively). Similar to Br-DBPs, I-DBPs with high O/C ratios were specifically captured by WAX cartridges, such as $\text{CH}_2\text{SO}_3\text{ClI}$, which exhibited approximately a 10-fold greater abundance in WAX extracted samples (abundance 7.31×10^5) than in the HLB_pH2 samples (abundance 8.26×10^4). This observation could be driven by differences in the treatment processes during sampling events, as well as extraction efficiencies. Limited information is available for I-DBPs especially in samples of drinking water collected directly from a treatment plant (Gong and Zhang, 2015; Li et al., 2016). In fact, we report here the largest mass spectrometric library of I-DBPs currently available for chlorinated drinking water. The DIPIC-Frag method was demonstrated to be a robust method to detect unknown I-DBPs in chlorinated water with good sensitivity and specificity.

Variations in m/z values (195.9253 - 476.8304) and retention times (2.4-16.2 min) were also observed for I-DBPs, indicating their chemical diversity, with the number of incorporated iodine atoms in each compound being 1 or 2 (Fig. A.6B). Abundances of peaks associated with I-DBPs ranged from 10^4 to 1.17×10^6 (Fig. 2.3B), approximately 5-fold less than that of Br-DBPs (Fig. 2.3A). Lesser abundances of I-DBPs compared to Br-DBPs and Cl-DBPs have been widely documented in previous studies (Plewa et al., 2004b; Richardson et al., 2007; Richardson et al.,

2008). Simultaneous determinations of Br-DBPs and I-DBPs in chlorinated water provided an opportunity to compare relative abundances of these analogues for individual DBPs. A significant correlation ($r=0.61$, $p<0.001$) was observed between abundances of Br-DBPs and corresponding I-DBP analogues in water samples extracted by WAX cartridges. Despite the strong correlation, ratios of abundances of I-DBPs to Br-DBPs varied considerably (geometric mean \pm geometric standard deviation, 0.27 ± 3.5). The ratio of I to Br incorporated in a halogenated acetic acid ($C_2H_2O_2ClI$, 0.59 ± 0.23) was 2-fold greater than that of a sulfonic acid (CH_2SO_3ClI , 0.31 ± 0.06), and 10-fold greater than those of DBPs with aromatic rings (ratios were 0.10 ± 0.01 and 0.02 ± 0.005 for $C_9H_7O_5I$ and $C_8H_4O_5ClI$, respectively) (Fig. A.8). Such results indicate different reaction efficiencies with NOM to produce Br-DBPs and I-DBPs, but future studies are warranted to clarify exact mechanisms.

2.3.4 Minor Effects of Quenching Reagents on the Profile of DBPs

Quenching reagents are commonly added to chlorinated water samples to prevent additional reactions from occurring between residual chlorine and previously formed DBPs (Kristiana et al., 2014). The untargeted screening strategy used in this study provides an opportunity to investigate the potential impact of quenching reagents on the profile of DBPs. None of the 50 most abundant Br-DBPs or 10 most abundant I-DBPs were detected in raw water samples, trip blanks, the ultrapure water blank or ultrapure water samples treated with sodium hypochlorite. In preGAC waters, 25 high-abundant DBPs were detected and confirmed by their isotopic peaks in at least one sample (Fig. A.9). Ascorbic acid treated samples exhibited a profile of DBPs that was very similar to samples untreated by quenching reagents, without any significant impact on abundances of detected DBPs. This is not surprising, since drinking water samples were extracted by SPE cartridges within a few hours after sample collection in the present study. The residual chlorine (0.12 mg/L) (Table A.4) in collected samples was 10-fold lower than that typically found in chlorinated drinking waters (1.5 mg/L). The results indicate that low-level residual chlorine did not lead to significant increase of DBPs in short-term sample storage. Unexpectedly, samples treated with sodium thiosulfate showed a specific loss of detection for $C_5H_2O_3ClBr$ and $C_5HO_3ClBr_2$, whose structures were predicted to be unstable ketones as mentioned below (Section 2.3.6). While this is the first time to show that sodium

thiosulfate may cause decomposition of halo-hydroxy-cyclopentene-diones, these sulfur-based quenching reagents have been reported to cause decomposition of other DBPs, such as haloacetonitriles, chloropicrin, and chlorate (Boal and Patsalis, 2017; Munch and Hautman, 1995). These results indicate that fast extraction of drinking water without any quenching reagent (the present study) or quenching with ascorbic acid are the best approaches for untargeted comparative analysis of DBPs.

2.3.5 Comparative Analysis of DBPs

Compared to direct infusion FT-ICR MS methods, the DIPIC-Frag method might present challenges in analysis such as shorter peak times and potential column problems. However, one advantage of the DIPIC-Frag method is that coupling to HPLC separation should result in lesser matrix effects. Thus, semi-quantitative comparative analysis might be conducted as was done for sediments and house dust (Peng et al., 2016a; Peng et al., 2016c). To test this, the precision of three SPE methods with good chemical coverage (C18_pH2, HLB_pH2 and WAX) were determined by calculating the relative standard deviation (RSD) of individual DBPs among triplicate samples. While a few DBPs exhibited poor precision ($>30\%$), most DBPs exhibited sufficient precision ($<30\%$) using C18_pH2 (mean precision was 22.5% and 21.2% for Br-DBPs and I-DBPs) or WAX (mean precision was 18.8% and 19.1% for Br-DBPs and I-DBPs) for extraction (Fig. 2.4). Reproducibility was better when HLB_pH2 was used; the mean precision was 13.3% and 15.1% for all detected Br-DBPs and I-DBPs, respectively. Such precision was comparable to those of targeted methods for analyzing DBPs based on surrogate standards (precision was 10-12% for chlorinated nonylphenol) in drinking water (Fan et al., 2013), which encouraged us to use the DIPIC-Frag method for comparative analysis of DBPs among samples.

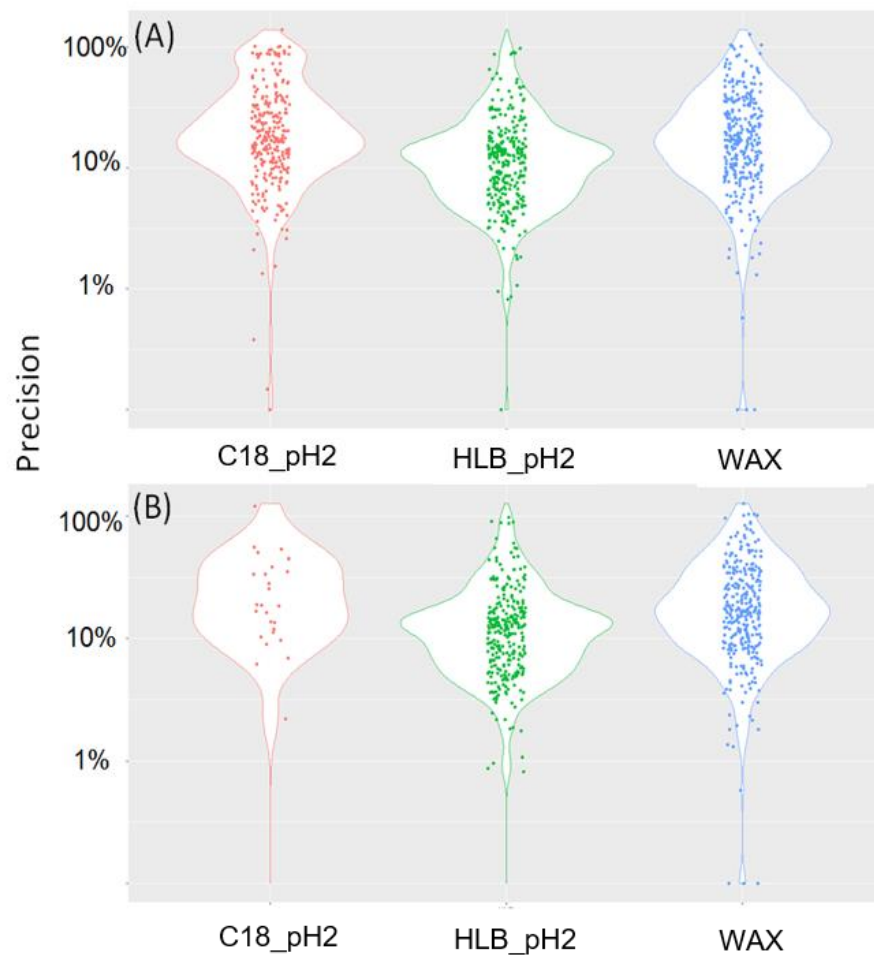


Fig. 2.4. Frequency distributions of method precision for (A) Br-DBPs and (B) I-DBPs shown as violin plots for the C18_pH2, HLB_pH2, and WAX sample pretreatment methods. Precision was calculated as relative standard deviation of each DBP to the mean value of abundances. Width of the violin indicates frequency at that precision.

Under HLB extraction methods, profiles of DBPs in water collected in October 2015 and April 2016 were compared. These samples differed by the season in which they were collected, but more importantly by the stage of treatment at which they were collected. Chlorinated raw water collected in October 2015 had not undergone treatments such as coagulation, unlike conventionally treated water collected in April 2016. Coagulation alters the profile of NOM in water with preferential removal of hydrophobic and high molecular molar mass compounds, which would change what precursors were present at the different points of chlorination (Matilainen et al., 2010). As expected, these samples exhibited unique profiles of Br-DBPs and I-

DBPs (Fig. 2.2). Water collected in April 2016 generally exhibited greater abundances of Br-DBPs (Fig. 2.2A). This observation is supported by the idea that the ratio of bromide ions to organic matter is one of the most important factors for determining concentrations of Br-DBP (Francis et al., 2010; Watson et al., 2014). Concentrations of bromide were 0.04 mg/L in both October and April, but at the point of chlorination there were differences in the parameter UV_{254} , which measures light absorbed by aromatic organic matter (0.1735 and 0.0729 cm^{-1} , respectively) (Conrad, 2017). Therefore, the ratio of bromide to organic matter was greater in April samples (Table A.3), thereby enhancing production of Br-DBPs. Additionally, some compound-specific shifts were observed: Br-DBPs with greater O/C ratios, *e.g.* $C_2H_2O_2ClBr$, CH_2O_3SClBr , $C_5HO_3Cl_2Br$, were detected with greater abundances in samples collected in April; but Br-DBPs with lesser O/C ratios, *e.g.* $C_9H_{10}O_3ClBr$, $C_8H_7O_3Br$, exhibited greater abundances in October (Fig. 2.2A).

In contrast to Br-DBPs, chlorinated raw water collected in October generally exhibited greater abundances of I-DBPs than did conventionally treated samples collected in April. This phenomenon was even more pronounced for I-DBPs with lesser O/C ratios, *e.g.* $C_8H_7O_3I$, while some I-DBPs with greater O/C ratios (*e.g.* CH_2O_3SClI , CH_3O_3SI) still showed greater abundances in samples collected in April. Again, we can attempt to explain these observations by investigating differences in the treatment processes. The longer chlorine contact time in April, 190 min compared to 49 min in October, could have resulted in conversion of generated I-DBPs to their chlorinated or brominated analogues, as was observed in samples of simulated drinking water (Conrad, 2017; Zhu and Zhang, 2016). Concepts such as this support the findings of this study and further validate the application of the DIPIC-Frag method for comparisons of DBPs in spatially and temporally unique water samples. Due to the different collection points between our October and April samples, a more systematic understanding of seasonal changes of Br-DBPs and I-DBPs in chlorinated waters is warranted in future studies.

2.3.6 Proposed Chemical Structures of High Abundance DBPs

Despite variations in abundances of Br-DBPs, a limited number of high-abundance DBPs were detected with peak abundances greater than 10^6 . In fact, of the 553 Br-DBPs, the 50 most abundance Br-DBPs contributed 45.3% of the total abundance, and the 100 most abundant Br-

DBPs contributed 62.5% of the total abundance (Fig. 2.3A). This indicated that, within the specific analytical window of negative mode ESI, it is possible to establish a relatively short list of Br-DBPs to become the focus of future research efforts.

One advantage of the DIPIC-Frag method, is the ability to simultaneously acquire high-resolution MS¹ and MS² spectra, with narrow DIA isolation window and chromatographic information recorded. This provides an opportunity to retrospectively evaluate MS² spectra and predict potential structures. Due to the relatively small molecular mass ($m/z < 400$) of the more abundant Br-DBPs, the number of possible chemical structures is limited for most. By combining fragment patterns and possible structures searched from public databases (*e.g.*, ChempSpider), structures for 40 of the 50 most abundant Br-DBPs were predicted (Table A.1). Many of the Br-DBPs are acidic, or methoxylated compounds and neutral loss of CO₂ or CH₄O provided abundant information for use in predicting structures (Fig. 2.5). As an example, the 3rd most abundant Br-DBP whose formula was predicted to be C₅H₃O₃Cl₂Br, has also been detected by FT-ICR MS, but the exact chemical structure could not be predicted using the MS¹ spectrum only (Gonsior et al., 2014). Further evaluation of the MS² spectra collected during application of the DIPIC-Frag method demonstrated loss of CO, which indicated that a ketone moiety was contained in the molecule and thus, a dione compound was concluded to be the only possible structure (Fig. 2.5A). This compound, C₅H₃O₃Cl₂Br, has also been detected in simulated and real drinking water samples by UPLC/ESI-triple quadrupole MS, and confirmed as a trihalo-hydroxycyclopentene-dione (trihalo-HCD) (Pan et al., 2016a; Zhai & Zhang, 2011).

Among the 40 Br-DBPs with predicted structures, 17 were aromatic acids or phenols (Table A.1 and Fig. 2.5B-C), representing the largest class of abundant Br-DBPs. This result is consistent with results of FT-ICR MS (Gonsior et al., 2014). Considering similarities of structures of these DBPs to those of lignin phenols, the most abundant plant component and one of the major precursors for DBPs, future studies are warranted to clarify the exact contribution of lignin phenols to DBPs (Hua et al., 2014). A novel class of methoxylated DBPs were also detected with characteristic loss of CH₄O (Fig. 2.5C). These compounds typically showed low O/C ratios (*e.g.*, C₉H₁₀O₃ClBr) compared to acidic compounds (*e.g.*, C₈H₅O₅Br), and showed distinct seasonal changes compared to other DBPs, as previously discussed (Section 2.3.5).

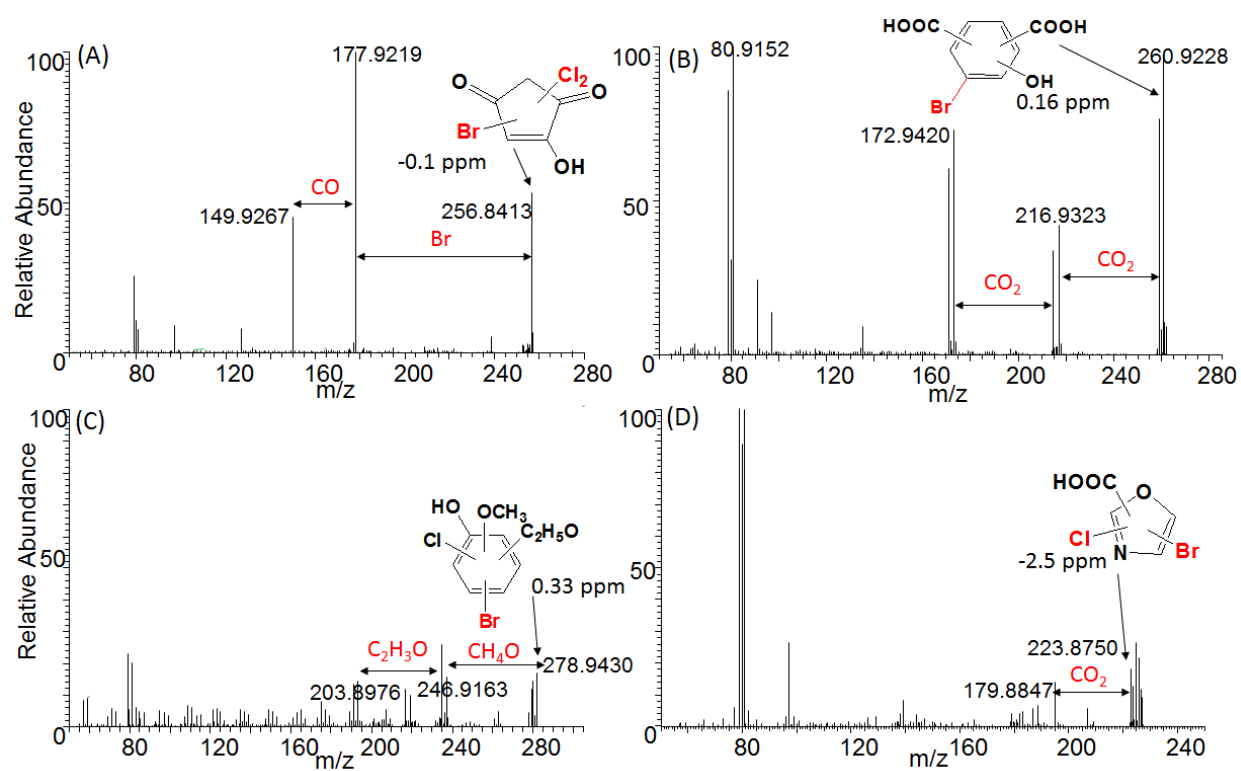


Fig. 2.5. Prediction of four typical Br-DBPs using high-resolution MS² spectra. The red formulae indicate the expected loss. Positions of bromine, chlorine, carboxylic acid or hydroxyl groups in compounds could not be exactly predicted.

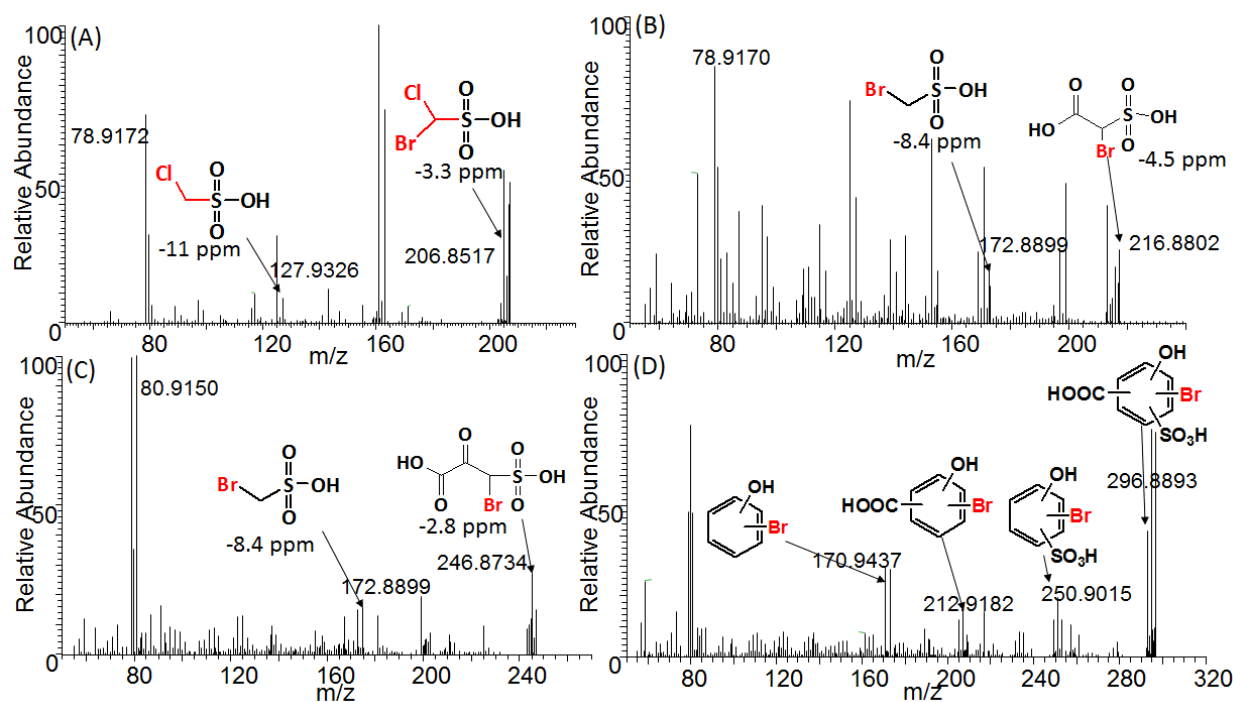


Fig. 2.6. MS² spectra for the detected class of high abundance sulfonic acid DBPs. The position of bromine, sulfonic acid, carboxylic acid or hydroxyl groups in compounds from panel B-D could not be exactly predicted.

Seven high-abundance Br-DBPs were predicted to contain nitrogen or sulfur (Table A.1 and Fig. 2.5D). For the most abundant Br-DBP, whose formula was predicted to be CH₂SO₃ClBr, the only plausible structure was predicted as a halogenated methanesulfonic acid (Fig. 2.6A). Several sulfonic acid DBPs were detected in our study (Fig. 2.6), but bromomethanesulfonic acid (CH₃SO₃Br) was the only compound for which an authentic standard was available for validation. Retention times were consistent between the authentic standard and the putative compound recovered from chlorinated water samples (Fig. A.10). The retention time of bromomethanesulfonic acid was also consistent with the corresponding chlorinated analogue bromochloromethanesulfonic acid (CH₂SO₃ClBr); the retention time of a compound on an Amide column is mainly determined by functional groups rather than halogen atoms. The detection of halogenated sulfonic acids as DBPs in this study supports previous work conducted on European drinking water by Zahn et al. (2016). However, there are still uncertainties with regards to what precursors could be converted to sulfur-containing DBPs. Considering the similar structures, it is possible that algal and bacterial metabolites such as

dimethyl sulfide or the release of compounds such as methanethiol from decaying plant matter could be involved but no data is available to support this yet (Bechard and Rayburn, 1979; Bentley and Chasteen, 2004; Lomans et al., 2001; Yoch, 2002). Several abundant, nitrogen-containing Br-DBPs were also detected, including C_4HNO_3ClBr , the structure of which was predicted to be an oxazole carboxylic acid (Fig. 2.5D). Several classes of nitrogen-containing DBPs (N-DBPs) including halonitriles and haloamides have been observed previously in drinking water but these structures are different from the N-DBPs detected in the present study (Muellner et al., 2007; Plewa et al., 2004a; Plewa et al., 2008; Shah & Mitch, 2012). These sulfur- or nitrogen-containing DBPs have not been observed in previous untargeted screening studies using FT-ICR MS, further indicating the complementary advantages of the FT-ICR and the DIPIC-Frag methods (Gonsior et al., 2014; Zhang et al., 2012; Zhang et al., 2014). Since N and S containing DBPs have been suggested to exhibit greater toxicity than purely carbonaceous DBPs (C-DBPs), the novel heteroatomic DBPs detected at relatively great abundances in the present study should be further investigated for potential toxicities (Muellner et al., 2007).

The lesser abundance of the I-DBPs made it challenging to obtain “clean” fragment patterns and, hence, prediction of structures for these compounds was difficult. Structures of I-DBPs were only predicted for the 10 most abundant compounds, with 9 of them being successfully assigned (Table A.2). Aromatic acids or phenols were the largest class of I-DBPs (Table A.2), and analogues of several Br-DBPs (*e.g.*, aromatic acid, $C_9H_7O_5I$) were detected. A recent study also reported the occurrence of iodinated aromatic phenols/acids during cooking with drinking water and iodized table salt (Pan et al., 2016b). Consistent with Br-DBPs, two sulfonic acid I-DBPs were also detected with relatively great abundances.

2.4 Conclusions

Identification of unknown Br- and I-DBPs in drinking waters is of importance because they often exhibit greater toxic potencies than do Cl-DBPs, yet a large proportion remain unidentified by traditional analytical methods. In this study:

- The DIPIC-Frag method exhibited sufficient sensitivity, specificity and reproducibility for detection of low abundant Br- and I-DBPs in plant-scale chlorinated drinking water.
- The largest mass spectrometric library of Br-DBPs and I-DBPs in plant-scale chlorinated

water was established, with 553 and 112 compounds detected, respectively.

- The 50 most abundant Br-DBPs contributed to almost half of the estimated total peak abundance of Br-DBPs, and chemical structures for 40 of these DBPs were predicted.
- The following analytical parameters are recommended for untargeted screening of DBPs: HLB_pH2 extraction method, Amide LC column, ESI ionization source, and either no quenching reagent or the use of ascorbic acid over sodium thiosulfate.

If combined with toxicity assays, this data provides the possibility to prioritize a relatively short list of Br-DBPs for water treatment quality management. Complementary advantages of the DIPIC-Frag method compared to previous FT-ICR MS method indicate that combination of these methods in future studies might further enhance the specificity of untargeted screening of DBPs. Application of the DIPIC-Frag method for comparative analysis of the fates of these unregulated DBPs in treatment processes and in response to seasonal changes in future studies are of interest, as is toxicological assessment.

2.5 Supporting Information

The supporting information provides text and figures addressing (1) chemicals and reagents; (2) the water treatment process; (3) LC-Q Exactive data acquisition; (4) chemometric analysis; (5) predicted chemical structures of the top 50 Br-DBPs; (6) predicted chemical structures of the top 10 I-DBPs; (7) raw water parameters and treatment conditions at the times and locations of water sample collection; (8) concentrations of free and total chlorine in samples collected for the quench study; (9) schematic workflow of the homologue models; (10) chromatograms of Br-DBPs with ESI or APCI ionization sources; (11) chromatograms of Br-DBPs on C18 or Amide columns; (12) chromatograms of Br-DBPs with different SPE methods; (13) plot of detected DBPs; (14) chromatograms of isomers of Br-DBPs; (15) detection of DBPs in the quench study; (16) the ratios of I-DBPs to corresponding Br-DBPs; (17) chromatograms of halogenated sulfonic acids.

2.6 Acknowledgements

This work was supported by a Discovery Grant from the Natural Science and Engineering Research Council of Canada [Project # 326415-07] and a grant from the Western Economic Diversification Canada [Projects # 6578, 6807 and 000012711]. Prof. Giesy was supported by the Canada Research Chair program, and the 2014 "High Level Foreign Experts" [#GDT20143200016] program, funded by the State Administration of Foreign Experts Affairs, the P.R. China to Nanjing University, and the Einstein Professor Program of the Chinese Academy of Sciences and a Distinguished Visiting Professorship in the School of Biological Sciences of the University of Hong Kong.

CHAPTER 3

MONTHLY VARIATIONS OF UNREGULATED BROMINATED DISINFECTION BY-PRODUCTS ARE PRIMARILY ASSOCIATED WITH TOTAL BROMINE IN CHLORINATED WATER

Christena Watts, Paul D. Jones, John P. Giesy, Hui Peng

Chapter 3 was formatted for submission to *Environmental Science & Technology* and will be submitted pending acceptance of Chapter 2 to *Water Research*. Author contributions are as follows:

Christena Watts (University of Saskatchewan) was responsible for collection of water samples, chemical extractions, data analysis, and writing of the manuscript.

Paul D. Jones and John P. Giesy (both University of Saskatchewan) provided scientific input and guidance, edited the manuscript, and secured funding for the research.

Hui Peng (University of Toronto) provided guidance in the laboratory, operated the analytical method for Br-DBP characterization, and contributed to creating the manuscript.

ABSTRACT

Numerous disinfection by-products (DBPs) form during chlorination of drinking water, but limited information exists on the seasonal trends of unregulated DBPs, particularly brominated DBPs (Br-DBPs). In this year-long study, monthly samples of raw, clearwell, and finished water were collected from a treatment plant in Saskatchewan, Canada. Fates of the 54 most abundant, unregulated Br-DBPs, determined from full-spectrum UHRMS analyses, were investigated. While abundances of most Br-DBPs increased between clearwell and finished stages, some Br-DBPs showed unexpected decreases significantly related to their chemical properties of low O/C and Br/C ratios. Occurrences of most Br-DBPs were positively correlated, indicating similar monthly trends, but monthly variations could not be significantly explained by parameters of raw water (e.g. turbidity, natural organic matter (NOM), temperature, bromine (Br)). A major finding that total concentrations of Br in finished water (0.04-0.12 mg/L) were significantly greater than in raw water (0.013-0.038 mg/L, $p < 0.001$) are suggestive of introduction of Br during disinfection. Total concentrations of Br in treatment units, instead of raw water, were significantly correlated to 34 Br-DBPs at $\alpha=0.05$, and 14 Br-DBPs at $\alpha=0.001$. This study provided the first evidence that monthly trends of unregulated DBPs were mainly associated with total concentrations of Br in treated waters.

Keywords: drinking water treatment; hypobromous acid; natural organic matter; bromine; chlorination

3.1 Introduction

Disinfection by-products (DBPs) form during treatment of drinking water when chlorine disinfectants, in the form of hypochlorous acid, react with natural organic matter (NOM) to produce a diverse profile of chlorinated compounds (Cl-DBPs). Hypochlorous acid (HOCl) also reacts with bromide found in source water to produce hypobromous acid (HOBr), which can react with NOM or Cl-DBPs to produce brominated disinfection by-products (Br-DBPs) (Richardson et al., 2007, 1999; Yang et al., 2014). Occurrence of DBPs in drinking water is ubiquitous around the globe, with particular focus in research paid to the four regulated trihalomethanes (THMs) and five regulated haloacetic acids (HAAs). These regulated DBPs are reported to induce cytotoxicity and genotoxicity in bench-scale experiments, and have been linked to elevated risks of bladder cancer and adverse pregnancy outcomes in epidemiological studies (Bull et al., 2011; Jeong et al., 2012; Michael J. Plewa et al., 2004; Richardson et al., 2007). Unregulated DBPs often show greater toxicities than THMs and HAAs, and a common trend has emerged that Br-DBPs are more toxic than Cl-DBP analogues (Li et al., 2016; Muellner et al., 2007; Plewa et al., 2008; Richardson et al., 2007; Yang and Zhang, 2013; Zhang et al., 2000). However, a large number of unregulated Br-DBPs remain uncharacterized due to their small abundances, chemical diversity, and lack of available authentic standards.

Ultrahigh-resolution mass spectrometry (UHRMS) provides a promising strategy to characterize previously unknown Br-DBPs. For example, direct infusion and Fourier transform ion cyclotron resonance mass spectrometry (FT-ICR MS) were used to detect more than 500 Br-DBPs in laboratory produced, chlorinated water and to confirm the existence of numerous, unregulated Br-DBPs in real samples of drinking water (Gonsior et al., 2014; Zhang et al., 2014). A data-independent precursor isolation and characteristic fragment (DIPIC-Frag) method was recently adapted to screen drinking water for unregulated Br-DBPs. That method was used to establish the largest library of 553 Br-DBPs detected in plant-scale chlorinated drinking water (Chapter 2). Due to compatibility with HPLC, the DIPIC-Frag method showed enhanced reproducibility and lesser matrix effects compared to direct infusion, which enabled comparative analysis of Br-DBPs in drinking waters collected at different time points.

Seasonal variations of regulated DBPs have been well documented in previous studies and several factors have been considered to affect seasonal trends. Most often, formation of

THMs has been reported to be favoured in summer due to warmer temperatures, increased reaction rates, and increased production of organic precursors by algae (Domínguez-Tello et al., 2015; Kim, 2009; Richardson et al., 2003; Rodriguez and Sérodes, 2001; Serrano et al., 2015). Other reports indicated that THMs and HAAs are more abundant in spring and fall when concentrations of dissolved organic carbon (DOC) are greatest (Chen et al., 2008; Uyak et al., 2008). Limited studies are available on seasonal variations of unregulated DBPs, in particular unregulated Br-DBPs. One study found that concentrations of bromochloroacetonitrile and dibromoacetonitrile were greater in winter (Mercier Shanks et al., 2013), while in contrast, another study reported greater occurrence of bromochloroacetonitrile in spring and autumn due to elevated concentrations of bromide (Serrano et al., 2015). With limited studies and conflicting findings such as these, there are still many gaps in understanding regarding what seasonal trends exist for unregulated Br-DBPs and what variables drive their formation.

The main objectives of this study were to explore monthly trends of unregulated Br-DBPs at a drinking water treatment plant (DWTP) in Saskatchewan, Canada and to identify factors that could predict their occurrence. To do this: 1) the DIPIC-Frag, UHRMS method was applied to screen unregulated Br-DBPs in samples of raw, clearwell, and fully treated samples of water collected over one year; 2) monthly trends of the most abundant Br-DBPs were investigated by comparing peak abundances through the treatment process as well as over time; and 3) correlation analysis was used to identify factors, such as bromine (Br), temperature, and UV₂₅₄ that could be driving the monthly trends of unregulated Br-DBPs.

3.2 Materials and Methods

3.2.1 Chemicals and Reagents

Oasis® HLB (500 mg, 6 cc) cartridges were purchased from Waters (Milford, MA, USA). Hydrochloric acid, ammonium hydroxide, and pH indicator strips (ColorpHast pH 0-6) as well as dichloromethane (DCM), methanol, and acetonitrile, Omni-Solv grade, were purchased from EMD Chemicals (Gibbstown, NJ, USA). G4 glass fibre filter circles were purchased from Fisher Scientific (Nepean, ON, Canada).

3.2.2 Collection of Water

Water was collected from a DWTP located in central Saskatchewan, Canada. Details of the treatment process can be found in the SI. Briefly, water undergoes treatment with potassium permanganate, coagulation, flocculation, a small dosage of chlorine gas (Cl_2) (pre-chlorine dose, ~ 0.4 mg/L), and silica sand/anthracite filtration. Then water is treated with UV irradiation followed by a second and greater dose of chlorine gas (post-chlorine dose, ~ 2.0 mg/L), which serves as the primary disinfection stage before water travels to the reservoir. Samples in this study were collected at the raw water intake (raw), just after UV irradiation before the post-chlorine dosage (clearwell), and at the fully treated stage after addition of the post-chlorine dose (finished). Water samples were collected in 4-L headspace-free, amber bottles that were previously rinsed with ultrapure water and methanol. Extractions were started within 4 hours of collection to minimize the loss of DBPs and effect of residual chlorine. No quenching reagent was added based on results from previous investigation that certain quenching reagents may lead to loss of some unregulated DBPs (Section 2.3.4).

Sampling began April 19, 2016, twelve days after the river ice broke, and continued on a monthly schedule until March 8, 2017. On July 21, 2016 an oil pipeline just over 300 km upstream of the DWTP ruptured and leaked 225,000 L of oil, with 40% of that reaching the North Saskatchewan River (Government of Saskatchewan, 2016). In response, the DWTP began withdrawing water from different sources and this interrupted sampling until September 2016, therefore, there is no data for August 2016. Following this date, supplementary quality controls were installed at the DWTP which provided additional data for September – March to be used in correlation analyses.

3.2.3 Sample Extraction

Based on a previously developed method (Chapter 2), samples of water were adjusted to pH 2 with 1 M hydrochloric acid and extracted by Oasis HLB cartridge for the best chemical coverage and reproducibility. Raw water samples required filtration with a G4 glass fibre filter prior to solid phase extraction. After pre-conditioning HLB cartridges with DCM, methanol, and ultrapure water, 1 L of samples were passed through the cartridges at a flow rate of 5-10 ml/min.

Cartridges were dried under a gentle flow of nitrogen and DBPs were eluted with 5 ml of methanol and 5 ml of DCM. Extracts were dried under a stream of nitrogen, reconstituted in 500 µl of methanol, and centrifuged (6000 rpm for 10 min) prior to instrumental analysis.

3.2.4 Quality Assurance and Control

Details are provided in Supporting Information.

3.2.5 Characterization of Br-DBPs by UHRMS

Aliquots of samples were analyzed for Br-DBPs by use of a Q ExactiveTM UHRMS (negative ion mode) equipped with a DionexTM UltiMateTM 3000 UHPLC system (Thermo Fisher Scientific). Based on method optimization (Chapter 2), a TSKgel Amide-80 column (4.6 mm ID x 15 cm, 3 µm) and electrospray ionization (ESI) were used. Ultrapure water containing 0.1% NH₄OH (A) and acetonitrile containing 0.1% NH₄OH (B) were used as mobile phases. Initially 95% of B was decreased to 90% over 18 min, then decreased to 30% over 8 min, followed by an increase back to 95% of B held for 3 min. Flow rate was 0.40 mL/min and temperatures of the column and sample compartments were maintained at 30 °C and 10 °C, respectively. Mass spectrometric settings for ESI (-) mode were: spray voltage, 2.8 kV; capillary temperature, 300 °C; sheath gas, 35 L/h; auxiliary gas, 8 L/h; and probe heater temperature, 325 °C. To avoid shifts in instrument sensitivity, extracts of samples from different months were analyzed at the same time. Details of instrument settings were described in our previous studies.

Using a library of 553 unregulated Br-DBPs established previously by use of full-spectrum analyses (Chapter 2), the 54 most abundant Br-DBPs detected at the DWTP in this study were selected for further investigation. Temporal trends as well as trends of Br-DBPs through the treatment process were investigated using the statistical software R (version 3.1.2; <http://www.R-project.org>; R Foundation for Statistical Computing, Vienna, Austria). It should be noted that absolute peak abundances were used for comparative statistical analysis, a strategy well documented in previous metabolomics studies, since authentic standards were not available for most of unregulated Br-DBPs.

3.2.6 Characterization of Natural Organic Matter by UHRMS

Aliquots of extracts were diluted with methanol to a concentration factor of 200x and analyzed for NOM by direct injection on a Q ExactiveTM HF Hybrid Quadrupole-OrbitrapTM mass spectrometer (Thermo Fisher Scientific). The data were collected at a resolution of 240,000 FWHM. Methods were modified from those outlined by Wang *et al.* (2017). Briefly, samples were injected at 3 μ l/min and data acquired in DIA mode for three minutes after signal stabilization. A scan range of 150-1000 m/z was used. Mass spectrometric settings for ESI (-) mode were: spray voltage, 3.0 kV; capillary temperature, 275 $^{\circ}$ C; sheath gas, 5 L/h; and AGC target, 2e5. Formulae were predicted based on the constraints of 0-200 12 C, 0-500 1 H, 0-60 16 O, 0-3 14 N₀₋₃, 0-2 32 S, and 0-1 13 C atoms.

Limitations exist in the characterization of NOM because extraction methods were optimized for DBPs. While enrichment of NOM by SPE cartridges under strongly acidic conditions (pH 2) is quite common, extraction efficiencies are reported to be low, particularly for nitrogenous and more polar compounds (Lavonen *et al.*, 2013; Reemtsma, 2009; Wang *et al.*, 2017; Zhang *et al.*, 2012a). HLB cartridges exhibit enhanced retention of both polar and nonpolar compounds compared to C18 cartridges, but it is understood that some compounds of NOM may not have been extracted by this method and therefore not characterized. As negative mode ESI was used, it is also possible that basic, nitrogen-containing NOMs were not efficiently ionized (Lavonen *et al.*, 2013).

3.2.7 Data Analyses

Correlation analysis was used to identify factors that could be used to predict occurrences of 54 unregulated Br-DBPs in finished water based on their measured peak abundances. Analyses were performed with eleven monthly measures of raw water parameters (temperature, turbidity, UV transmittance (UVT), colour, river level), treatment conditions (pre- and post-chlorine doses), and total concentrations of Br at the raw, clearwell, and finished stages of treatment. Seven monthly measures (September – March) of total organic carbon (TOC), absorbance at UV₂₅₄, and normalized specific absorbance (SUVA; UV₂₅₄/DOC) of raw water were available. Reported values can be found in Table B.1. The DWTP provided the above

information with the exception of measures of total concentrations of Br, which were analyzed by inductively coupled plasma mass spectrometry (ICP-MS) at the Environmental Analytical Laboratories of the Saskatchewan Research Council.

3.3 Results and Discussion

3.3.1 Occurrences of Unregulated Br-DBPs

The 54 most abundant, unregulated Br-DBPs were selected from the Br-DBP library established by our recent full-spectrum screening study (Chapter 2), for further investigations in the present study. These prioritized Br-DBPs were selected because they contributed more than half of the total peak abundance of all Br-DBPs and were detected relatively frequently (>90%) for effective statistical analysis. The selected Br-DBPs showed broad chemical diversity and, consistent with other studies, included sulfonated DBPs ($\text{CH}_2\text{O}_3\text{SClBr}$), halo-hydroxy-cyclopentene-diones (halo-HCDs; $\text{C}_5\text{HO}_3\text{Cl}_2\text{Br}$ and $\text{C}_5\text{HO}_3\text{ClBr}_2$), and halo-hydroxybenzoic acids ($\text{C}_7\text{H}_4\text{O}_3\text{ClBr}$ and $\text{C}_7\text{H}_4\text{O}_3\text{Br}_2$) (Gonsior et al., 2014; Pan et al., 2016a; Pan and Zhang, 2013; Zahn et al., 2016). The detection of high abundance, sulfur-containing DBPs is of concern since heteroatomic DBPs were suggested to have stronger toxicities. Consistent with other studies, carboxylic and phenolic aromatic compounds ($\text{C}_8\text{H}_5\text{O}_5\text{Br}$ and $\text{C}_7\text{H}_7\text{O}_6\text{Br}$) were also detected at high abundance (Gonsior et al., 2014). Bromochloroacetic acid ($\text{C}_2\text{H}_2\text{O}_2\text{ClBr}$), which is not included in the five HAAs currently regulated by the U.S. Environmental Protection Agency, was additionally included due to its high detection frequency.

Only two of the selected Br-DBPs (2/54, 3.7%) were detected in raw water with low frequencies (1/11, 9.1%), while 53 of the 54 Br-DBPs (98.1%) were detected in finished waters (Table B.2). These results confirmed that selected Br-DBPs were primarily produced during the disinfection process. Notably, 52 of 54 (96.3%) Br-DBPs were detected in clearwell waters, even though only relatively low pre-chlorination dosages are applied prior to the clearwell (0.46 ± 0.17 mg/L, compared to 2.0 ± 0.23 mg/L as the post-chlorine dose). This is consistent with results of a previous study, in which THMs, bromo-acids, and other halogenated DBPs were also detected after the pre-chlorination stage of treatment at a DWTP in Israel (Richardson et al., 2003). Detection of most Br-DBPs in clearwell water indicated effective formation of Br-DBPs

even at low chlorination dosage. Peak abundances for these 54 Br-DBPs showed large variation with several orders of magnitude difference, ranging from not detected to 1.64×10^7 in clearwell water and from not detected to 1.24×10^7 in finished water (Table B.2).

A Spearman's correlation matrix was used to explore co-occurrences of Br-DBPs based on peak abundances detected in clearwell and finished waters over the year (Fig. 3.1A). Most relationships were positive, which indicated similar trends through the treatment process and/or similar monthly trends for unregulated Br-DBPs. Positive correlations were still observed when only finished waters were included in analysis (Fig. B.1), albeit with weaker significance partly due to smaller sample size. Three clusters of correlated Br-DBPs were identified based on the correlation matrix (Fig. 3.1A). Isomers and structural analogues often fell into the same cluster. In the blue square were two trihalo-HCDs ($C_5HO_3Cl_2Br$ and $C_5HO_3ClBr_2$) as well as two dihalo-HCDs with the formula $C_5H_2O_3ClBr$. A significantly positive relationship ($R^2 = 0.95$, $p = 1.89 \times 10^{-14}$) was observed between $C_5HO_3Cl_2Br$ and $C_5HO_3ClBr_2$ (Fig. 3.1B). In the red square were four dihalo-hydroxybenzoic acids, two with the formula $C_7H_4O_3ClBr$ and two with the formula $C_7H_4O_3Br_2$ ($R^2 = 0.78 - 0.99$, $p = 1.27 \times 10^{-8} - < 2.20 \times 10^{-16}$) (Fig. B.2). The observation of strong positive relationships between analogues was not surprising since analogues generally form via the same reaction route and precursor compounds (Pan et al., 2017; Pan and Zhang, 2013; Zahn et al., 2016). Also in the red square were 7 of the 10 selected sulfur-containing DBPs with R^2 values ranging from 0.11 – 0.99 ($p = 0.14 - < 2.2 \times 10^{-16}$) (Table B.3). Limited information is available on formation mechanisms and precursor compounds of sulfur-containing DBPs. The positive relations found here indicate that they might form from common precursor compounds, and further studies to identify precursor compounds of sulfur-containing DBPs is warranted.

Unexpectedly, negative correlations were observed between some Br-DBPs as denoted by black rectangles in Fig. 3.1A. An example is shown in Fig. 3.1C between $C_7H_7O_6Br$ and $C_7H_4O_3ClBr$ ($R^2 = 0.10$, slope = -0.16, $p = 0.16$). Further investigation of the relationship showed that the negative trend was driven by the low abundance of $C_7H_7O_6Br$ in clearwell water and low abundance of $C_7H_4O_3ClBr$ in finished water (Fig. 3.1C). These results indicated that some Br-DBPs, e.g., $C_7H_4O_3ClBr$, degraded from clearwell to finished water.

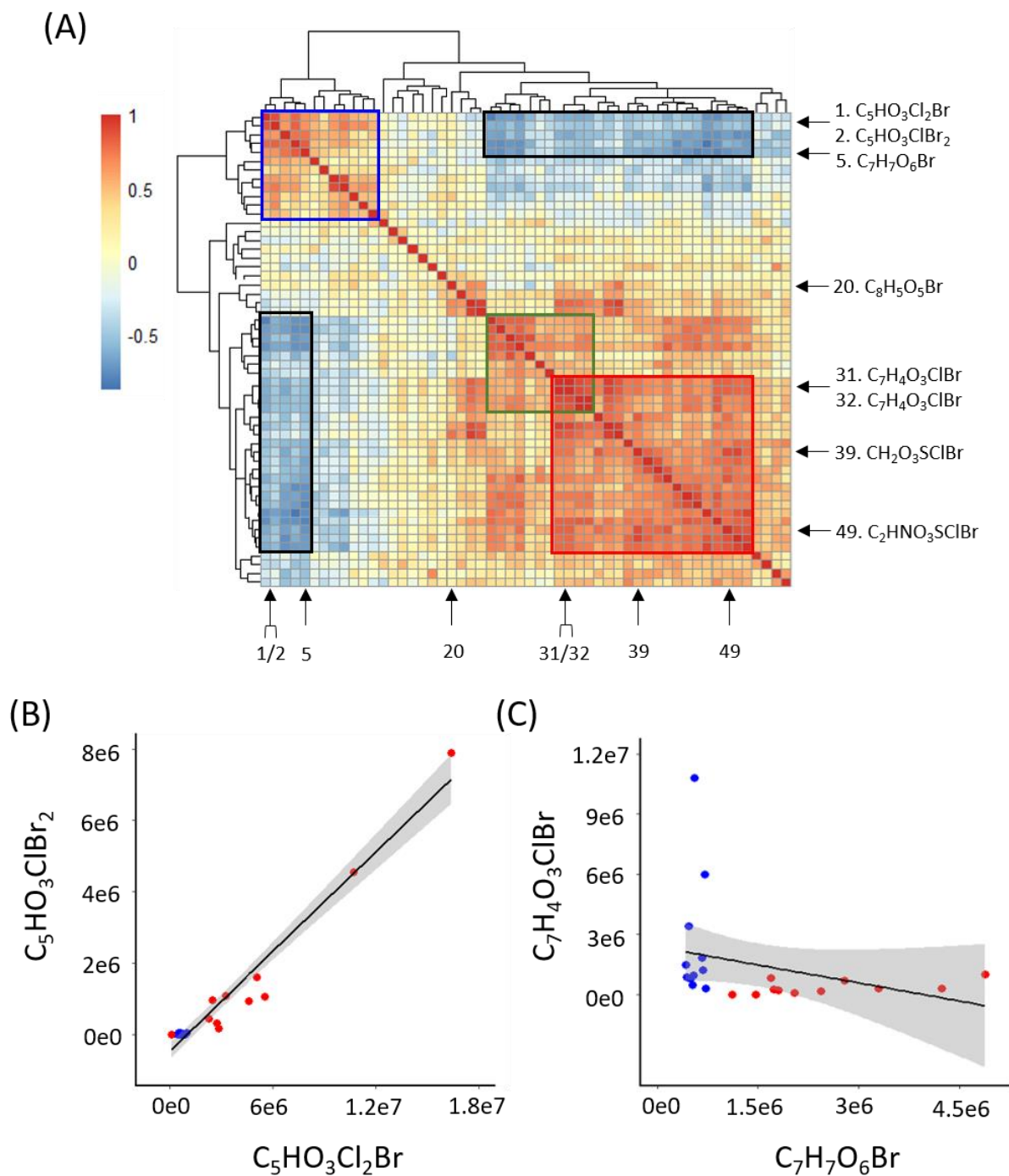


Fig. 3.1. (A) Spearman's correlation matrix based on ion abundances of 54 Br-DBPs detected in clearwell and finished water at 11 monthly time points ($n=22$). Representative compounds are indicated and a full list can be found in Table B.4. Examples are shown for (B) a strong positive correlation found between two trihalo-HCDs analogues and (C) a negative correlation found between $C_7H_7O_6Br$ and $C_7H_4O_3ClBr$. Red points represent ion abundances detected in clearwell water and blue points represent ion abundance detected in finished water, with 95% confidence intervals indicated in grey.

3.3.2 Fates of Br-DBPs are related to Chemical Properties

To further understand the fates of Br-DBPs between clearwell and finished water, soft clustering analysis was used and three general trends of Br-DBPs were identified through the treatment process (Fig. 3.2A). Cluster I Br-DBPs, such as $C_5HO_3Cl_2Br$, saw a large increase in abundance from raw to clearwell water, but a decrease in finished water. Cluster II Br-DBPs, exemplified by $C_8H_5O_5Br$, increased greatly from raw to clearwell water and then continued to increase in finished water at a lesser rate. The majority of investigated Br-DBPs (33/54), including all sulfur-containing Br-DBPs, were classified as cluster III which saw a modest increase from raw to clearwell water followed by a large increase in finished water. The decrease of cluster I but increase of cluster II and III Br-DBPs in finished water, indicated that cluster I Br-DBPs could possibly be converted to downstream DBPs (clusters II and III) in finished water with greater chlorine dosage. Identification of these different trends supports the dynamic vision model described by Li and Mitch (2018) in which the percent contribution of DBPs to total organic halide shifts as water interacts with chlorine for longer contact times and moves through treatment processes and distribution systems.

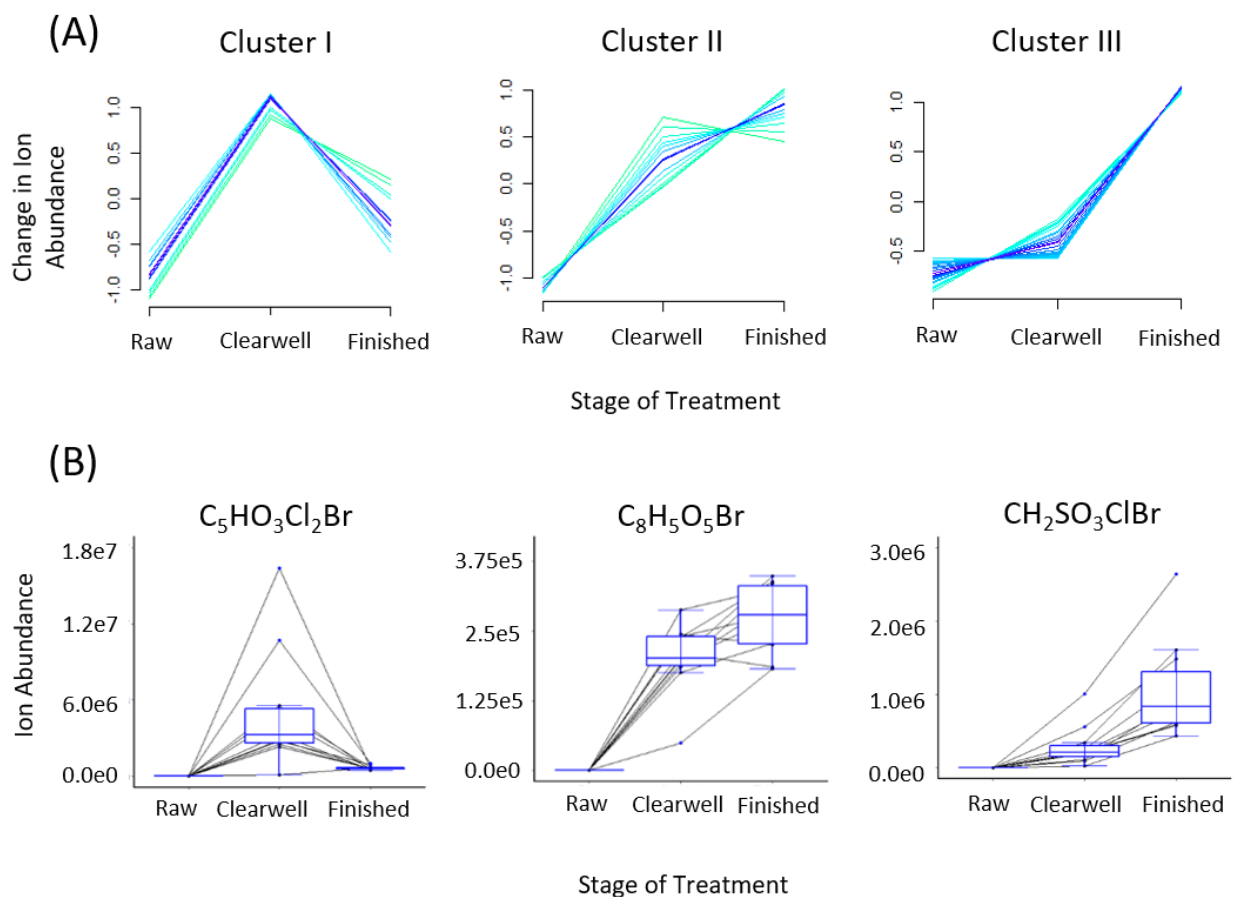


Fig. 3.2. (A) Three trends identified for Br-DBPs detected through the drinking water treatment process. Each coloured line represents one of 54 unregulated Br-DBPs. (B) Representative compounds are shown for each of the three clusters defined in (A). Data from eleven months is included to illustrate that trends were consistent through the year.

The chemical diversity of unregulated Br-DBPs provides a unique chance to investigate potential effects of chemical properties on their formation dynamics across treatment stages. While no significant differences were observed between molecular weights, number of carbon, or number of Br for Br-DBPs of each cluster, there were significant differences in Br/C and O/C ratios. The ratio of Br/C in cluster III Br-DBPs was greater compared to cluster I and II ($p=0.02$) Br-DBPs (Fig. B.3A), and compared to cluster I, Br-DBPs in cluster II and III had greater ratios of O/C ($p = 0.01$ and 0.06 , respectively) (Fig. B.3B). Because chlorination is an oxidative disinfection process, it is expected that DBPs contain more oxygen and halogen atoms than their

precursor compounds. The observations that cluster II and cluster III Br-DBPs have greater Br/C and O/C ratios make it possible that cluster I Br-DBPs could be converted to cluster II or III Br-DBPs at post-chlorination. For example, the average abundance of the trihalo-HCD $C_5HO_3Cl_2Br$ decreased from 5.1×10^6 in clearwell water to 6.6×10^5 in finished water (Fig. 3.2B; $p < 0.01$). Results of previous studies have shown that trihalo-HCDs form rapidly upon chlorination and then degrade to lower molecular weight DBPs such as THMs or HAAs with increased chlorine contact time, which is supported here by classification of $C_5HO_3Cl_2Br$ as cluster I (Zhai et al., 2014; Zhai and Zhang, 2011). Notably, all 10 sulfur-containing Br-DBPs (e.g. CH_2SO_3ClBr) were grouped in cluster III, indicating their persistence during disinfection. Thus, our study confirmed in actual drinking water samples that Br-DBPs may exhibit different reaction dynamics which are closely related to their chemical properties.

3.3.3 Monthly Variations of Br-DBPs are not correlated to NOM

Monthly trends of Br-DBPs in finished water were investigated by soft clustering (Fig. 3.3). While four diverse trends were observed, concentrations of three of four clusters (clusters 1, 3 and 4) had common peaks in abundance in summer (i.e. June or July), with decreased abundance in fall and winter for clusters 3 and 4. Similarities among monthly trends for most Br-DBPs is supported by their positive correlations (Fig. 3.1A), indicating the existence of common factors driving their co-occurrences.

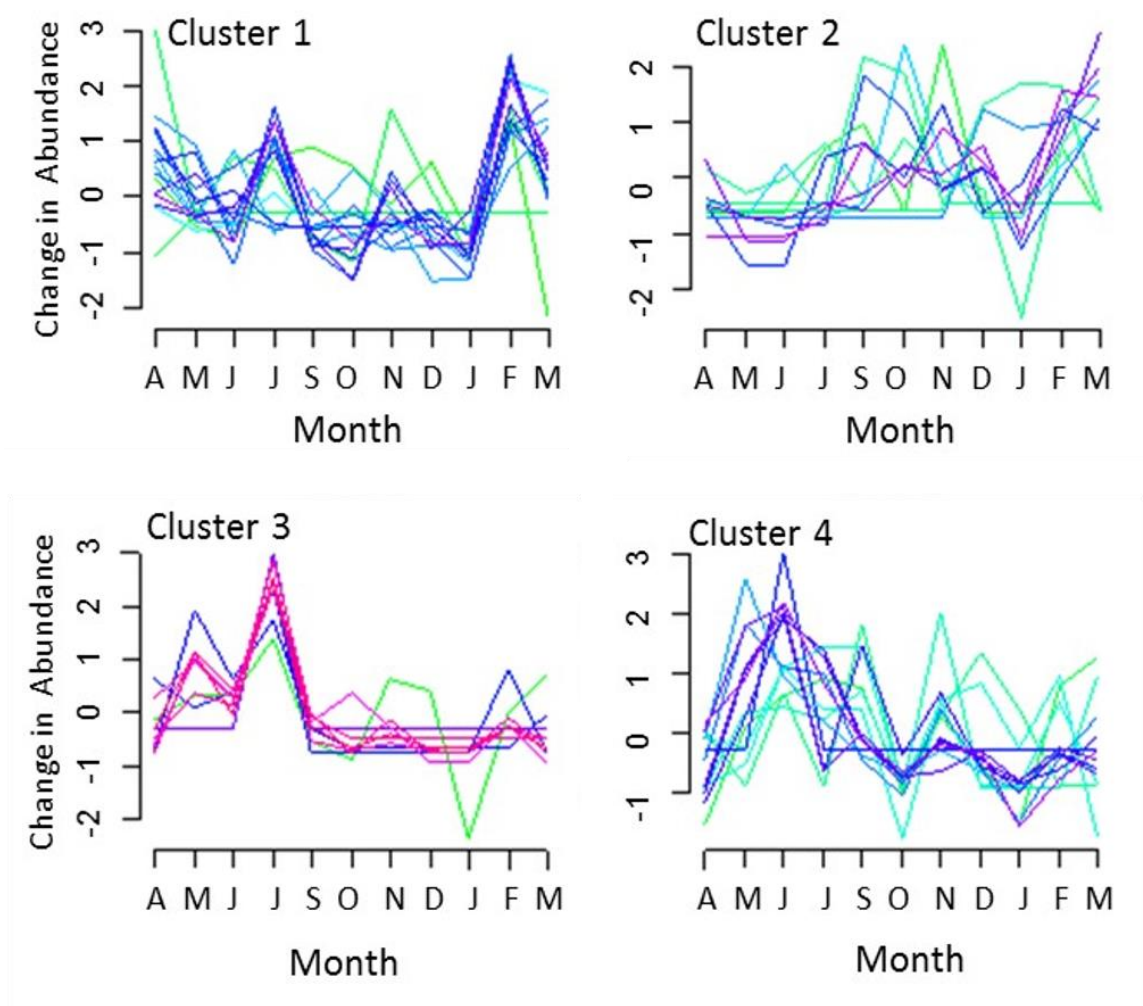


Fig. 3.3. Four temporal trends identified by soft clustering analysis for the detection of 54 unregulated Br-DBPs in finished water over 11 months.

Since NOM is known to provide precursors for formation of DBPs, the same samples of raw, clearwell, and finished waters were analyzed for NOM by use of direct infusion Orbitrap UHRMS. 394 peaks were assigned predicted formulae. CHO NOM was the major class (316 compounds), contributing to 86.6 ± 2.2 % of total ion abundance of NOM (Fig. B.4A). Detection of CHO compounds as the major class of NOM is consistent with previously reported results (Koch et al., 2007; Zhang et al., 2012b). Sulfur-containing NOM was detected at relatively high abundance, with 11 CHOS compounds (4.5 ± 2.4 %), and 56 CHOSN compounds (8.5 ± 0.7 %). Sulfur-containing NOM is rarely discussed in DBP research, but a previous study reported detection of sulfur-containing NOM molecules at an intensity of about 1/3 that of CHO NOM molecules in waters collected from China (Zhang et al., 2012a). The ubiquitous occurrence of

sulfur-containing NOM, the detection of high abundance sulfur-containing Br-DBPs, together with the reported enhanced toxicities of heteroatomic DBPs, indicates that sulfur-containing DBPs are an emerging concern (Muellner et al., 2007; Zahn et al., 2016). Overall, NOM was significantly ($p < 0.001$) reduced through the water treatment process with an average reduction in total ion abundance of 48.6 ± 7.1 % from raw to finished water (Fig. B.4B). This is not surprising since previous studies have shown that abundances of NOM are reduced along treatment units (Gonsior et al., 2014; Kim and Yu, 2005; Matilainen et al., 2010).

Soft clustering analysis was used to identify four trends in monthly variation of NOM (Fig. B.5). All four clusters of NOM peaked in December, showing distinct trends from Br-DBPs. Correlations between individual Br-DBPs and individual compounds of NOM were further explored by use of van Krevelen plots. A clear relationship between $C_7H_7O_6Br$ and NOM was observed, with significant correlations to > 50% of NOM that had O/C ratio > 0.5 and H/C ratio < 1 (Fig. B.6A). This is consistent with results of a recent, bench-scale study, in which NOM molecules with large O/C ratios and low H/C ratios were found to have the greatest potential to form chlorinated THM and HAA (Wang et al., 2017). However, clear correlations were not observed between any other Br-DBPs and NOM (Fig. B.6B), especially when p values were adjusted for multiple comparisons. Results of previous studies have documented the role of NOM in spatial distribution of regulated DBPs (Domínguez-Tello et al., 2015; Wang et al., 2017; Ye et al., 2009). In those studies, samples were collected from different geographical locations, and larger variations of NOM were observed which could drive spatial differences in DBP profiles. In contrast, in this study the magnitude of variation of NOM is minor because all samples were collected at the same location. Thus, NOM may not be a major driving factor for monthly variations of Br-DBPs at a specific site. Overall, in this study NOM was not a strong predictor for monthly variation of unregulated Br-DBPs due to lack of similarities in soft clustering analyses as well as lack of correlations in van Krevelen plots.

3.3.4 Monthly Variations of Br-DBPs are Primarily Correlated to Total Bromine

Correlations were further investigated between detections of Br-DBPs in finished water and eleven monthly measures of raw water parameters including river level, turbidity, colour, temperature and UV transmittance (UVT) of raw water, applied doses of chlorine (pre- and post-

It was expected that concentrations of bromide (Br^-) in raw water would be correlated with production of Br-DBPs. Concentrations of Br^- at the studied DWTP were particularly small, and traditional detection by use of ion chromatography was not sufficiently sensitive for this study (detection limit of ~ 0.04 mg/L). Therefore, more sensitive ICP-MS was adopted and concentrations of total Br in raw water were determined to range from 0.013 - 0.038 mg/L. Concentrations of Br in raw water in the present study are 3-10 fold less than concentrations of bromide reported in other regions, e.g. 0.095 ± 0.013 mg/L (mean \pm sd) in U.S. drinking water sources and as much as 0.09 mg/L in a Saskatchewan lake located approximately 300 km from the DWTP in this study (Buffalo Pound Water Board of Directors, 2016; VanBriesen, n.d.). With this result, total concentrations of Br in raw water were not found to be significantly correlated with abundances of any investigated, unregulated Br-DBPs (Fig. 3.4).

With ICP-MS, concentrations of total Br could be measured in treated waters as well since bromide and other Br species could be converted to elemental Br for analysis. Concentrations of Br ranged from 0.018 - 0.065 mg/L in clearwell water and 0.040 - 0.120 mg/L in finished water (Fig. 3.5). Interest was created in exploring total concentration of Br in more depth due to the unexpected observation that it increased through the treatment process with statistical significance ($p = 1.98 \times 10^{-6}$) (Fig. 3.5). These findings were unexpected since Br^- in drinking water is suggested to be present primarily due to natural background concentrations of Br^- in source water, thus concentrations of total Br across treatment units should be similar.

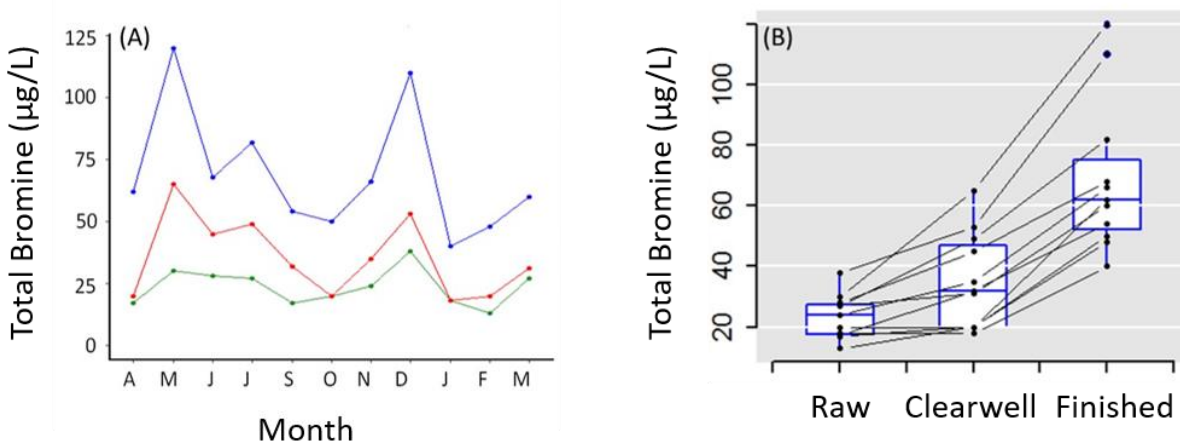


Fig. 3.5. Concentrations of total Br in samples of water collected over a year at the raw, clearwell, and finished stages of treatment. (A) Results are shown across different months for raw (green), clearwell (red) and finished water (blue). (B) Increasing concentrations of total Br across treatment stages.

Motivated by this observation, potential correlations between Br-DBPs and concentrations of Br in finished water, rather than raw water were investigated. Significant correlations were found for nine Br-DBPs (Fig. 3.4). When data from clearwell and finished stages of treatment were used to increase the sample size, the majority of Br-DBPs (34/54) were significantly correlated to total Br at $\alpha=0.05$, with 26 of those significant at $\alpha=0.01$ and 14 significant at $\alpha=0.001$ (Fig. 3.6A). For example, the sulfur-containing Br-DBP $\text{CH}_2\text{O}_3\text{SClBr}$ showed significantly positive correlation with concentrations of total Br ($R^2=0.59$, $p = 2.8 \times 10^{-5}$) (Fig. 3.6B). The positive correlation was preserved when finished and clearwell data were considered separately (Fig. 6C). While previous studies have documented effects of concentrations of Br on formation of Br-DBPs in both laboratory and field work, this is the first field study to observe that total concentration of Br, not background concentration of Br^- in source water, is a major driving factor for monthly variations of most unregulated Br-DBPs.

While the exact source of additional Br introduced throughout the treatment process remains unconfirmed, it must be related to the disinfection process since the only treatment step between clearwell and finished water is post-chlorination. Br_2 , bromine chloride (BrCl), and other brominated contaminants are known to occur as impurities in chlorine gas used for disinfection of drinking water, and current NSF 60 criteria specify 1 mg Br/L as the single product allowable concentration for any reagents used in the production of chlorine disinfectants (De Nora Water Technologies, 2015; MacPhee et al., 2002; The NSF Joint Committee on Drinking Treatment Chemicals, 2013). The acceptable concentration of Br impurities is small, but might be enough to affect concentrations of Br at the DWTP studied here, where background concentrations of Br in raw water are particularly low.

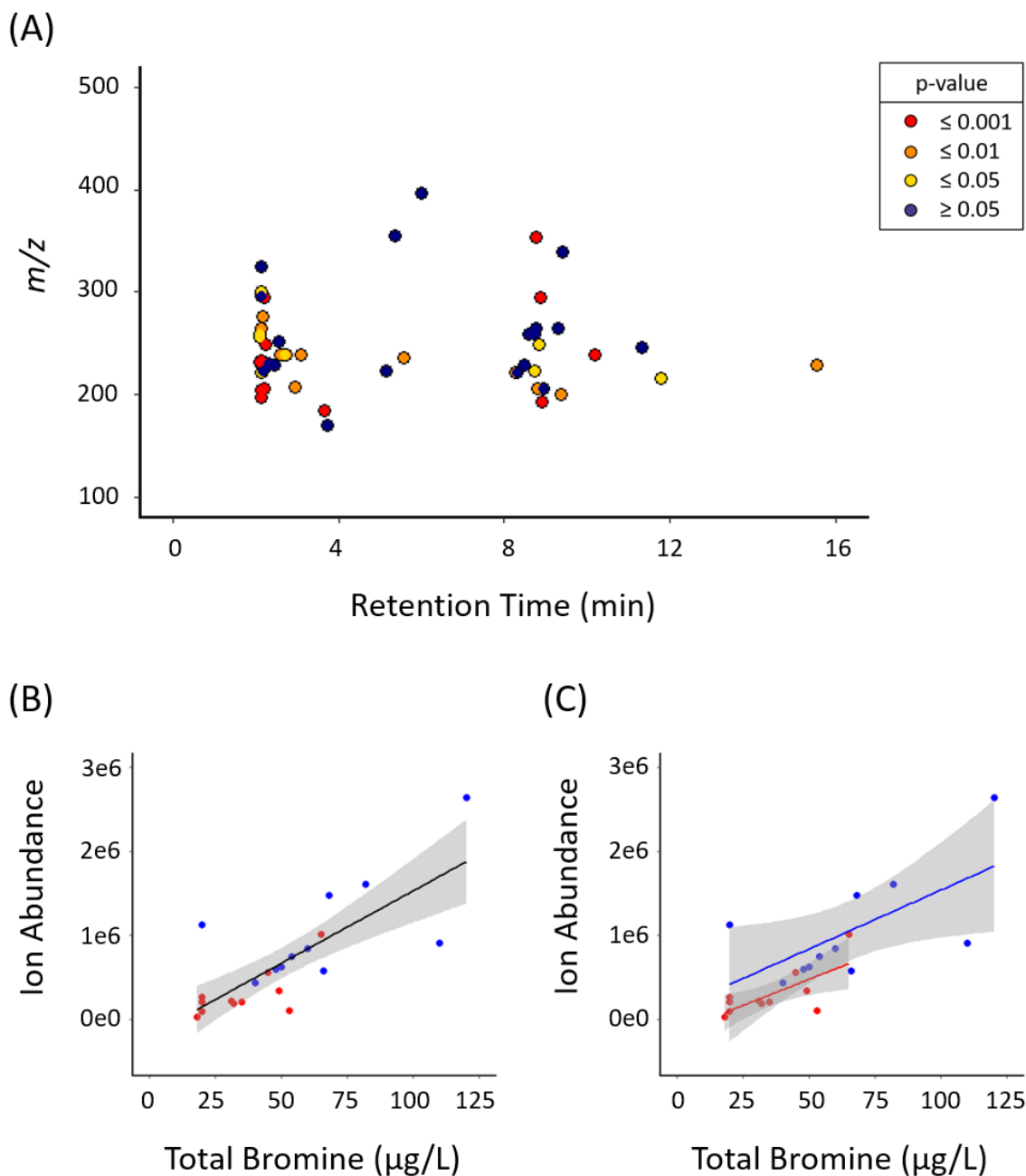


Fig. 3.6. (A) Distribution of retention times and m/z values for 54 abundant Br-DBPs, with the significance (p -value) of correlation to total concentrations of Br at the clearwell and finished stages of treatment represented by colour. The relationship between $\text{CH}_2\text{O}_3\text{SClBr}$ and total Br is shown with (B) one linear model incorporating both clearwell and finished data ($R^2 = 0.59$, $p = 2.8 \times 10^{-5}$), and (C) two linear models that consider clearwell and finished water data separately (Clearwell: $R^2 = 0.51$, $p = 0.013$; Finished: $R^2 = 0.41$, $p = 0.034$). Red points represent data from clearwell and blue points represent data from finished water, with 95% confidence intervals shown in grey.

3.3.5 Implications

The occurrence and potential health risks of unregulated DBPs are of concern since several studies have documented their stronger toxicities compared to regulated DBPs. UHRMS-based, untargeted chemical analysis provides a new strategy to investigate the occurrence, and even spatial and temporal trends of unregulated DBPs. In the present study, chemical-specific trends of unregulated Br-DBPs were reported for the first time. The observation that concentration of total Br increased through the treatment process and the hypothesis that it might be a major driving factor for monthly variations of abundances of Br-DBPs is significant at two levels: i) reduction of concentrations of Br might be the most effective way to decrease levels of Br-DBPs; ii) if concentrations of Br are added during the disinfection process, from impurities of disinfection reagents, there might be an early process modification that could reduce concentrations of Br-DBPs.

It should be noted the conclusion from the current study may be region-specific. For other regions where background concentrations of Br⁻ are greater, Br introduced during disinfection might not significantly affect concentrations of total Br, and other factors may drive monthly variations of Br-DBPs. Further application of the untargeted chemical analysis strategy to more DWTPs for investigation of spatial and temporal trends of Br-DBPs is of great interest.

3.4 Acknowledgements

This work was supported by a Discovery Grant from the Natural Science and Engineering Research Council of Canada [Project # 326415-07] and a grant from the Western Economic Diversification Canada [Projects # 6578, 6807 and 000012711]. Prof. Giesy was supported by the Canada Research Chair program, and the 2014 "High Level Foreign Experts" [#GDT20143200016] program, funded by the State Administration of Foreign Experts Affairs, the P.R. China to Nanjing University, and the Einstein Professor Program of the Chinese Academy of Sciences and a Distinguished Visiting Professorship in the School of Biological Sciences of the University of Hong Kong. Prof. Peng was supported by a Discovery Grant from the Natural Science and Engineering Research Council of Canada [Project # RGPIN-2018-06511] and University of Toronto Start-up Funds.

3.5 Supporting Information

This supporting information provides text and figures addressing (1) the water treatment process; (2) quality control and assurance; (3) conditions reported at the water treatment plant on sampling dates; (4) detection frequencies and maximum ion abundances for 54 abundant Br-DBPs; (5) R^2 and p - values for linear models calculated based on detections of sulfur-containing DBPs; (6) ID# and precursor formulae of Br-DBPs in correlation matrices found in Fig. 3.1A and Fig. B.1; (7) correlation matrix of Br-DBPs detected in finished water; (8) linear models for isomers of $C_7H_3O_3ClBr$ and $C_7H_3O_3Br_2$ at the clearwell and finished stages; (9) Br/C and O/C ratios of Br-DBPs compared based on clusters defined in Fig. 2A; (10) temporal and spatial trends of NOM; (11) example van Krevelen plots representing relationships between NOM and Br-DBPs; and (12) correlation matrices between raw water parameters and ion abundances of individual Br-DBPs (seven months of data).

CHAPTER 4

PREDICTING *IN VITRO* TOXICITY OF MIXTURES OF DISINFECTION BY-PRODUCTS BY INVESTIGATING SEASONAL CHANGES IN WATER QUALITY

Christena Watts, Paul D. Jones, John P. Giesy, and Hui Peng

Chapter 4 will be submitted to either *Water Research* or *Environmental Science & Technology*, pending acceptance of Chapters 2 and 3 to these journals. Currently, it is formatted for *Water Research* and contributions from each author are as follows:

Christena Watts (University of Saskatchewan) was responsible for chemical analysis, *in vitro* assays, data analysis, and creation of the manuscript.

Paul D. Jones and John P. Giesy (University of Saskatchewan) secured funding for the project and contributed by editing the manuscript.

Hui Peng (University of Toronto) assisted with chemical analysis and editing of the manuscript.

ABSTRACT

Over 700 disinfection by-products (DBPs) have been detected in drinking water. They fall into diverse chemical classes, yet there is limited information on toxic potencies of mixtures of DBPs. In this study, raw, clearwell, and fully treated waters were collected at a drinking water treatment plant at six time points in a year. Toxicities of concentrated extracts were investigated by use of CHO-K1 cytotoxicity and Nrf2/ARE oxidative stress assays. Cytotoxicity was greatest in finished water collected in November and March, while oxidative stress was greatest in June and November, both of which could be related to seasonal trends in unregulated Br-DBPs. These toxic endpoints were significantly correlated ($R^2 = 0.53$, $p = 7.4 \times 10^{-3}$) and three classes of Br-DBPs (Br_2 , BrCl , S-DBPs) demonstrated significant correlations to both endpoints. Parameters of water quality were not strong predictors of finished water toxicity, but concentrations of total bromine and applied doses of chlorine demonstrated significant correlations to both cytotoxicity ($R^2 = 0.43$, $p = 0.002$) and oxidative stress ($R^2 = 0.67$, $p = 0.001$) of water at related treatment units. This study represents the first to explore temporal trends in whole mixture toxicity of DBPs and to suggest concentration of total Br as a surrogate measure.

Keywords: chlorination; disinfection by-product; oxidative stress; cytotoxicity; bromine

4.1 Introduction

Disinfection by-products (DBPs) can be found globally in treated drinking water. They are produced through reactions between natural organic matter (NOM), inorganic precursors such as bromide, and disinfectants used during the treatment process. The two major classes of regulated DBPs are trihalomethanes (THMs) and haloacetic acids (HAAs); however, over 700 halogenated DBPs have been detected and even more remain unknown due to the small concentrations at which they exist, complicated interferences, and the lack of available standards for targeted analyses (Yang and Zhang, 2016). The field of DBP research is further complicated by seasonal and geographical variations in detection of DBPs, which makes generalization of findings difficult.

To understand what drives formation of DBPs, several parameters of water quality have been explored. In a controlled setting, predictive models for THMs and HAAs were developed based on dissolved organic carbon (DOC), UV absorption at 254 nm (UV_{254}), and the concentration of bromide (Br^-) (Chen and Westerhoff, 2010). In a 25-week field study, a multivariate analysis of three distribution systems in Canada found water temperature was a better predictor of THM seasonal variation than chlorine dose, surrogates of NOM, and pH (Rodriguez and Sérodes, 2001). Studies such as these are valuable in understanding how regulated DBPs form, but the practice has not been expanded to all unregulated DBPs. In one approach, our research group explored correlations between parameters of water quality and detection of 54 unregulated brominated DBPs (Br-DBPs) in samples of drinking water collected over a period of twelve months (Chapter 3). Temperature of raw water and concentration of total bromine (Br) at each stage of treatment were identified to have the strongest relationships with unregulated Br-DBPs, while turbidity, colour, and UV transmittance (UVT) demonstrated few significant correlations.

For characterization and comparison of toxicities of unregulated DBPs, efforts have been made by The Water Research Foundation to create standardized tests (Plewa and Wagner, 2009; Wagner and Plewa, 2017). Protocols have been published for a 72 h chronic mammalian cell cytotoxicity assay and a 4 h single cell gel electrophoresis assay (comet assay) that both use a Chinese hamster ovarian (CHO) cell line. By 2009, these assays had been used to characterize forty-seven DBPs from seven chemical classes ranked from most toxic to least toxic as:

haloacetaldehydes > haloacetamides > halonitromethanes > haloacetonitriles > >2C-haloacids > haloacetic acids > halomethanes (Plewa and Wagner, 2009). By 2017, the number of DBPs assessed by these assays grew to 103 and a general trend was observed that iodinated DBPs were more toxic than brominated analogues, which were more toxic than chlorinated analogues (Wagner and Plewa, 2017). While many advances in understanding can be taken from this work, there is still a need to integrate results with chemical profiles of actual drinking water to determine which unregulated DBPs pose the greatest risks. There is also potential to extend the application of these assays from the assessment of individual, chemically synthesized DBPs to the assessment of mixtures of DBPs. For example, these assays were used to assess mixture toxicity of laboratory-produced, chlorinated water concentrated by XAD resin. Strong correlations were identified between total organic Br (TOBr) measured in unchlorinated water with genotoxicity and cytotoxicity of corresponding chlorinated water ($r = 0.85$ and $r = 0.92$, respectively) (Yang et al., 2014). Relationships between total organic chlorine (TOCl) and these toxic endpoints were weak and inverse ($r = -0.56$ and $r = -0.39$, respectively), further supporting the supposition that Br-DBPs are of greater concern than chlorinated DBPs (Cl-DBPs) (Yang et al., 2014).

Previous work with a data-independent precursor isolation and characteristic fragment method (DIPIC-Frag) established a library of 553 Br-DBPs detected in chlorinated water collected from a drinking water treatment plant (DWTP) in Saskatchewan, Canada (Chapter 2). Based on this library, fates of the 54 most abundant Br-DBPs detected at a second DWTP in Saskatchewan, Canada were explored (Chapter 3). Concentration of Br at each stage of treatment and temperature of raw water were identified to have the strongest relationships to unregulated Br-DBPs. The goal of this research chapter is to build off of Chapter 3 by assessing toxicities of these complex mixtures of unregulated DBPs detected throughout the year. This was done by use of a 72 h CHO-K1 cytotoxicity assay and a 16 h Nrf2/ARE oxidative stress assay. Similar to Chapter 3, seasonal trends were explored and correlation analysis was performed to identify relationships between parameters of water quality, treatment conditions, Br-DBPs, and observed toxic responses.

4.2 Materials and Methods

4.2.1 Chemicals and Reagents

Details in Appendix C4.

4.2.2 Collection of Water Samples

Water samples were collected from a DWTP located in central Saskatchewan that is supplied by the North Saskatchewan River. Here, treatment begins with addition of potassium permanganate as well as seasonal use of powdered activated carbon to control taste and odour in warmer months. This is followed by coagulation with poly-aluminum chloride, flocculation assisted by an additional polymer, a small dose of chlorine gas (Cl_2) (pre-chlorine dosage, ~ 0.4 mg/L), and silica sand/antracite filtration. Then water is treated with UV irradiation followed by a second and greater dose of chlorine gas (post-chlorine dose, ~ 2.0 mg/L), which serves as the primary disinfection stage before water travels to the reservoir. Samples in this study were collected at the raw water intake (raw), just after UV irradiation before the post-chlorine dose (clearwell), and at the fully treated stage (finished). Water was collected in 4 L headspace-free, amber bottles previously rinsed with ultrapure water and methanol (MeOH). Extractions were started within 4 h of collection to minimize effects of residual chlorine. No quenching reagent was added based on results from previous investigations which indicated that some quenching reagents might lead to the loss of some unregulated DBPs (Section 2.3.4).

Sampling began April 19, 2016, twelve days after the river ice broke. Sampling was planned to occur every month for a year, with samples from every month analyzed for Br-DBPs (Chapter 3) and samples from every other month subjected to toxicity assessment. On July 21, 2016 an oil pipeline just over 300 km upstream of the DWTP ruptured and leaked 225,000 L of crude blended with condensate, with 40% of that reaching the North Saskatchewan River (Government of Saskatchewan, 2016). In response, the DWTP began withdrawing water from different sources and this interrupted sampling in August. Sampling resumed September 29, 2016. Samples for toxicity assessment were therefore collected in April, June, September, November, January, and March.

4.2.3 Chemical Analysis for Br-DBPs

Based on a previously developed method (Chapter 2), samples of water were adjusted to pH 2 with 1 M hydrochloric acid and extracted by Oasis HLB cartridge for the best chemical coverage and reproducibility. Raw water samples required filtration with a G4 glass fibre filter prior to solid phase extraction (SPE). After pre-conditioning HLB cartridges with DCM, MeOH, and ultrapure water, 1 L of samples were passed through the cartridges at a flow rate of 5-10 ml/min. Cartridges were dried under a gentle flow of nitrogen and DBPs were eluted with 5 ml of MeOH and 5 ml of DCM. Extracts were dried under a stream of nitrogen and reconstituted in 500 µl of MeOH. A procedural blank of ultrapure water acidified to pH 2 with hydrochloric acid and extracted by the SPE protocol above was included in the study design.

Aliquots of samples were analyzed for Br-DBPs by use of a Q Exactive™ UHRMS (negative ion mode) equipped with a Dionex™ UltiMate™ 3000 UHPLC system. Based on method optimization (Chapter 2), a TSKgel Amide-80 column (4.6 mm ID x 15 cm, 3 µm) and electrospray ionization (ESI) were used. More detailed analytical conditions can be found in Appendix C4.

Using a library of Br-DBPs established previously by use of full-spectrum analyses (Section 2.3.2), the 54 most abundant Br-DBPs detected at this DWTP were identified and selected for further investigation (Chapter 3). To avoid shifts in instrument sensitivity, extracts of samples from different months were analyzed at the same time. It should be noted that absolute peak abundances were used for comparative statistical analysis, a strategy well documented in previous metabolomics studies, since instrument sensitivity is similar for the same DBPs from different samples.

4.2.4 72 h CHO-K1 Cytotoxicity Assay

CHO-K1 cells (ATCC® CCL-61™) were cultured in F-12 nutrient medium supplemented with 5% FBS and maintained at 37 °C with 5% CO₂. Methods for assessment of cytotoxicity were adapted from protocols used by the Water Research Foundation to evaluate toxicities of DBP standards (Plewa and Wagner, 2009; Wagner and Plewa, 2017). In this assay, reduction in cell density is measured after a 72 h exposure period, or approximately 3 cell divisions, by

measuring absorbance of crystal violet dye at $\lambda = 595$ nm. 100 μ l aliquots of CHO-K1 cell suspension (3×10^4 cells/ml) were seeded in 96-well F-bottom plates and mixed with 100 μ l of concentrated water extracts prepared in F-12 nutrient medium with 5% FBS. In preliminary studies, cytotoxicity of the procedural blank began to occur at a concentration factor of 70 x likely due to solvent, therefore, extracts of raw, clearwell or finished water were tested at a maximum concentration factor of 60 x, which kept solvent below 1% in each well.

Nine concentration factors (60 x, 45 x, 30 x, 15 x, 7.5 x, 3.75 x, 1.875 x, 0.9375 x, and 0.46875 x) were tested in triplicate. Positive control wells were exposed to 2.95 μ M iodoacetic acid, negative control wells contained CHO-K1 cells and growth medium, and blank control wells contained only growth medium. Iodoacetic acid was selected as the positive control because it is a potent cytotoxic DBP (Zhang et al., 2010). A concentration of 2.95 μ M was chosen based on reported LC₅₀ values in the literature and a dose-response curve calculated in-house (Fig. C.1). Plates were sealed with Aeraseal™ sealing film and incubated at 37 °C with 5% CO₂ for 72 h. After exposure, media was removed and cells were fixed with ice-cold MeOH for 10 min. MeOH was removed and 100 μ l of 2% Accustain® crystal violet solution prepared in 50:50 MeOH:ultrapure water was used to stain proteins and DNA for 10 min. Plates were washed three times with PBS and the crystal violet dye solubilized with 50 μ l of DMSO:MeOH (3:1 v/v) for 10 min. Absorbance was measured at 595 nm on a SpectraMAX 190 instrument. Absorbance values in sample wells were corrected by average absorbance in blank wells and converted to mean cell density as a percentage of negative control response. Dose-response curves and predicted LC₅₀ values were produced in R using the ‘drc’ package (Ritz et al., 2015).

4.2.5 16 h Nrf2/ARE Oxidative Stress Assay with MCF7 Cell Line

The Nrf2/ARE luciferase reporter MCF7 cell line was cultured in DMEM high glucose medium supplemented with 10% FBS and grown at 37 °C with 5% CO₂. The assay was performed as outlined by Signosis Inc. (SL-0010-NP). White 96-well plates were seeded with 100 μ l of 5×10^5 cells/ml. After 24 h, media was removed and cells were exposed in triplicate to 150 μ l of concentrated extracts of water prepared at three concentration factors (15 x, 7.5 x, and 3.75 x) in DMEM high glucose supplemented with 0.1% FBS. Negative control wells were exposed to DMEM high glucose supplemented with 0.1% FBS, while positive control wells were

exposed to 50 μ M t-BHQ prepared in the same medium. Plates were sealed with Aeraseal™ sealing film and incubated for 16 h at 37 °C with 5% CO₂. After exposure, wells were washed twice with PBS and then 75 μ l of DPBS and 75 μ l of ‘Steadylite plus’ buffer solution was added. Plates were incubated for 30 min in the dark before luminescence was recorded. Data was reported as fold increase over negative control.

The MTT assay was performed in parallel to the Nrf2/ARE oxidative stress assay to monitor cytotoxicity, which could reduce luminescent responses. All procedural conditions were kept consistent. After 16 h exposure, positive control wells were treated with MeOH for 5 min. Media was aspirated and wells washed with HBSS to remove any phenol red interferences. MTT solution (Biotium; MTT Cell Viability Assay Kit) was mixed with HBSS at a ratio of 1:10, and 110 μ l was added to each well. After 50 min of incubation at 37 °C with 5% CO₂, 150 μ l of DMSO was added to solubilize crystals and absorbance at 570 nm was recorded. Average absorbance of sample wells were corrected by positive control wells and converted to percent of negative control response.

4.2.6 Correlation Analysis for Predicting Toxicity of DBP Mixtures

A correlation matrix was produced based on data for samples of raw, clearwell, or finished water collected in April, June, September, November, January, and March. Included in the analysis were: predicted LC₅₀ values from the 72 h CHO-K1 cytotoxicity assay (Table 4.1); fold induction of the Nrf2/ARE oxidative stress pathway at a concentration factor of 15 x (Table 4.2); temperature of raw water; turbidity of raw water; UV transmittance (UVT) of raw water; colour of raw water; river level; pre-chlorine dose; post-chlorine dose; and concentrations of Br at the raw, clearwell or finished stages. Raw water parameters and treatment conditions were provided by the DWTP, while concentrations of total Br were determined by inductively coupled plasma mass spectrometry (ICP-MS) at the Environmental Analytical Laboratories of the Saskatchewan Research Council. These variables were checked for normality using the Shapiro-Wilk test. At $\alpha = 0.05$, some deviations from normality were observed, therefore, Spearman’s correlation was chosen as the most suitable approach. Analysis was performed in R using the ‘corrplot’ package (Wei et al., 2017). Significance was defined at $\alpha = 0.05$. In the interpretation of results, the small samples size ($n = 6$) for each parameter should be taken into consideration.

4.3 Results and Discussion

4.3.1 Trends in the Occurrences of Unregulated Br-DBPs

Trends in occurrences of the 54 most abundant Br-DBPs were discussed in Chapter 3. General findings included identification of three trends of formation through the treatment process (Cluster I, II, and III; Fig. 3.2) and four general trends in monthly variation (Cluster 1, 2, 3, and 4; Fig. 3.3). Many isomers and analogues co-occurred. Using Spearman's correlation, it was determined that few significant relationships existed between parameters of water quality (e.g. turbidity, UV transmittance, and colour) and the ion abundances of unregulated Br-DBPs (Fig. 3.4). Temperature of raw water showed the most number of significant correlations to individual Br-DBPs (6 positive and 3 negative relationships at $\alpha = 0.05$). A major finding was the consistent increase in concentration of total Br from raw water, to clearwell water, to finished water (Fig. 3.5). When the concentration of Br in clearwell and finished waters were compared to the detection of Br-DBPs at corresponding stages 34/54 relationships were significant at $\alpha = 0.05$ (Fig. 3.6). While the exact source of additional Br was unconfirmed, the overall conclusion was that the concentration of total Br at the clearwell and finished stages was the greatest predictor for occurrences of unregulated Br-DBPs in chlorinated water.

4.3.2 Monthly Trends in Cytotoxicity of Mixtures of DBPs

Dose-response curves for concentrated extracts of raw, clearwell or finished water, assessed by the 72 h CHO-K1 cytotoxicity assay can be found in Fig. C.2 (A - C). Predicted LC_{50} values are reported in Table 4.1. In general, there was a trend of increasing cytotoxicity as water moved from raw water intake, to clearwell water, to fully treated water (Fig. 4.1A). As expected, this supports the hypothesis that chlorination and subsequent formation of DBPs causes increased cytotoxicity, however, there are exceptions to this trend. In June, clearwell water was less cytotoxic than raw water, and in April, raw and clearwell water had similar predicted LC_{50} values (Fig. 4.1B). In dependent 2-group Wilcoxin signed rank tests (Mann-Whitney U tests), finished water was significantly more cytotoxic than clearwell water ($p =$

0.03), but finished water was not significantly more cytotoxic than raw water ($p = 0.06$). Raw water and clearwell water were not significantly different in their cytotoxic potentials ($p = 0.53$).

Table 4.1. LC_{50} values for 72 h CHO-K1 cytotoxicity tests of water samples collected at three stages of treatment (raw, clearwell, finished) and at six time points over a year. LC_{50} values (mean \pm se in units of concentration factor (x)) were predicted by a Weibull dose-response model with the lower limit fixed at zero (see Fig. C.2).

	Raw	Clearwell	Finished
April	57.0 \pm 1.9	60.9 \pm 3.6	54.5 \pm 1.8
June	28.5 \pm 2.4	57.8 \pm 8.1	28.6 \pm 1.8
September	50.2 \pm 2.0	42.8 \pm 1.7	30.1 \pm 2.0
November	40.5 \pm 1.1	37.1 \pm 1.2	12.4 \pm 1.2
January	77.0 \pm 13.2	70.6 \pm 5.3	24.3 \pm 1.4
March	84.6 \pm 15.7	40.0 \pm 2.1	15.4 \pm 1.3

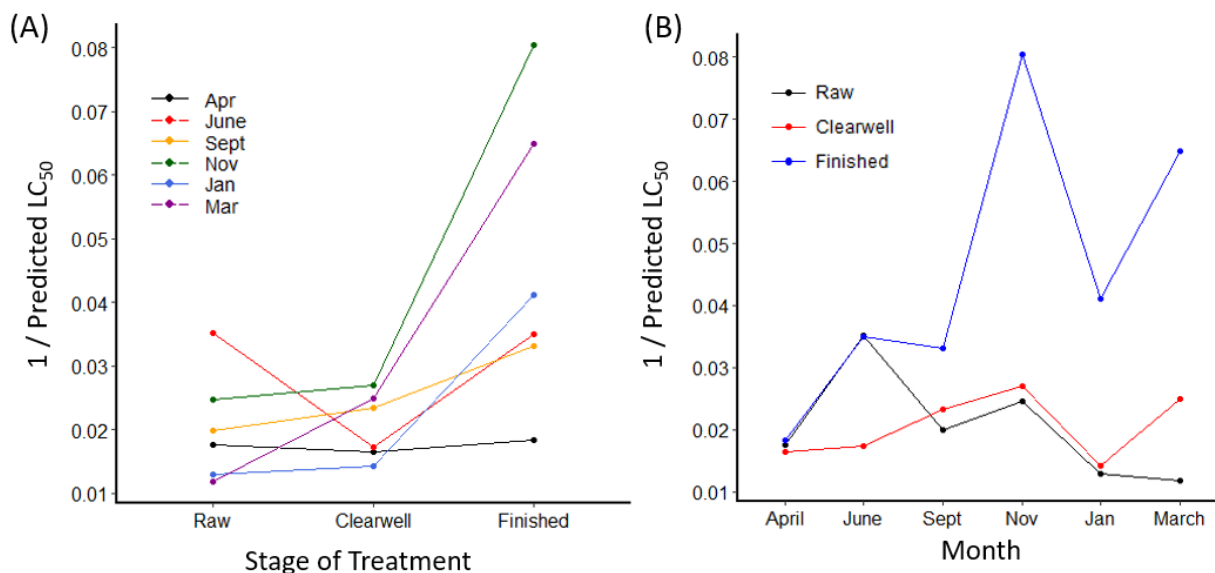


Fig. 4.1. Trends in cytotoxicity (plotted as $1/LC_{50}$ (mean)) for concentrated extracts of water visualized by (A) stage of treatment and (B) month of sampling. Predicted LC_{50} values can be found in Table 4.1.

Analysis of raw water determined that cytotoxicity was most induced by water collected in June ($LC_{50} = 28.5 \pm 2.4$ x), followed by November, September, and April. Determination of LC_{50} values for raw water collected in January and March were less accurate because 100% reduction in cell density compared to the negative control was not achieved at the greatest tested concentration of 60 x. For clearwell water, cytotoxicity increased from April through to November, with the greatest cytotoxicity induced in November ($LC_{50} = 37.1 \pm 1.2$ x). The order of cytotoxicity for all six months was: November > March \approx September > June \approx April > January. Similarly, the greatest cytotoxicity of finished water was determined for water collected in November ($LC_{50} = 12.4 \pm 1.2$ x) and March ($LC_{50} = 15.4 \pm 1.3$ x). This was followed by January > June \approx September > April. Cytotoxicity of raw water was not correlated to cytotoxicity of finished water ($R^2 = 0.015$, $p = 0.82$; Fig. C.3A). Cytotoxicity of clearwell water was also not correlated to cytotoxicity of finished water ($R^2 = 0.28$, $p = 0.28$; Fig. C.3B), which implies that the post-chlorine dose shifts the profile of DBPs to such a degree as to change the cytotoxic potency of the water. This might suggest that under environmentally relevant conditions and concentrations, Br-DBPs classified as cluster III (Fig 3.2A) possess greater cytotoxic potential as a whole than Br-DBPs classified as cluster I.

When trends in cytotoxicity were compared to seasonal trends of Br-DBPs (Fig. 3.3A) interest was created for Br-DBPs represented by cluster 1 and cluster 2 due to spikes in detections in November and March. In contrast, cluster 3 Br-DBPs were not detected at great abundance in any of the six months assessed for cytotoxicity and many Br-DBPs in cluster 4 showed peak detection in June, which was ranked 4th for cytotoxicity of finished water. Based on these results, future cytotoxicity work could focus on Br-DBPs that fall under both cluster III (trend through process) and cluster 1 and cluster 2 (trend over time).

4.3.3 Monthly Trends in Oxidative Stress

Results for induction of the Nrf2/ARE oxidative stress pathway by raw, clearwell, and finished water at concentration factors of 3.75 x, 7.5 x, and 15 x can be found in Table 4.2 and Fig. C.4A. As determined by the MTT assay, no significant cytotoxicity was induced by extracts of water at concentrations tested in this 16 h assay (Fig. C.4B). At 3.75 x there were no significant increases in oxidative stress for samples of water. At 7.5 x significant increases were

observed for three raw water samples (April, September, and November), one clearwell water sample (November), and five finished water samples (all excluding April). At 15 x all samples of raw, clearwell, and finished water induced significant oxidative stress, therefore, subsequent discussion will focus on data based on the concentration factor 15 x.

Table 4.2. Fold induction of the Nrf2/ARE oxidative stress pathway by extracts of raw, clearwell, and finished water at three concentration factors (3.75 x, 7.5 x, and 15 x) compared to the negative control. Samples were collected at 6 monthly time points (April 2016 – March 2017).

	Raw			Clearwell			Finished		
	3.75 x	7.5 x	15 x	3.75 x	7.5 x	15 x	3.75 x	7.5 x	15 x
April	1.06 ± 0.11	1.26 ± 0.08*	1.54 ± 0.05**	1.09 ± 0.07	1.15 ± 0.14	1.87 ± 0.19*	1.13 ± 0.07	1.23 ± 0.20	2.19 ± 0.08**
June	1.01 ± 0.02	1.16 ± 0.08	1.54 ± 0.11*	0.95 ± 0.04	1.11 ± 0.07	1.38 ± 0.07*	1.20 ± 0.10	1.92 ± 0.04**	3.59 ± 0.12**
Sept.	0.98 ± 0.01*	1.06 ± 0.02*	1.35 ± 0.04**	0.94 ± 0.02*	1.01 ± 0.10	1.45 ± 0.06**	1.13 ± 0.06	1.47 ± 0.17*	2.96 ± 0.18**
Nov.	1.24 ± 0.14	1.32 ± 0.08*	1.53 ± 0.09*	1.18 ± 0.09	1.41 ± 0.07**	1.97 ± 0.02 **	1.26 ± 0.12	1.70 ± 0.03**	3.30 ± 0.29**
Jan.	0.92 ± 0.06	0.98 ± 0.09	1.34 ± 0.12*	0.99 ± 0.11	0.96 ± 0.05	1.28 ± 0.06*	1.05 ± 0.10	1.24 ± 0.02**	2.19 ± 0.18**
March	0.93 ± 0.06	1.06 ± 0.06	1.19 ± 0.07*	0.91 ± 0.07	1.07 ± 0.08	1.37 ± 0.11*	1.03 ± 0.07	1.37 ± 0.07*	2.68 ± 0.08**

Notes: n=3; * significant fold-induction at $\alpha=0.05$; ** significant fold-induction at $\alpha=0.01$.

Similar to cytotoxicity, there was a general trend of increasing oxidative stress as water moved from raw intake water, to clearwell, to the finished stage of treatment with the greatest increase occurring after application of the post-chlorine dose (Fig. 4.2A). This is consistent with other studies that have shown treatment processes such as pre-chlorination and post-chlorination increase the potential for water extracts to induce oxidative stress (Escher et al., 2012; Xie et al., 2010). Again, this trend was similar to that observed for Br-DBPs classified as cluster III based on their formation through the treatment process (Fig. 3.2A). Independent 2-group Wilcoxon signed rank tests (Mann-Whitney U tests), raw and clearwell water were not significantly different ($p = 0.22$), but it was determined that finished water was more toxic than raw and clearwell water (both $p = 0.031$). Oxidative stress of raw water was not significantly correlated to oxidative stress of finished water ($R^2 = 0.13$, $p = 0.49$; Fig. C.5A). Oxidative stress of clearwell water was also not significantly correlated to that of finished water ($R^2 = 0.64$, $p = 0.91$; Fig. C.5B).

This assay could statistically differentiate more stages of the water treatment process than could the CHO cytotoxicity assay; therefore, oxidative stress might be a more selective and sensitive endpoint for characterizing toxicity of mixtures of DBPs. This conclusion was also drawn in studies that compared toxicities of DBPs via Nrf2/ARE oxidative stress and Microtox® cytotoxicity assays (Escher et al., 2012; Stalter et al., 2016). Use of the Nrf2/ARE pathway for comparison of toxicities induced by mixtures of DBPs is further supported by the observation that 49/50 investigated DBPs were capable of activating this pathway (Stalter et al., 2016).

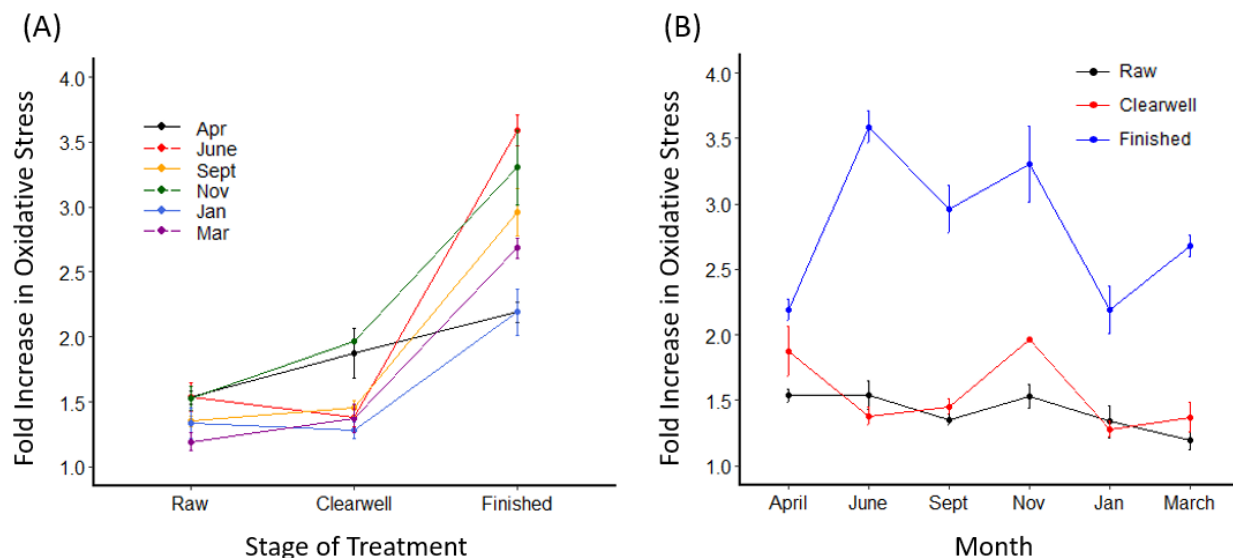


Fig. 4.2. Fold induction of the Nrf2/ARE oxidative stress pathway (mean \pm sd) in MCF7 cell line after 16 h exposure to 15 x concentrated extracts of water, visualized by (A) stage of treatment and (B) month of sampling. Average fold increase (n=3) normalized as percent of negative control response. Results are reported in Table 4.2.

At 15 x, there was little monthly variation in oxidative stress induced by raw water (Fig. 4.2B). Raw water collected in April and June demonstrated the greatest oxidative stress, with fold-increases over the negative control of 1.54 ± 0.05 x and 1.54 ± 0.11 x, respectively. For clearwell water, the greatest induction of oxidative stress was reported in November (1.97 ± 0.02 x), followed by April (1.87 ± 0.19 x) and September (1.45 ± 0.06 x). At 15 x, oxidative stress of finished water was significant at $\alpha=0.01$ for all months assessed in this study. June induced the greatest oxidative stress (3.59 ± 0.12 x) and November the second greatest (3.30 ± 0.29 x). While still significant, April and January caused the least oxidative stress (2.19 ± 0.08 x and 2.19 ± 0.18 x, respectively).

When comparing trends in oxidative stress with monthly variations of Br-DBPs (Fig. 3.3), Br-DBPs of cluster 4 showed peaks in detection in the same three months that induced greatest oxidative stress: June, November and September (Fig. 4.2B). Seasonal trends of cluster 1, 2, and 3 Br-DBPs do not directly reflect the trend observed in induction of oxidative stress, but there are similarities. For example, cluster 2 Br-DBPs were detected at greatest abundance in March, September, October and November, which includes the months that ranked second, third, and fourth in the oxidative stress assay. Moving forward, Br-DBPs of cluster 4, and possibly

cluster 2, could become the focus for more targeted assessments of individual chemical oxidative stress, in particular if they were also classified as cluster III based on their formation through the treatment process.

4.3.4 Predicting Toxicity of DBP Mixtures

4.3.4.1 Oxidative Stress and Cytotoxicity of DBP Mixtures are related

Predicted LC₅₀ values and fold-induction of oxidative stress by extracts of raw, clearwell or finished water (at 15 x) were compared. Although not attributed to DBPs, these endpoints were significantly correlated in raw water ($R^2 = 0.69$, $p = 0.041$), which could suggest that similar compounds are responsible for both cytotoxicity and oxidative stress of river water, and that these compounds follow a distinct trend through the year (i.e. peaks in June and November in this study). For clearwell and finished waters, the lack of correlation between monthly trends in these endpoints ($R^2 = 0.10$ and 0.20 ; $p = 0.53$ and 0.37 , respectively) suggests that DBPs responsible for cytotoxicity do not elicit such response primarily through oxidative stress; however, it is possible that small sample size ($n = 6$) contributed to this lack of significance.

When both clearwell and finished water were incorporated into the same linear model a significant correlation was found between cytotoxicity and oxidative stress ($R^2 = 0.53$, $F_{1,10} = 11.18$, $p = 7.4 \times 10^{-3}$) (Fig. 4.3). Both clearwell and finished waters contained complex mixtures of DBPs (Table B.2), although they showed distinct differences in detection frequencies and ion abundances. Based on this work, oxidative stress might be a primary molecular initiation event for cytotoxicity induced by mixtures of DBPs. Correlations between these endpoints have been previously identified for halomethanes ($\rho = 0.93$) as well as for concentrated extracts of treated water (Escher et al., 2012; Stalter et al., 2016). Oxidative stress has also commonly been identified as a molecular initiating event for genotoxicity induced by DBPs (Dad et al., 2013; Neale et al., 2012; Pals et al., 2013; Stalter et al., 2016; Xie et al., 2010). Causative relationships have been identified between oxidative stress and genotoxicity of mono-HAAs, and in a study of 50 DBPs, each DBP that activated the p53 tumour suppressor pathway also induced the Nrf2 oxidative stress pathway (Dad et al., 2013; Pals et al., 2013; Stalter et al., 2016). To further confirm relationships between oxidative stress, cytotoxicity, and genotoxicity the methods of

this paper could be applied to a large number of spatially and temporally unique samples of chlorinated drinking water.

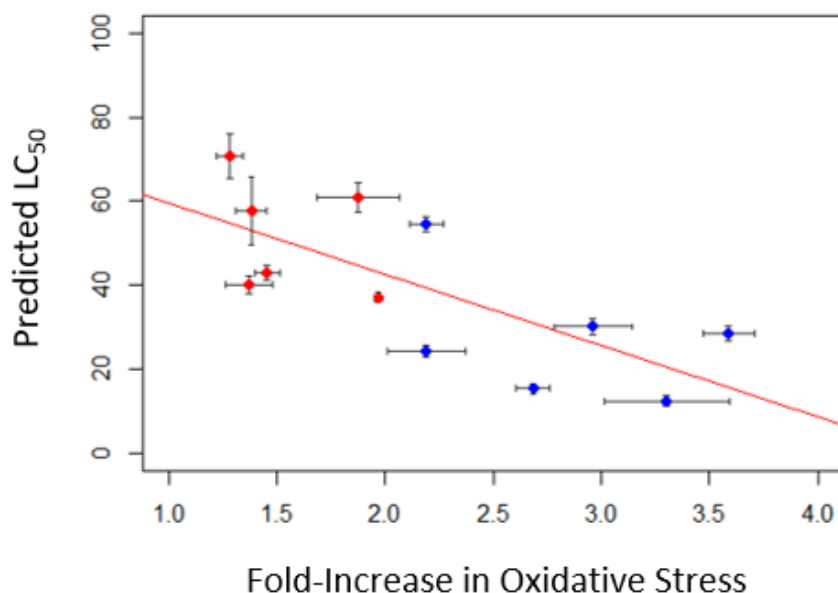


Fig. 4.3. Relationship between oxidative stress and cytotoxicity induced by 15 x concentrated extracts of clearwell (red) and finished (blue) water. Linear model $R^2 = 0.53$, $F_{1,10} = 11.18$, $p = 7.4 \times 10^{-3}$.

4.3.4.2 Classes of Br-DBPs Contribute to Whole Mixture Toxicity to Varying Degrees

To assess contributions of various classes of Br-DBPs to whole mixture toxicities, cumulative ion abundances were calculated based on the 54 most abundant Br-DBPs. Linear models were used to define relationships, with analyses performed on finished water alone ($n = 6$) as well as with data from clearwell and finished water combined to increase sample size and expand models to more distinct mixtures of DBPs ($n = 12$) (Table 4.3). For finished water alone, no significant linear relationships were identified. When clearwell and finished water were combined, significant relationships were identified. Cytotoxicity was correlated to Br_2 , BrCl , and sulfur-containing Br-DBP (S-DBPs) classes while oxidative stress was correlated to Br_2 , BrCl , S-DBPs, nitrogen-containing Br-DBPs (N-DBPs), and all Br-DBPs. Compared to cytotoxicity, unregulated Br-DBPs were more significantly correlated to oxidative stress induced by mixtures

of DBPs which further supports the use of oxidative stress as an endpoint in comparing DBP mixtures.

As previously mentioned, there are few studies that compare whole mixture toxicity of DBPs found in drinking water. In the HIWATE study, Br-DBPs were significantly correlated to cytotoxicity of spatially distinct samples of water concentrated by XAD resin ($R^2 = 0.46$, $p \leq 0.022$), which differs from results of this study (Jeong et al., 2012). These differences might be explained by the number and types of Br-DBPs included in each study. The HIWATE study assessed eleven Br-DBPs and of those eleven, five were regulated (BDCM, DBCM, bromoform, MBA, and DBA) and six were unregulated (bromochloroacetonitrile, dibromoacetonitrile, bromochloroacetic acid, bromodichloroacetic acid, dibromochloroacetic acid, and tribromoacetic acid). In contrast, 54 unregulated Br-DBPs were analyzed in the study, results of which are presented here. Therefore, the lesser toxic potencies of some Br-DBPs in this study might have weakened the strength of correlation or the most cytotoxic Br-DBPs might not have been included in the 54 most abundant Br-DBPs.

Table 4.3. Statistically significant correlations between detected classes of Br-DBPs and measured toxicities of concentrated extracts of clearwell and finished water.

Class of DBP ^c	Finished Water Only ^a		Clearwell and Finished Water ^b	
	Cytotoxicity (LC ₅₀)	Oxidative Stress ^d	Cytotoxicity (LC ₅₀)	Oxidative Stress ^d
All Br-DBPs	NS	NS	NS	R ² = 0.37 p = 0.037*
Br (n = 20)	NS	NS	NS	NS
Br₂ (n = 7)	NS	NS	R ² = 0.42 p = 0.023*	R ² = 0.85 p = 0.000022**
BrCl (n = 24)	NS	NS	R ² = 0.35 p = 0.041*	R ² = 0.57 p = 0.0047**
Br₂Cl (n = 2)	NS	NS	NS	NS
C-DBPs (n = 28)	NS	NS	NS	NS
S-DBPs (n = 10)	NS	NS	R ² = 0.40 p = 0.027*	R ² = 0.76 p = 0.00021**
N-DBPs (n = 20)	NS	NS	NS	R ² = 0.54 p = 0.0068**
NS = not significant; ^a p-value based on F _{1,4} ; ^b p-value based on F _{1,10} ; ^c Cumulative ion abundance calculated from the 54 most abundant Br-DBPs; ^d Fold increase in oxidative stress compared to negative control at concentration factor of 15 x; *significant at α = 0.05; **significant at α = 0.01				

The observation that N-DBPs were more significantly correlated to oxidative stress than C-DBPs is consistent with the general conclusion that N-DBPs exhibit greater toxic potencies than do C-DBPs (Krasner et al., 2016; Muellner et al., 2007; Plewa et al., 2008). There is little to no data available on toxic potencies of S-DBPs, but recent discussions of their high-abundances in drinking water, and significant correlation to toxicity identified here creates interest in further

exploring toxicity of these compounds (Zahn et al., 2016). In future work it will be important to determine occurrences of Cl-DBPs and I-DBPs to compare contributions of other halogen classes to whole mixture toxicity of DBPs. Cl-DBPs typically occur at greater concentrations than analogous Br-DBPs and have been correlated to cytotoxicity of spatially distinct samples of drinking water ($R^2 = 0.61$, $p \leq 0.005$), although in a bench-scale study TOCl was not correlated to cytotoxicity ($R^2 = 0.31$) (Jeong et al., 2012; Yang et al., 2014). I-DBPs typically occur at lesser concentrations than Cl- or Br-DBPs; however, they demonstrate enhanced toxicity and total organic iodine (TOI) was significant correlated to cytotoxicity of chlorinated water ($R^2 = 0.77$) (Yang et al., 2014).

4.3.4.3 Toxicities of Mixtures of DBPs are Primarily Associated with Total Br and Chlorine Dose

With six months of data, there were no significant correlations ($\alpha < 0.05$) between endpoints of toxicity with temperature of raw water, concentrations of Br in raw water or finished water, and applied doses of chlorine (Fig. 4.4). Concentrations of Br at the clearwell stage were positively correlated to oxidative stress of finished water (Fig. C.6A). This could mean that Br-DBPs produced primarily by the post-chlorine dose (cluster III) contribute more to oxidative stress of finished water than those produced primarily by the pre-chlorine dose (cluster I and II). Other significant findings include that as river level increases the DWTP can be expected to output finished water with decreased potential to cause oxidative stress (Fig. C.6B). At this site, river level followed a seasonal pattern of being greater than 2 m between December and April and being less than 2 m between May and November (Table B.1). Increased river level could result in dilution of NOM precursors, which is supported by the negative correlation of river level with turbidity (Fig. 3.4). Turbidity was positively correlated with predicted LC_{50} values of finished water meaning that more turbid raw water was related to lesser cytotoxic potencies of finished drinking water, but this linear relationship might have been driven by the outlier value reported in April (Fig. C.6C). While, increases in colour and decreases in UVT of raw water were significantly correlated to increases in oxidative stress of raw water, they could not predict toxicity of finished water.

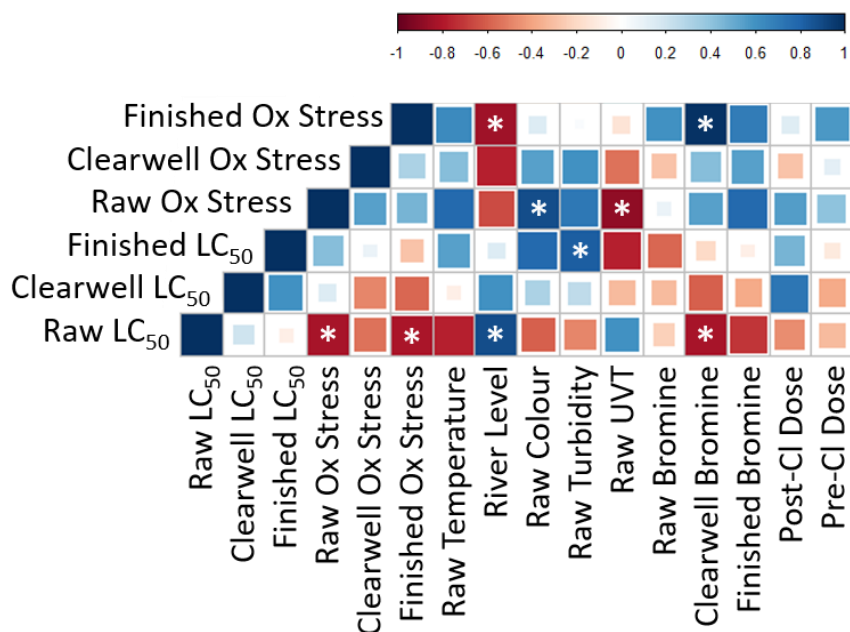


Fig. 4.4. Spearman's correlation matrix indicating significant* ($\alpha=0.05$) correlations between measures of toxicity, parameters of water quality, and doses of chlorine (n=6).

Concentrations of Br in raw or finished water alone were not strong predictors for toxicity of finished water with $R^2 = 0.0007 - 0.45$ and $p = 0.15 - 0.96$ (Fig. C.7). However, the observation that Br increased through the treatment process and that concentrations of Br at each stage of treatment could predict occurrences of many unregulated Br-DBPs (Section 3.3.4) created interest in further exploring this relationship. When concentrations of Br in clearwell and finished water were incorporated into the same linear model and used to predict associated toxicities, significant relationships were identified (Fig. 4.5). For cytotoxicity $R^2 = 0.43$ and $p = 0.021$ and for oxidative stress $R^2 = 0.67$ and $p = 0.0011$. While this increase in significance might in part be driven by increased sample size, it indicated that concentration of Br might be a single parameter that DWTPs could monitor to predict whole mixture toxicity of DBPs as opposed to focussing on concentrations of individual DBPs.

In DBP research, concentration of Br⁻ in raw water is the main parameter used to quantify Br. Increased concentrations of Br⁻ in source water have been correlated to increased formation of Br-DBPs, shifts in speciation to more highly brominated DBPs, as well as increased cytotoxicity and genotoxicity of drinking water (Chen and Westerhoff, 2010; Hua et al., 2006; Pan and Zhang, 2013; Sawade et al., 2016; Sohn et al., 2006). Total organic Br of source water

has also been shown to correlate well with cytotoxicity and genotoxicity of laboratory-produced chlorinated water concentrated by XAD resin ($r = 0.85$ and $r = 0.92$, respectively) (Yang et al., 2014). This however, is the first paper to investigate total Br at treated stages of treatment as a viable surrogate for predicting whole mixture toxicity of DBPs.

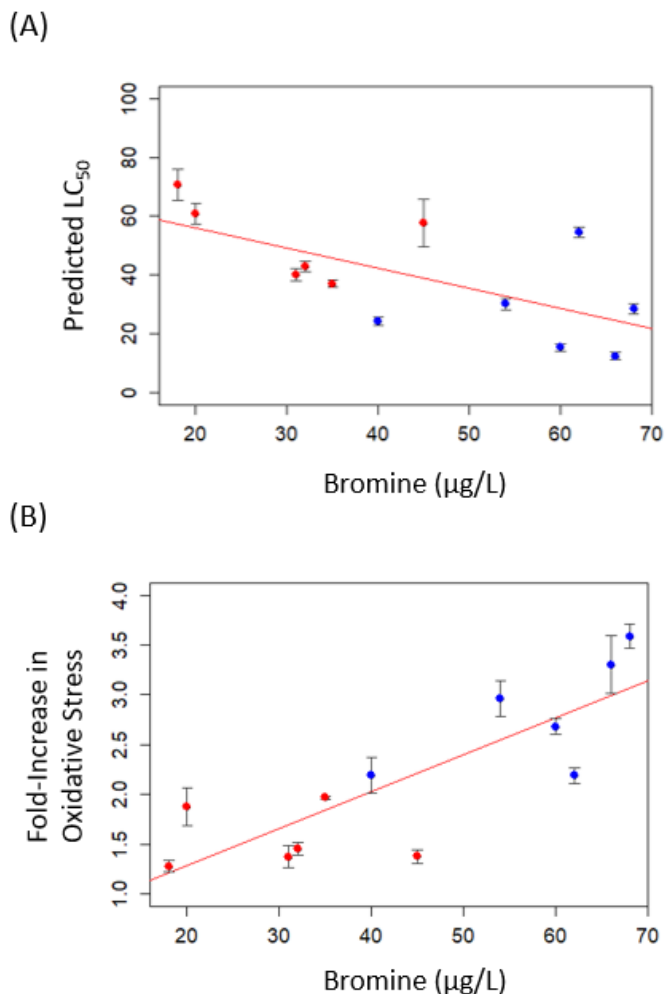


Fig. 4.5. Relationships between concentrations of total Br and (A) predicted LC₅₀ values and (B) oxidative stress induced by concentrated water extracts (15 x) collected at the clearwell (red) and finished stages (blue) of treatment. Linear model for predicted LC₅₀: $R^2 = 0.43$, $F_{1,10} = 7.44$, $p = 0.021$. Linear model for oxidative stress: $R^2 = 0.67$, $F_{1,10} = 20.68$, $p = 0.0011$.

Interestingly, very similar correlations were found between chlorine doses (pre- and post-chlorine) and toxic potencies of clearwell and finished water when both stages of treatment were incorporated into a single model (Fig. 4.6). R^2 , p , and F-statistics were nearly identical to those

determined between concentrations of Br and toxic potencies. This indicated that doses of chlorine and concentrations of Br have equal power in predicting mixture toxicity of DBPs. A linear correlation was found between applied doses of chlorine and the concentration of additional Br introduced at associated stages of treatment, corrected by concentrations of Br present at previous treatment units ($R^2 = 0.63$, $F_{1,10} = 17.29$, $p = 0.002$) (Fig. C.8). While this relationship was significant, it cannot account for the fact that different tanks of Cl_2 were supplied to and used by the DWTP throughout the year. These tanks could have varying amounts of Br impurities that could weaken the strength of the linear correlation.

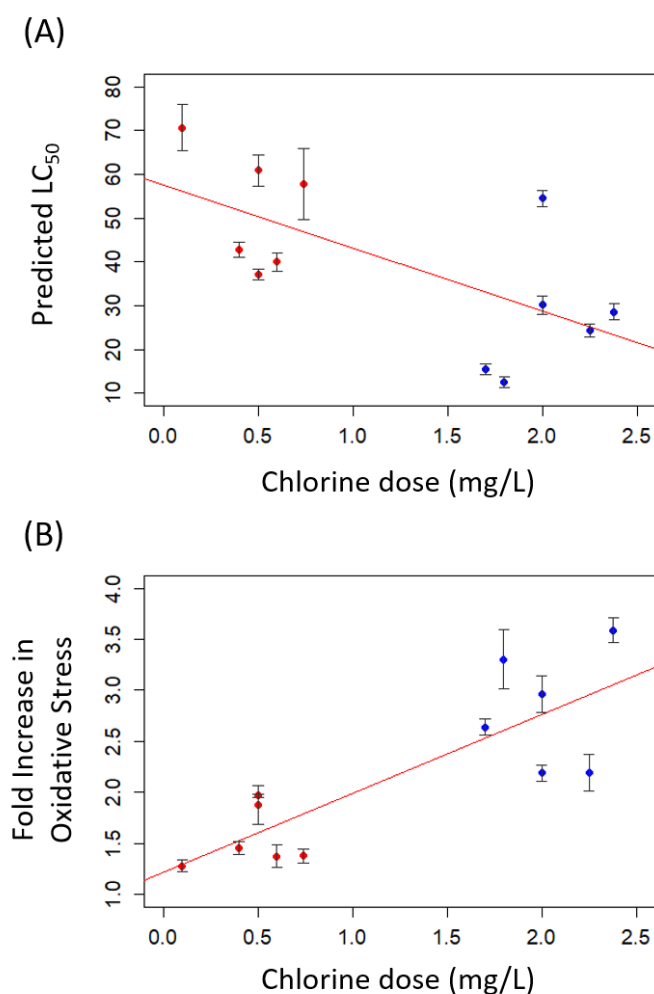


Fig. 4.6. Relationships between pre- and post-chlorine doses with (A) predicted LC_{50} values and (B) oxidative stress induced by concentrated water extracts (15 x) collected at the clearwell (red) and finished stages (blue) of treatment. Linear model for predicted LC_{50} : $R^2 = 0.43$, $F_{1,10} = 7.44$, $p = 0.021$. Linear model for oxidative stress: $R^2 = 0.68$, $F_{1,10} = 21.0$, $p = 0.001$.

Uncertainties remain as to why concentrations of total Br increased through the treatment process at the DWTP studied in this project, but correlations to occurrences of unregulated Br-DBPs (Section 3.3.4), mixture toxicities, and applied doses of chlorine are intriguing. If Br impurities found in chlorine disinfectants were confirmed as the source of additional Br, this would be a considerable finding that could result in stricter regulations for Br impurities in chlorine disinfectants used in drinking water systems, particularly for DWTPs that source low-Br containing waters. In doing so, an early process modification could allow DWTPs to reduce the occurrences of Br-DBPs as well as reduce whole mixture toxicity of drinking water.

4.4 Conclusions

There are few studies in the literature that explore whole mixture toxicity of DBPs found in plant-scale, chlorinated samples of drinking water. While the HIWATE project was able to identify significant correlations between cytotoxicity of XAD extracted samples of drinking water and occurrences of 21 DBPs in spatially unique samples, this study represents the first to explore temporal changes in toxicity associated with complex mixtures of DBPs. In this study, measures of toxicity do not indicate that there is great risk posed to those who drink public water; rather, they act as a tool for comparison of trends. Primary findings include:

- Cytotoxicity was greatest in finished water collected in November and March, which created interest in exploring cluster 1 and cluster 2 compounds (Fig. 3.3) in more targeted cytotoxicity assessments.
- Oxidative stress was greatest in finished water collected in June and November, which created interest in exploring cluster 4 compounds (Fig. 3.3) in more targeted assessments of oxidative stress.
- Oxidative stress and cytotoxicity were significantly correlated when data from both clearwell and finished stages were compared, which suggests DBPs that cause cytotoxicity might primarily act via oxidative stress.
- Br-DBPs classified as Br₂, BrCl, N-DBPs, and S-DBPs might represent the classes that contribute most significantly to whole mixture toxicity, however, characterization of Cl-DBPs and I-DBPs should be performed in future work.

- 16 h Nrf2/ARE oxidative stress assay might be a more sensitive and selective assay than the 72 h CHO cytotoxicity assay for comparing toxicity of mixtures of DBPs.
- Concentrations of Br in treated water showed similar predictive capacity as applied chlorine doses in predicting whole mixture toxicity of DBPs; Concentration of Br has potential to be used as a surrogate measure for whole mixture toxicity of DBPs.

This work is limited by the fact that only abundances of Br-DBPs were characterized. Cl-DBPs are generally detected at greater abundances than Br-DBPs and likely contributed to cytotoxicity and oxidative stress observed in this study, but Br-DBPs are consistently more toxic than their chlorinated analogues which is why they were the focus of this research. Additionally, some volatile DBPs might not have been captured by the SPE methods used for extraction. That said, the versatility of HLB cartridges and demonstrated enhanced extractability of many Br-DBPs after pH adjustment to 2 (Fig. 2.2) supports the belief that extracts used in this study are representative of real mixtures of DBPs found in drinking water. As samples from only six months were extracted for toxicity assessment, future work would benefit from including all 12 months of the year to capture a full picture of how toxicity changes with time. In particular, correlations in seasonal trends might have been strengthened with inclusion of samples from August, as it possesses the greatest mean temperature, and July and February, as they correspond to months that saw peaks in detection of Br-DBPs classified as cluster 3 and 1, respectively (Fig. 3.3). Perhaps with a greater understanding of what conditions drive the overall toxicity of complex mixtures of DBPs, DWTPs could focus on risk reduction rather than control of individual DBPs.

4.5 Supporting Information

Supporting information can be found in Appendix C4 and provides details on (1) chemicals and reagents; (2) conditions for chemical analysis of Br-DBPs; (3) standard curve produced for iodoacetic acid; (4) dose-response curves for concentrated water extracts subjected to the 72 h CHO-K1 cytotoxicity assay; (5) relationships between cytotoxicity of raw and clearwell waters with that of finished water; (6) results from the Nrf2/ARE oxidative stress assay and the MTT cytotoxicity assay; (7) relationships between oxidative stress of raw and clearwell

waters with that of finished water; (8) significant relationships identified to toxicity of finished water; (9) linear models between concentration of total Br and endpoints of toxicity; and (10) correlation between applied doses of chlorine and introduction of Br to the water treatment process.

4.6 Acknowledgements

This work was supported by a Discovery Grant from the Natural Science and Engineering Research Council of Canada [Project # 326415-07] and a grant from the Western Economic Diversification Canada [Projects # 6578, 6807 and 000012711]. Prof. Giesy was supported by the Canada Research Chair program, and the 2014 "High Level Foreign Experts" [#GDT20143200016] program, funded by the State Administration of Foreign Experts Affairs, the P.R. China to Nanjing University, and the Einstein Professor Program of the Chinese Academy of Sciences and a Distinguished Visiting Professorship in the School of Biological Sciences of the University of Hong Kong. Prof. Peng was supported by a Discovery Grant from the Natural Science and Engineering Research Council of Canada [Project # RGPIN-2018-06511] and University of Toronto Start-up Funds.

CHAPTER 5

GENERAL DISCUSSION

5.1 Project Rationale and Summary

There are many challenges in the study of DBPs that have created gaps in understanding, particularly for DBPs for which there are no regulatory guidelines. The small abundances at which these DBPs exist, their chemical diversity, and the lack of available chemical standards have contributed to only half of total organic halogen (TOX) of disinfected water being accounted for by described DBPs (Plewa and Wagner, 2009). Furthermore, temporal and spatial variations in the detection of DBPs makes generalization of findings difficult. One of the goals of this project was to increase understanding of occurrences of unregulated DBPs in drinking water, in particular, unregulated Br-DBPs due to their enhanced toxicities compared to Cl-DBPs. To do this, a DIPIC-Frag method previously used to detect organo-bromine compounds in sediment was adapted for full spectrum screening of plant-scale chlorinated water (Chapter 2). A mass spectrometry library of Br-DBPs and I-DBPs was established and the method was shown to be reproducible and reliable for comparative analysis of unique samples of water. This encouraged application of the method for investigation of temporal trends of unregulated Br-DBPs.

A year-long study was then conducted in which samples of raw, clearwell, and finished water were collected each month from a second DWTP (Chapter 3). Trends in occurrences of Br-DBPs through the treatment process as well as over time were investigated. There are multiple factors thought to influence formation of regulated THMs and HAAs, such as temperature or TOC of raw water, but less is known for unregulated Br-DBPs. Therefore, correlation analyses based on parameters of raw water, chlorine doses, and concentrations of Br were used to identify variables that may favour formation of unregulated Br-DBPs. While correlation analysis of field samples cannot define causative relationships, in this study it was used for preliminary investigations to suggest parameters for further study. The use of field samples collected from an operational DWTP is advantageous because chlorine doses and contact times accurately describe methods used in the real world. Additionally, the use of samples from DWTPs provided an opportunity to explore formation of DBPs with regard to regional interests rather than producing data based on reference materials such as Suwannee River NOM.

Another challenge in studies of DBPs is the fact that DBPs exist in mixtures, yet most research on toxicity focusses on chemical synthesis and *in vitro* toxicity assessment of individual compounds. It is a challenge to assess each DBP individually because more than 700 DBPs have

been identified in drinking water and that number continues to increase with the development of analytical instruments with enhanced sensitivity and resolution. Therefore, the last research chapter (Chapter 4) provides insight into how toxicities of DBP mixtures change over time. Multiple assays were tested for their ability to quantify and compare toxicity induced by concentrated extracts of water including the Microtox[®], Micro Ames, and single cell gel electrophoresis (SCGE) assay (results not shown), but it was the 72 h CHO-K1 cytotoxicity assay and the 16 h Nrf2/ARE oxidative stress assay that demonstrated the required sensitivity and specificity. The 72 h CHO-K1 cytotoxicity assay was adapted from a protocol published by The Water Research Foundation for assessment of toxicity of individual DBPs, while the 16 h Nrf2/ARE oxidative stress assay was chosen based on numerous publications that have linked oxidative stress with cytotoxicity and genotoxicity induced by DBPs (Austin et al., 1996; Cemeli et al., 2006; Dad et al., 2013; Gao et al., 1996; Lilly et al., 1997; Pals et al., 2013). The Nrf2/ARE pathway is a general, downstream response activated by both ROS and electrophiles, which is advantageous for assessing toxicity of chemically diverse compounds such as DBPs (Kansanen et al., 2013; Nguyen et al., 2009). After temporal trends in toxicity were described, correlation analysis was again performed to determine if parameters of water quality or treatment conditions could explain observed patterns.

5.1.1 Application of the DIPIC-Frag Method for Untargeted Detection of Br-DBPs

The DIPIC-Frag method has previously been used to screen sediments and house dust for brominated compounds (Peng et al., 2016c, 2016a, 2015). To apply the method to samples of drinking water, conditions of chemical extraction, liquid chromatography, and mass spectrometry needed to be modified due to differences in matrices as well as properties of brominated compounds found in each matrix. For sediment, analysis required use of accelerated solvent extraction, Florisil SPE cartridges, a Hypersil GOLD[™] C18 column, and atmospheric pressure chemical ionization (APCI-) (Peng et al., 2015). 1593 unique brominated compounds were detected and assigned formulae with m/z ranging from 170.9438 – 997.5217 and number of bromine atoms ranging from 1 – 8. For house dust, analysis required two-step organic extraction, Florisil SPE cartridges, a Hypersil GOLD[™] C18 column, and atmospheric pressure photoionization (APPI-) (Peng et al., 2016c). 738 unique brominated compounds were detected

and assigned formulae with m/z ranging from 229.9558 – 1000.868 and number of bromine atoms ranging from 1 – 9. In contrast, the greatest chemical coverage of DBPs in drinking water was achieved by use of an HLB_pH2 SPE method, Amide LC column, and ESI- source. A non-redundant library of 553 Br-DBPs was established with m/z ranging from 170.884 – 497.0278 and the number of bromine atoms ranged from 1 – 3. Greater polarities of Br-DBPs compared to organo-bromine compounds found in other matrices probably explains why they were poorly retained on a C18 column and required a hydrophilic interaction chromatography (HILIC, Amide) column, as well as why better ionization was achieved by ESI (Michael J Plewa et al., 2004; Richardson et al., 2008; Zhang et al., 2008). Another major difference between Br-DBPs and organo-bromines found in sediment or house dust is the degree of halogenation. It is possible that with additional research, degree of halogenation could be used to differentiate emission sources of brominated compounds found in the environment.

Compared to other analytical methods used in studies of DBPs, the DIPIC-Frag method has many advantages. For example, FT-ICR MS has been a useful tool for detection of novel DBPs. It was used to detect ~ 800 Cl-DBPs in drinking water and ~ 500 Br-DBPs in laboratory-produced chlorinated water (Gonsior et al., 2014; Zhang et al., 2014). Although FT-ICR MS is rapidly improving, direct injection methods are often used (Junot et al., 2010). Direct injection methods are more likely to suffer from matrix effects and thereby poses a challenge for comparative analysis of drinking water, especially since internal/external standards are not available for most detected DBPs. Compatibility of the DIPIC-Frag method with HPLC also made it possible to differentiate isomers of DBPs that have the same exact m/z value, an objective that could not be achieved by previous direct infusion methods (Gong & Zhang, 2015; Zhang et al., 2014). This is a significant advantage because of the 553 Br-DBPs detected (Chapter 2), 204 (37%) had isomers.

The library created by the DIPIC-Frag method (Chapter 2) represents the largest mass spectrometry library for Br-DBPs and I-DBPs detected in plant-scale chlorinated water. The use of plant-scale chlorinated water is significant because the treatment conditions represent those used in real-world scenarios. In Chapter 2, conditions of the DWTP represented two time points (October 2015 and April 2016) as well as two treatment processes that differed in the point at which chlorine was added (at raw water intake or after clarification). On sampling dates, concentrations of bromide in source water were 0.04 mg/L, temperature of raw water was 11.5

and 5.1 °C, primary chlorination doses were 4.38 and 3.45 mg/L, and chlorine contact times were 49 and 190 min, respectively. In contrast, the 478 Br-DBPs detected in laboratory-scale chlorinated drinking water were produced by water containing 2.0 mg/L sodium bromide and 3.0 mg/L Suwannee River fulvic acid standard material, treated with 5 mg/L Cl₂ at 20 °C for five days (Zhang et al., 2014). Concentration of bromide, chlorine dose, temperature, and chlorine contact time are all known to affect concentration and speciation of DBPs in dynamic ways, and often in laboratory chlorination experiments they are elevated to create favourable conditions. So, while controlled laboratory experiments can contribute valuable information to literature by isolating the effect of individual variables, responses are often amplified compared to what might be expected in actual drinking water.

5.1.2 Unregulated Br-DBPs in Saskatchewan Drinking Water Treatment Plants

MS² spectra and public databases were used to predict structures for 41/50 and 9/10 of the most abundant Br-DBPs and I-DBPs, respectively (Section 2.3.6). Identified in the list of abundant Br-DBPs were many aromatic acids or phenols, five heteroatomic compounds, and four sulfonic acids (Table A.1). Types of predicted structures were consistent with results of analyses with FT-ICR MS or UPLC/ESI triple quad MS (Gonsior et al., 2014; Pan et al., 2016a; Zhang et al., 2014). An optimized analytical method and established library were used to screen samples of raw, clearwell, and fully treated samples of water collected at a second DWTP located in central Saskatchewan (Chapter 3). The 54 most abundant Br-DBPs were identified with ten being similarly abundant between the two studied DWTPs: C₈H₅O₅Br, CH₂O₃SClBr, C₅H₂O₃ClBr, C₅HO₃ClBr₂, C₅HO₃Cl₂Br, C₇H₇O₆Br, C₇H₄O₃Br₂, C₇H₄O₃ClBr, C₂H₂O₂ClBr, and C₈H₄O₅Br₂. Predicted structures for this list include a methanesulfonic acid, two trihalo-HCDs, various carboxylic and phenolic aromatic compounds, and bromochloroacetic acid which is not included in the five HAAs currently regulated by the US EPA (Table A.1). Trihalo-HCDs and methanesulfonic acids emerged as two classes of interest based on their recent identification as DBPs and their relatively great ion abundances detected at two distinct DWTPs in Saskatchewan (Pan et al., 2016a; Zahn et al., 2016). A correlation matrix of the 54 most abundant, unregulated Br-DBPs indicated that many Br-DBPs were positively associated in their occurrences, with

isomers and structural analogues co-occurring together in time as well as through the treatment process.

Fifty three (53) of the 54 investigated Br-DBPs (98.1%) were detected in finished waters and 52 of 54 (96.3%) Br-DBPs were also detected in clearwell waters even though only relatively small pre-chlorination dosages were applied prior to the clearwell (0.46 ± 0.17 mg/L, compared to 2.0 ± 0.23 mg/L as the post-chlorine dose) (Table B.2) (Chapter 3). Three trends were identified for formation of unregulated Br-DBPs through treatment processes (clusters I, II, and III; Fig. 3.2A). While abundances of most Br-DBPs increased through the process, Br-DBPs of cluster I showed unexpected decreases between clearwell and finished waters, which was significantly related to chemical properties of low O/C and Br/C ratios. Four monthly trends were also identified for formation of Br-DBPs over time (clusters 1-4, Fig. 3.3). While the trends were diverse, three of four (clusters 1, 3, and 4) showed common peaks in abundance in summer (June or July). This was consistent with the common conclusion in literature that regulated DBPs are most common during summer months (Domínguez-Tello et al., 2015; Kim, 2009; Richardson et al., 2003; Rodriguez and Sérodes, 2001; Serrano et al., 2015; Zhang et al., 2005).

5.1.3 Toxicity of Unregulated Br-DBP Mixtures

Raw, clearwell, and finished samples of water from the months April, June, September, November, January, and March were tested by two *in vitro* assays: 1) a 72 h CHO-K1 cytotoxicity assay; and 2) a 16 h Nrf2/ARE oxidative stress assay (Chapter 4). Observed responses did not indicate that there is a risk for public consumption of chlorinated water, but rather these assays allowed for comparative analysis of trends in toxic potencies. For both assays there was a general trend of increasing toxicity as water moved through the treatment process, which was similar to the trend in formation for cluster III Br-DBPs (Fig. 4.1A and 4.2A). Differences were observed in temporal trends of toxic endpoints (Fig. 4.1B and 4.2B). Cytotoxicity was greatest in finished water collected in November and March, which created interest in exploring seasonal clusters 1 and 2 (Fig. 3.3) in more targeted cytotoxicity assessments. Oxidative stress was greatest in finished water collected in June and November, which created interest in exploring compounds in seasonal cluster 4 (Fig. 3.3) in more targeted assessments of oxidative stress. Cytotoxicity and oxidative stress were not significantly

correlated in clearwell or finished water when stages of treatment were considered separately ($R^2 = 0.10$ and 0.20 ; $p = 0.53$ and 0.37 , respectively), in part due to small sample size. However, when data from both stages were incorporated in the same model these endpoints were significant correlated ($R^2 = 0.53$, $p = 7.4 \times 10^{-3}$) (Fig. 4.4). This may indicate that in complex mixtures of DBPs, compounds responsible for cytotoxicity may act primarily via mechanisms of oxidative stress.

When classes of unregulated Br-DBPs were assessed for their contribution to toxic potencies of mixtures, a greater number of classes were correlated to oxidative stress (Table 4.3). Br₂, BrCl, and S-DBPs were significantly correlated to cytotoxicity, while all Br-DBPs (54), Br₂, BrCl, S-DBPs, and N-DBPs were significantly correlated to oxidative stress. Overall, results indicated that the 16 h Nrf2/ARE oxidative stress assay may be a more sensitive and selective assay for comparing toxicity of mixtures of DBPs. This is consistent with results of other studies that have compared cytotoxicity of DBPs by Microtox[®] assay to activation of the Nrf2/ARE oxidative stress pathway (Escher et al., 2012; Stalter et al., 2016).

5.1.4 Predicting the Occurrence of Br-DBPs and Toxicity of DBP Mixtures

With temporally unique samples of raw, clearwell, and finished drinking water correlation analyses were performed to identify parameters that could potentially predict occurrences of unregulated Br-DBPs as well as the toxicity associated with real mixtures of DBPs. Parameters of interest included raw water temperature, turbidity, UVT, colour, river level, SUVA, UV₂₅₄, concentrations of total organic carbon (TOC), Br as determined by ICP-MS, and applied doses of chlorine. Few significant correlations were identified between ion abundances of Br-DBPs and these parameters (Fig. 3.4 and B.7). Temperature of raw water demonstrated the greatest number of significant correlations to Br-DBPs with six positive and three negative relationships. Similarly, parameters of water quality were not strongly correlated to temporal trends in toxic potencies of mixtures (Fig. 4.4), but as river level increased the DWTP might expect to output finished water with decreased potential to cause oxidative stress.

The most significant finding of the study reported in this thesis was the unexpected increase in concentration of Br as water moved from the raw water intake (0.013-0.038 mg/L), to clearwell (0.018-0.065 mg/L), to the finished stage of treatment (0.040-0.120 mg/L) (Fig. 3.5).

Rather, it was expected that the concentration of total Br would remain relatively constant or decrease due to volatilization of some Br-DBPs. This encouraged further exploration of relationships between concentrations of Br, Br-DBPs, and toxic potencies of mixtures at related stages of treatment. When clearwell and finished stages were investigated together, concentrations of Br were found to be significantly correlated to detection of 34/54 unregulated Br-DBPs at $\alpha = 0.05$. Those that were not significantly correlated with concentration of Br were typically formed via the cluster I trend through the treatment process. Concentrations of Br were also significantly correlated to cytotoxicity ($R^2 = 0.43$, $p = 0.021$) and oxidative stress ($R^2 = 0.67$, $p = 0.0011$) of corresponding waters (Fig. 4.5). Similar correlations were found between chlorine doses (pre- and post-chlorine) and toxic potencies of clearwell and finished water when both stages of treatment were incorporated into a single model (Fig. 4.6). R^2 , p , and F-statistics were nearly identical to those determined between concentrations of Br and toxic potencies. This indicated that doses of chlorine and concentrations of Br had equal power in predicting toxic potencies of mixtures of DBPs and that concentration of Br might be the single parameter that DWTPs could monitor to predict whole mixture toxicity of DBPs.

While the exact source of additional Br throughout the treatment process remains unconfirmed, it must be related to disinfection since the only treatment step between clearwell and finished water is post-chlorination. The relationships between applied doses of chlorine (pre- and post-) with changes in concentration of Br at related stages was significant ($R^2 = 0.63$, $p = 0.002$), which seems to support this conclusion (Fig. C.8). Br₂, bromine chloride (BrCl), and other brominated contaminants are known to occur as impurities in chlorine gas used for disinfection of drinking water, and current NSF 60 criteria specify 1 mg Br/L as the single product allowable concentration for any reagents used in the production of chlorine disinfectants (De Nora Water Technologies, 2015; MacPhee et al., 2002; The NSF Joint Committee on Drinking Treatment Chemicals, 2013). The acceptable concentration of Br impurities is small, but might be enough to affect concentrations of Br at the DWTP studied here, where background concentrations of Br in raw water were particularly low. If Br impurities found in chlorine disinfectants were confirmed as the source of additional Br, this would be a considerable finding that could result in stricter regulations for Br impurities in chlorine disinfectants used in drinking water systems, particularly for DWTPs that source low-Br containing waters. In doing so, an early process modification could allow DWTPs to reduce the occurrences of Br-DBPs as

well as reduce whole mixture toxicity, thereby increasing safety of drinking water. Future work is warranted to discern whether or not impurities in chlorine disinfectants are truly the source.

5.2 Limitations

This work is limited by the fact that in Chapter 3 and 4 only abundances of Br-DBPs were characterized. Br-DBPs consistently have greater toxic potencies than do their chlorinated analogues; however, Cl-DBPs are generally detected at greater abundances than Br-DBPs and likely contributed to some of the cytotoxicity and oxidative stress observed in this study. There is a plan to screen the same samples in this study for Cl-DBPs, but the scope of that research is beyond this thesis. Additionally, some volatile DBPs may not have been captured by the SPE methods used for extraction. The versatility of HLB cartridges (all purpose, strong hydrophilic polymer with lipophilic balance) and demonstrated enhanced extractability of many Br-DBPs after pH adjustment to 2 (Fig. 2.2) supports the belief that extracts used in this study are representative of real mixtures of DBPs found in drinking water.

Another limitation of this work is the number of observations used to create correlation matrices in Chapter 3 and 4. In Fig. 3.1A, there were 22 observations for each Br-DBP, but for Fig. 3.4 and A.1 there were only 11 observations, and for the correlation matrix produced with toxicity values (Fig. 4.4) there were only 6 observations. With these sample sizes, particularly Fig. 4.4, the correlations and significance levels are questionable. With greater sample sizes some relationships may have become significant, but that would have required greater investment of resources to complete. Since samples from only six months were extracted for toxicity assessment, future work would benefit from including all 12 months of the year to capture a full picture and reduce uncertainty in predictions. Sampling in August was interrupted by an oil spill, which affected this study because August typically experiences the warmest weather in Saskatchewan. Toxicity data for July and February would have also been valuable for comparing seasonal trends since these two months saw spikes in detection of Br-DBPs of cluster 3 and 1, respectively.

Lastly, since there were so many variables that could affect profiles of Br-DBPs produced within a DWTP, conclusions drawn in this thesis may not be true across all geographical locations. For example, at DWTPs where source water contains elevated background

concentrations of bromine, Br impurities in chlorine disinfectants may not result in an increase in Br of the same relative magnitude. DWTPs that employ ozonation as opposed to chlorination would also not expect to see changes in concentration of Br during treatment.

5.3 Future Research Considerations

This research project has provided insight on the occurrences of unregulated Br-DBPs as well as the toxicities of complex mixtures of DBPs, with focus placed on identification of predictors for observed temporal trends. It has also created a framework for future projects as follows:

- 1) Both DWTPs studied in this project use chlorination as their primary disinfectant. It would be interesting to collect samples of treated water from plants that use alternative disinfectants such as ozone, chloramines, or a combination of disinfectants. This would certainly expand the library of known Br-DBPs and I-DBPs detected in drinking water. For example, chloramination is known to produce more nitrogenous DBPs. The library could also be expanded by applying the DIPIC-Frag method to geographically distinct DWTPs that source water of varying characteristics.
- 2) The 16 h Nrf2/ARE oxidative stress assay was able to statistically differentiate raw, clearwell, and finished stages of treatment. Potentially, it could be used to compare samples of water collected from additional stages of treatment. Operators at DWTPs could then gain a more in-depth understanding of what processes increase or decrease whole mixture toxicity and modify their processes as needed.
- 3) There is also potential to apply methods in this thesis to bench-scale chlorination experiments, which would allow variables to be isolated and causative relationships to be confirmed. For example, it is uncommon for bench-scale chlorination experiments to assess whole mixture toxicity but with the HLB_pH2 extraction method and 16 h Nrf2/ARE oxidative stress assay the relationship between water temperature and toxicity of DBP mixtures could be evaluated.
- 4) An attempt was made to use the HLB_pH2 extraction method and 16 h Nrf2/ARE oxidative stress assay in an effects-directed analysis; however, the chosen HPLC method did not separate the complex mixture of DBPs sufficiently. Changes in column pressure,

small injection volumes, and limited elution volumes made it difficult to accurately predict concentration factors and limited the number of assays that could be completed. Perhaps with a preparative column, an effects-directed analysis could be performed to identify fractions of concentrated water extracts that induce the greatest oxidative stress. Paired with chemical analysis, this could reveal unregulated DBPs of greatest concern.

- 5) The Water Research Foundation has published protocols for a standardized SCGE assay that uses a CHO AS52 cell line for comparison of genotoxicity induced by DBP standards (Plewa and Wagner, 2009; Wagner and Plewa, 2017). Time was dedicated to optimizing this assay for the purpose of evaluating whole mixture toxicity of concentrated water extracts, however, the CHO AS52 cell line is not commercially available and efforts to obtain the cell line were unsuccessful. In place, a CHO-K1 cell line ((ATCC® CCL-61™) was purchased from Cedarlane (Burlington, ON, CA). Unfortunately, the CHO-K1 cell line lacks *gpt*, an E.coli gene that CHO AS52 possesses (Tindall and Stankowski Jr, 1989). This gene is responsible for enhanced susceptibility to mutagenicity. Therefore, future work could also focus on obtaining the CHO AS52 cell line and comparing seasonal trends in whole mixture genotoxicity.
- 6) Based on this thesis, future work could focus on Br-DBPs detected at high abundance at both DWTPs ($C_8H_5O_5Br$, CH_2O_3SClBr , $C_5H_2O_3ClBr$, $C_5HO_3ClBr_2$, $C_5HO_3Cl_2Br$, $C_7H_7O_6Br$, $C_7H_4O_3Br_2$, $C_7H_4O_3ClBr$, $C_2H_2O_2ClBr$, and $C_8H_4O_5Br_2$), Br-DBPs that followed cluster III through the treatment process (Fig. 3.2), or Br-DBPs that followed cluster 4 over time due to similar peaks in occurrence with peaks in oxidative stress (Fig. 3.3 and 4.2B).

5.4 Conclusion

The three main research objectives of this thesis were as follows:

- Develop a reproducible method for untargeted screening and semi-quantitative comparison of Br-DBPs in samples of drinking water (Chapter 2).
- Identify fates and behaviours of unregulated Br-DBPs in drinking water, and determine if parameters of source water can explain their occurrences (Chapter 3).

- Explore monthly trends in the toxicity of real DBP mixtures by use of *in vitro* assays, and identify variables that may predict whole mixture toxicity of DBPs (Chapter 4).

These objectives were achieved and this thesis contributes novel findings and concepts to the field of DBP research. First, a reproducible and semi-quantitative method was developed for untargeted screening of Br-DBPs and I-DBPs in chlorinated water. Using this method, the largest mass spectrometry library of Br-DBPs and I-DBPs in real drinking water was established. Then, initial work was completed to better understand how unregulated Br-DBPs change through the treatment process as well as over time. Of most significance was the conclusion that concentrations of Br increased through the treatment process, and that it was the best predictor for occurrences of unregulated Br-DBPs. Temporal trends in toxicity were explored by use of a 72 h CHO-K1 cytotoxicity assay and a 16 h Nrf2/ARE oxidative stress assay. This study represents the first to explore temporal changes in toxicity associated with complex mixtures of DBPs and the first to correlate concentration of Br and applied doses of chlorine to toxicities of plant-scale chlorinated water. The 16 h Nrf2/ARE oxidative stress assay demonstrated to be more sensitive for comparison of *in vitro* toxicity associated with DBP mixtures compared to the 72 h CHO chronic cytotoxicity assay. Oxidative stress has been correlated to both cytotoxicity and genotoxicity of DBPs, therefore, it is recommended that oxidative stress, specifically the general downstream response of the Nrf2/ARE pathway, be used in future work to compare toxicities of complex mixtures of DBPs. Perhaps with an understanding of what conditions drive the overall toxic potencies of complex mixtures of DBPs, DWTPs could focus on risk reduction rather than control of individual DBPs.

APPENDICES

APPENDIX A

CHAPTER 2 SUPPORTING INFORMATION

This supporting information provides text and figures addressing: (1) chemicals and reagents; (2) the water treatment process; (3) LC-Q Exactive data acquisition; (4) chemometric analysis; (5) predicted chemical structures of the top 50 Br-DBPs; (6) predicted chemical structures of the top 10 I-DBPs; (7) raw water parameters and treatment conditions at the times and locations of water sample collection; (8) concentrations of free and total chlorine in samples collected for the quench study; (9) schematic workflow of the homologue models; (10) chromatograms of Br-DBPs with ESI or APCI ionization sources; (11) chromatograms of Br-DBPs on C18 or Amide columns; (12) chromatograms of Br-DBPs with different SPE methods; (13) plot of detected DBPs; (14) chromatograms of isomers of Br-DBPs; (15) detection of DBPs in the quench study; (16) the ratios of I-DBPs to corresponding Br-DBPs; (17) chromatograms of halogenated sulfonic acids.

Chemicals and Reagents

4-bromophenol, bromoacetic acid, iodoacetic acid, bromomethanesulfonic acid, ascorbic acid, and sodium thiosulfate were purchased from Sigma-Aldrich Chemical Co. (St. Louis, MO, USA). Oasis HLB (6 cc, 500 mg, 30 μ m), WAX (6 cc, 150 mg, 30 μ m) and C18 (6 cc, 1 g, 30 μ m) solid phase extraction cartridges were purchased from Waters (Milford, MA, USA). Dichloromethane (DCM), methanol, and acetone, Omni-Solv grade, were purchased from EMD Chemicals (Gibbstown, NJ, USA).

Water Treatment Process

At the water treatment plant, which is the subject of this report, the process begins at a lake pumping station where water from a small, eutrophic lake is pre-chlorinated (primary disinfection) before being pumped 3 km to the main building to undergo cascade degasification, alum coagulation, flocculation, clarification, sand filtration, and a final dosing of chlorine (Fig. A.1). It is not typical for primary disinfection to occur at the beginning of the drinking water treatment process, but this treatment plant chooses to do so to reduce bacterial growth in the water transport pipe and to reduce issues with taste and odour compounds. In April 2016 the plant was operating a test in which pre-chlorination was removed. Instead, primary disinfection occurred between clarification and sand filtration, therefore, samples collected in April 2016 were collected post-sand filtration.

August 17, 2017, samples were collected for the quench study. At this time the plant had returned to performing pre-chlorination and their granular activated carbon (GAC) filter was in operation after sand filtration. The GAC filter removes many compounds including DBPs by adsorption, therefore, samples were collected before this stage of treatment (preGAC).

LC-Q Exactive Data Acquisition

Aliquots of extracts were analyzed using a Q ExactiveTM UHRMS (Thermo Fisher Scientific) equipped with a DionexTM UltiMateTM 3000 UHPLC system (Thermo Fisher Scientific). TSKgel Amide-80 (3 μ m; 4.6 mm \times 150 mm; TOSOH) was selected for the present method based on its ability to separate DBPs in preliminary investigations. Injection volume was 5 μ L. Ultrapure water containing 0.1% NH₄OH (A) and acetonitrile containing 0.1% NH₄OH (B)

were used as mobile phases. Initially 95% of B was decreased to 90% in 18 min, then decreased to 30% at 26 min, followed by an increase to initial conditions of 95% of B held for 3 min to allow for equilibration. The flow rate was 0.40 mL/min. Temperatures of the column and sample compartment were maintained at 30 °C and 10 °C, respectively.

Data were acquired in data-independent acquisition (DIA) mode. Parameters for DIA were one full MS¹ scan recorded at resolution R=70,000 (at m/z 200) with a maximum of 3×10^6 ions collected within 100 ms, followed by six DIA MS/MS scans recorded at a resolution R=35,000 (at m/z 200) with a maximum of 1×10^5 ions collected within 60 ms. DIA data were collected using 5- m/z -wide isolation windows per MS/MS scan. Each DIA MS/MS scan was chosen for analysis from a list of all 5 m/z isolation windows. In these experiments, 80 5- m/z -wide windows between 100 and 500 m/z , were grouped into four separate methods, each of which contained 20 windows. Mass spectrometric settings for APCI (-) mode were: discharge current, 10 μ A; capillary temperature, 225 °C; sheath gas, 20 L/h; auxiliary gas, 5 L/h; and probe heater temperature, 350 °C. Mass spectrometric settings for ESI (-) mode were: spray voltage, 2.8 kV; capillary temperature, 300 °C; sheath gas, 35 L/h; auxiliary gas, 8 L/h; and probe heater temperature, 325 °C.

Quality Control and Assurance

To avoid contamination of samples, all equipment was rinsed regularly with methanol. One procedural blank using ultrapure water was incorporated in the analytical procedure. 17 brominated compound peaks and 3 iodinated compound peaks were detected in the blank. Background contamination from blanks was subtracted from samples for downstream data analysis, and those DBPs whose abundance was less than 3 times the background abundance in blanks were considered non-detected. Some halogenated compounds were also detected in source water, and thus only those compounds showing >3-fold higher abundance in chlorinated water samples than source water samples were considered to be DBPs produced during chlorination process.

Because most detected DBPs were unregulated compounds for which no authentic standards were available, intensities of peaks were used to semi-quantify their relative abundances, as has been done previously for organo-bromine compounds (Peng et al., 2016a,

2015). To enhance comparability among samples and avoid potential shifts in sensitivity among compounds during multiple injections, the methods (4 methods in total for each sample, to cover all the mass range) were run at the same time for all samples. Method detection limits (MDLs) could not be calculated for DBPs, but a peak intensity cutoff of 50,000 (Br-DBPs) or 10,000 (I-DBPs) was incorporated into the DIPIC-Frag method as described previously (Peng et al., 2016a), and used as the MDL for the DBPs. For DBP peaks detected in blanks, 3× the peak abundance were used as MDLs.

Chemometric Analysis of DIPIC-Frag Results

A novel chemometric strategy was developed to expand the number of DBPs detected and reduce rates of false positives of predicted precursor ions and compound formulae.

Peak detection and matching among samples. Detection of Br-DBPs or I-DBPs was accomplished by extracting m/z values of iodine fragment ($m/z=126.9045$) or bromine fragment ($m/z=78.9171$) in each of the 80 DIA windows (10 ppm mass window). Only those peaks exceeding the cutoff peak intensity (50,000 and 10,000 for Br-DBPs and I-DBPs respectively) were analyzed further. For isomers with similar retention times and m/z values, a local regression fitting method (LOESS) was used to adjust for shifts between runs, as done in a previous metabolomics study (Smith et al., 2006), in order to avoid potential effects of shifts in retention time on alignments of peaks among samples.

Precursor ion alignment and formula prediction. While there are 37 known isotopes of iodine with masses ranging from 108 to 144, all but ^{127}I undergo radioactive decay. To identify precursor ions and propose compound formulae with confidence, a robust scoring system was developed to determine precursor ions and compound formulae of DBPs.

(1) *Elution profiles.* The initial step in the analysis required a reduction of the number of precursor ions. This was facilitated by correlation of iodine/bromine peaks with each of the precursor ions from “precursor ion regions” detected at the exact scanning point at the top of the bromine/iodine peaks. But different from our previous studies using correlation to align precursor ions, here all the ions from “precursor ion regions” showing the same retention time as corresponding bromine/iodine fragment peak were included for further data analyses.

Because of the greater peak abundances of precursor ions than product ions after adjustment of the product ion number as described in our previous study (Peng et al., 2015), the precursor ion candidates having intensities less than 20-fold that of iodine peaks were excluded from subsequent analyses.

(2) *Molecular formulae and seven golden standard.* Based on results of previous studies (Peng et al., 2016a, 2015), chemical formulae of DBPs were set to contain up to 100 C, 200 H, 5 N, 30 O, 8 I, 8 Cl, 8 Br, 1 P and 2 S atoms per molecule. Then the mass error (MSerror) of the predicted formulae for each candidate precursor ion was calculated (Equation 1).

$$MSerror = \exp\left\{-0.5 \times \left(\frac{MZ_{act} - MZ_{pred}}{\delta}\right)^2\right\} \quad (1)$$

Where: MZ_{act} is the observed m/z value of precursor ions, and MZ_{pred} are the predicted m/z values of chemical formulae, and δ is the standard derivation of the instrument, which was set to 2.3 ppm according to the well curated library for brominated compounds (Peng et al., 2016a, 2015). The seven golden rules algorithm was used for further filtering of molecular formulae (Kind and Fiehn, 2007). To derive parameters for the seven heuristic rules, which were derived from multiple databases (Kind and Fiehn, 2007), the library of brominated compounds was used to parameterize these rules (Peng et al., 2015). This was found to be more useful to filter incorrect precursor ions and formulae.

(3) *Isotopic peak.* Similarities of isotopic peaks between actual mass spectra and predicted molecular formula were useful to filter out incorrect formulae, especially for sulfur, chlorinated and brominated compounds. According to previous studies (Tsugawa et al., 2015), the similarity of the isotopic peaks could be calculated (Equation 2).

$$Isotope = 1 - \sum |r_{act,i} - r_{pred,i}| \quad (2)$$

$$r_i = \frac{I_{M+i}}{I_M}$$

Where: $r_{act,i}$ is the actual mass spectrum of peakⁱ, $r_{pred,i}$ is the isotopic peak distribution pattern of the predicted formulae, and I_M is the abundance of the monoisotopic compound peak with the greatest abundance.

(4) *Homologue model.* Information for iodinated compounds and brominated homologues could be useful to reduce rates of false positives (-CH₂ and halogen models; Fig. A.1). A score of 1.0 was given to those predicted molecular formulae with homologues detected in the

brominated compounds library.

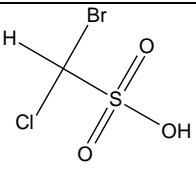
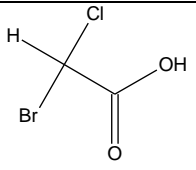
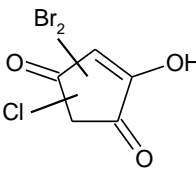
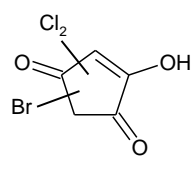
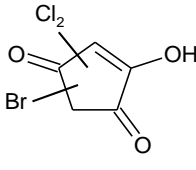
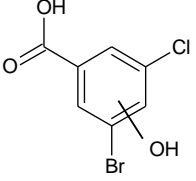
$$\text{Homologue} = \begin{cases} 0, no \\ 1, yes \end{cases} \quad (3)$$

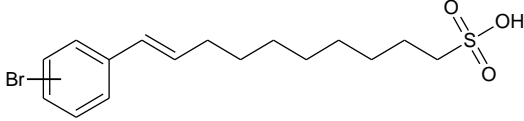
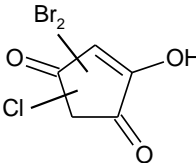
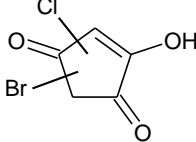
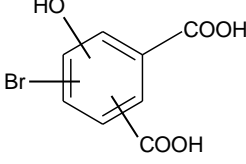
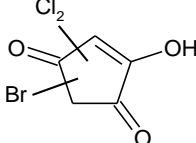
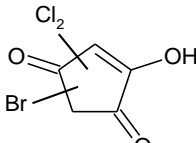
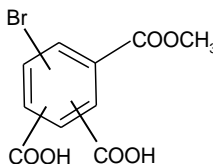
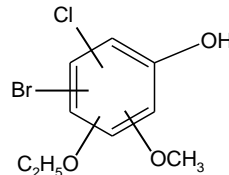
(5) *Final library output.* The total score for each precursor ion and molecular formula was calculated by summing all scores from previous determinations (Equation 4):

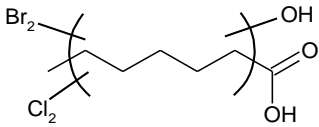
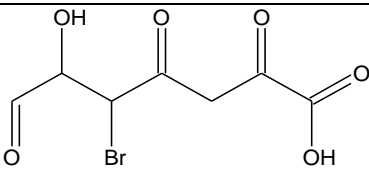
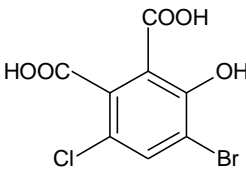
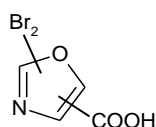
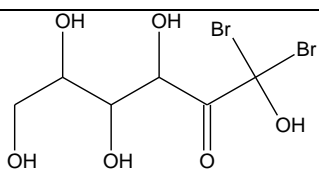
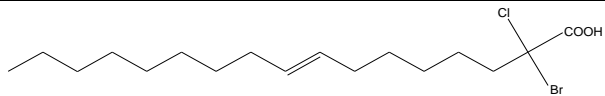
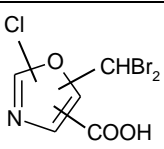
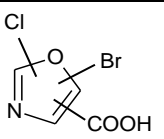
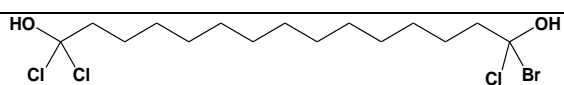
$$\text{Score} = \text{MSerror} + 0.5 \times \text{Isotope} + \text{homologue} \quad (4)$$

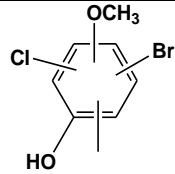
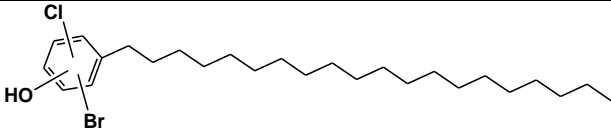
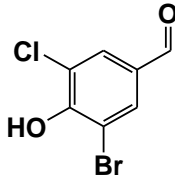
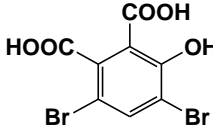
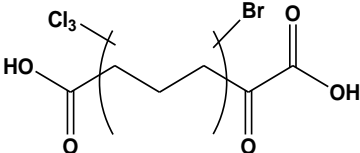
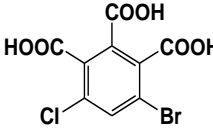
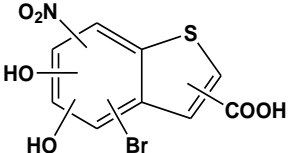
The precursor ion and molecular formulae with the greatest score for each DBP peak were used to establish the final DBP library.

Table A.1. Formulae of compounds, m/z values, peak abundances, and predicted chemical structures of the 50 most abundant Br-DBPs. The relative position of halogen or phenol/hydroxyl groups on the alkyl chain or aromatic ring could not be accurately determined for some DBPs. The exact structures of some chemicals were determined according to previous studies. Considering the potential existence of multiple adducts for a given detected ion, only the formula was shown for detected ions. m/z values were shown for most abundant isotopic peak or monoisotopic peak. Several Br-DBPs were predicted as isomers with same formulae.

Molecular Formula	m/z	Abundance	Structure
$\text{CH}_2\text{O}_3\text{SClBr}$	206.8516	6.2e6	
$\text{C}_2\text{H}_2\text{O}_2\text{ClBr}$	170.8843	4.5e6	
$\text{C}_5\text{HO}_3\text{ClBr}_2$	302.7889	2.5e6	
$\text{C}_5\text{HO}_3\text{Cl}_2\text{Br}$	256.8413	1.9e6	
$\text{C}_5\text{HO}_3\text{Cl}_2\text{Br}$	256.8413	1.8e6	
$\text{C}_7\text{H}_4\text{O}_3\text{ClBr}$	248.8960	1.7e6	

$C_{16}H_{23}O_3SBr$	373.0480	1.7e6	
$C_5HO_3ClBr_2$	300.7909	1.7e6	
$C_5H_2O_3ClBr$	222.8794	1.4e6	
$C_8H_5O_5Br$	258.9249	1.4e6	
$C_5HO_3Cl_2Br$	258.8389	1.3e6	
$C_5HO_3Cl_2Br$	258.8389	1.3e6	
$C_{10}H_7O_6Br$	300.9357	1.1e6	
$C_9H_{10}O_3ClBr$	278.9430	1.1e6	

$C_7H_{10}O_3Cl_2Br_2$	368.8312	1.1e6	
$C_7H_7O_6Br$	264.9357	1.1e6	
$C_8H_4O_5ClBr$	292.8862	1.0e6	
$C_4HNO_3Br_2$	269.8231	1.0e6	
$C_6H_{10}O_6Br_2$	334.8755	9.7e5	
$C_4HO_5SBrCl_2$	310.7995	9.6e5	
$C_{17}H_{30}O_2ClBr$	381.1015	9.5e5	
$C_5H_2O_3NClBr_2$	317.7999	9.3e5	
C_4HNO_3ClBr	227.8699	9.1e5	
$C_{15}H_{28}O_2Cl_3Br$	423.0284	8.6e5	

$C_8H_8O_2ClBr$	249.9392	5.9e5	
$C_{26}H_{44}OClBr$	485.2200	5.7e5	
$C_{20}H_{36}SOClBr$	439.1264	5.7e5	
$C_7H_4O_2ClBr$	232.9013	5.4e5	
$C_8H_4O_5Br_2$	336.8352	5.2e5	
$C_6H_5O_5Cl_3Br$	340.8228	5.2e5	
$C_9H_4O_6BrCl$	320.8820	5.1e5	
$C_{10}H_4NO_7SBr$	359.8836	5.1e5	
$C_9H_4NO_6SBr$	331.8830	4.7e5	
$C_{14}H_{29}N_2O_3SBr$	383.0999	4.5e5	
$C_{31}H_{46}O_2Br$	529.2505	4.4e5	

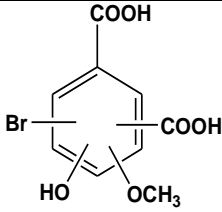
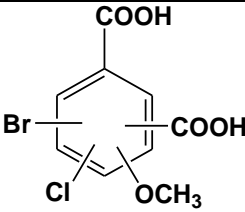
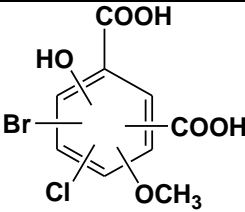
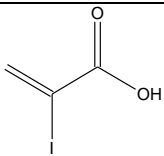
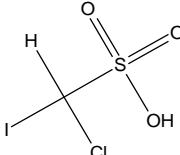
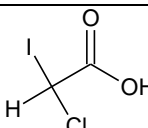
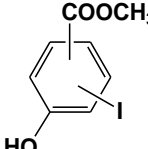
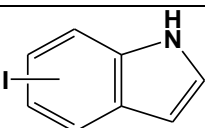
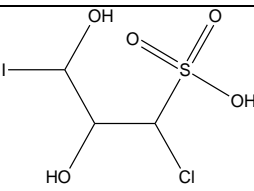
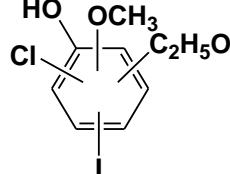
$C_9H_7O_6Br$	272.9419	4.4e5	
$C_9H_6O_5ClBr$	306.9030	4.2e5	
$C_9H_6O_6ClBr$	322.8978	4.1e5	
$C_{17}H_{14}O_{10}ClBr$	492.9345	4.0e5	
$C_7H_7O_6Br$	264.9353	4.0e5	

Table A.2. Formulae for compounds, m/z values, peak abundances and predicted chemical structures of the top 10 I-DBPs. The relative position of halogen or phenol/hydroxyl groups on the alkyl chain or aromatic ring could not be accurately determined.

Molecular Formula	m/z	Abundance	Structure
$C_3H_3O_3I$	196.9093	1.2e6	
CH_2SO_3ClI	254.838	7.3e5	
$C_2H_2O_2ClI$	218.8707	2.0e5	
$C_{15}H_{16}O_8I$	449.9822	3.1e5	
$C_8H_7O_3I$	276.937	3.0e5	
C_8H_6NI	241.9466	2.6e5	
$C_3H_6SO_5ClI$	314.8598	2.5e5	
$C_9H_{10}O_3ClI$	326.9282	2.5e5	

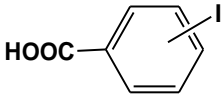
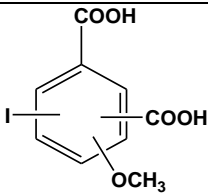
$C_7H_5O_2I$	246.9257	2.4e5	
$C_9H_7O_5I$	320.9261	1.9e5	

Table A.3. Comparison of water quality parameters and details for treatment processes for the two sampling dates and sampling points used in method development. Information obtained through personal communication with the Manager of Laboratory & Research at the water treatment plant (Conrad, 2017).

		8-Oct-15	15-Apr-16
Point of sample collection		Before Treatment (Pre Flash Mix)	After Treatment Clear Well
Chlorination point		Raw Water Intake	Post Clarification
Pre-chlorine dose	mg/L	4.38	0
Alum dose	mg/L	NA	100
Clarifier channel chlorine dose	mg/L	NA	3.45
Chlorine contact time	min.	49	190
Raw Water Analyses (immediately before chlorination point in October)			
Colour	Pt/Co	40	30
Dissolved oxygen	mg/L	9.3	11.4
Odor	TON	80	72
pH		8.42	8.36
Temperature	°C	11.5	5.1
Turbidity	NTU	5.4	5.2
Alkalinity	mg CaCO ₃ /L	193	200
Bromide	mg/L	0.04	0.04
TOC	mg/L	9.8	7.7
UV ₂₅₄	cm ⁻¹	0.1735	0.1331
SUVA	L./(mg.M)	1.770	1.774
Clarifier Effluent Analyses (immediately before chlorination point in April)			
pH		NA	6.93
Turbidity	NTU	NA	0.52
DOC	mg/L	NA	4.7
UV ₂₅₄	cm ⁻¹	NA	0.0729
SUVA	L./(mg.M)	NA	1.551

Table A.4. Concentrations of free and total chlorine in water collected August 17, 2017 as determined by an Orion AQUAfast™ AQ4000 colorimeter (Thermo Scientific).

Sample	Free chlorine (mg/L)	Total chlorine (mg/L)
Blank	0.020	< DL
Blank-NaOCl-1	0.687	0.756
Blank-NaOCl-2	0.683	0.676
preGAC-No quench	0.124	0.603
preGAC-Ascorbic acid	0.023	< DL
preGAC-Sodium thiosulfate	0.018	0.023

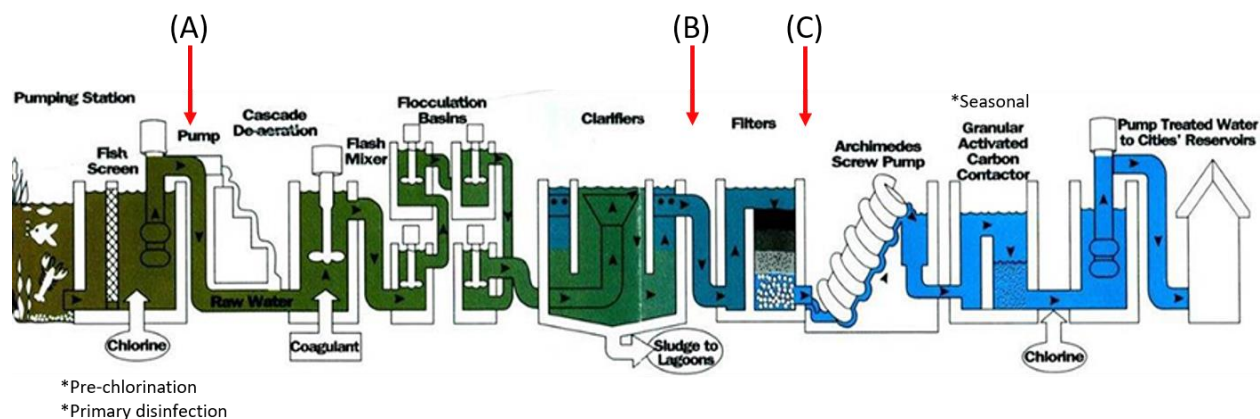


Fig. A.1. Typical process employed at the DWTP where samples were collected for this study. In October 2015, samples of raw chlorinated water were collected at (A). In April 2016, the point of chlorination changed to post-clarification (B) and samples were collected after sand filtration (C). In August 2017, the plant had returned to operating with pre-chlorination and the granular activated carbon (GAC) filter was in operation. Samples collected in August 2017 were sampled pre-GAC (C). Adapted from <http://www.buffalopoundwtp.ca/plant/water-treatment-process>.

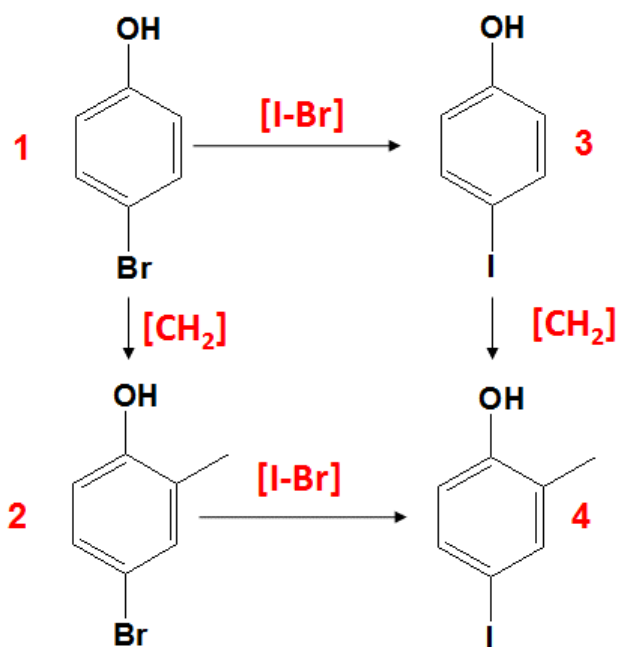


Fig. A.2. Schematic workflow of homologue models incorporated in the DIPIC-Frag method. 1) Br-DBP compound 1 was predicted; due to the characteristic peak and lower mass values, the formula of this compound could be predicted reliably; 2) Br-DBP compound 2 was then predicted based on a homologue model with $-CH_2$ difference to compound 1; 3) I-DBP compound 3 was then predicted, and the homologue information from compound 1 would increase the score and prediction accuracy of this compound; 4) I-DBP compound 4 was then confidently predicted with homologue information from compound 2 (I-Br) and compound 3 ($-CH_2$).

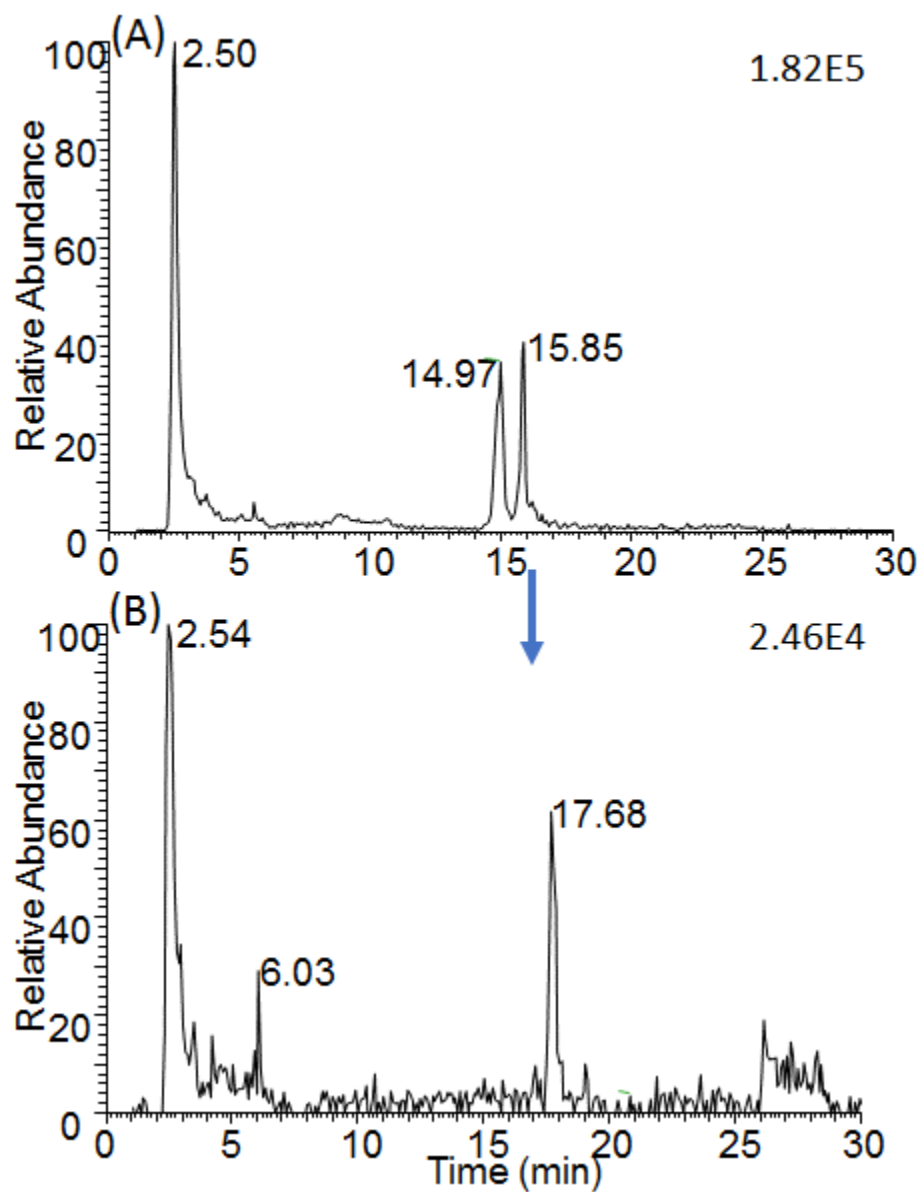


Fig. A.3. Typical chromatograms of Br-DBP peaks (230 ± 2.5 m/z DIA window) using ESI (A) or APCI (B) ionization sources.

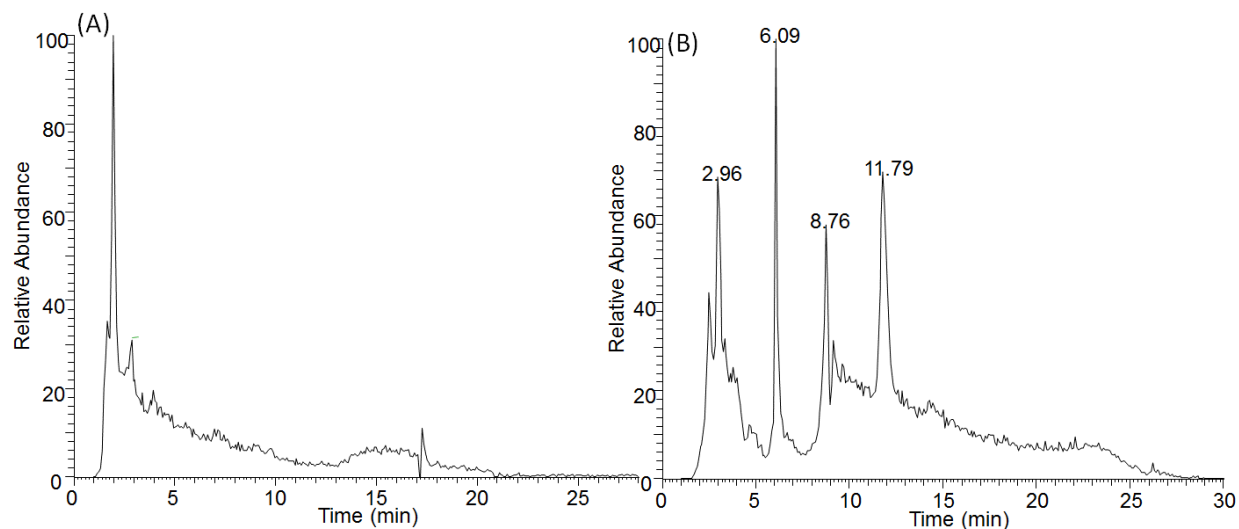


Fig. A.4. Typical chromatograms of Br-DBPs peaks under (A) Hypersil GOLDTM C18 column (3 μ m; 2.1 mm \times 50 mm; Thermo Fisher Scientific) and (B) TSKgel Amide-80 column (3 μ m; 4.6 mm \times 150 mm; TOSOH). Most abundant peaks on C18 columns were eluted in the first 3 min with poor separation, indicating poor retention ability of Br-DBPs on C18 columns. Ultrapure water containing 0.1% NH₄OH (A) and acetonitrile containing 0.1% NH₄OH (B) were used as mobile phases. Initially 95% of B was decreased to 90% in 18 min, then decreased to 30% at 26 min, followed by an increase back to 95% of B held for 3 min.

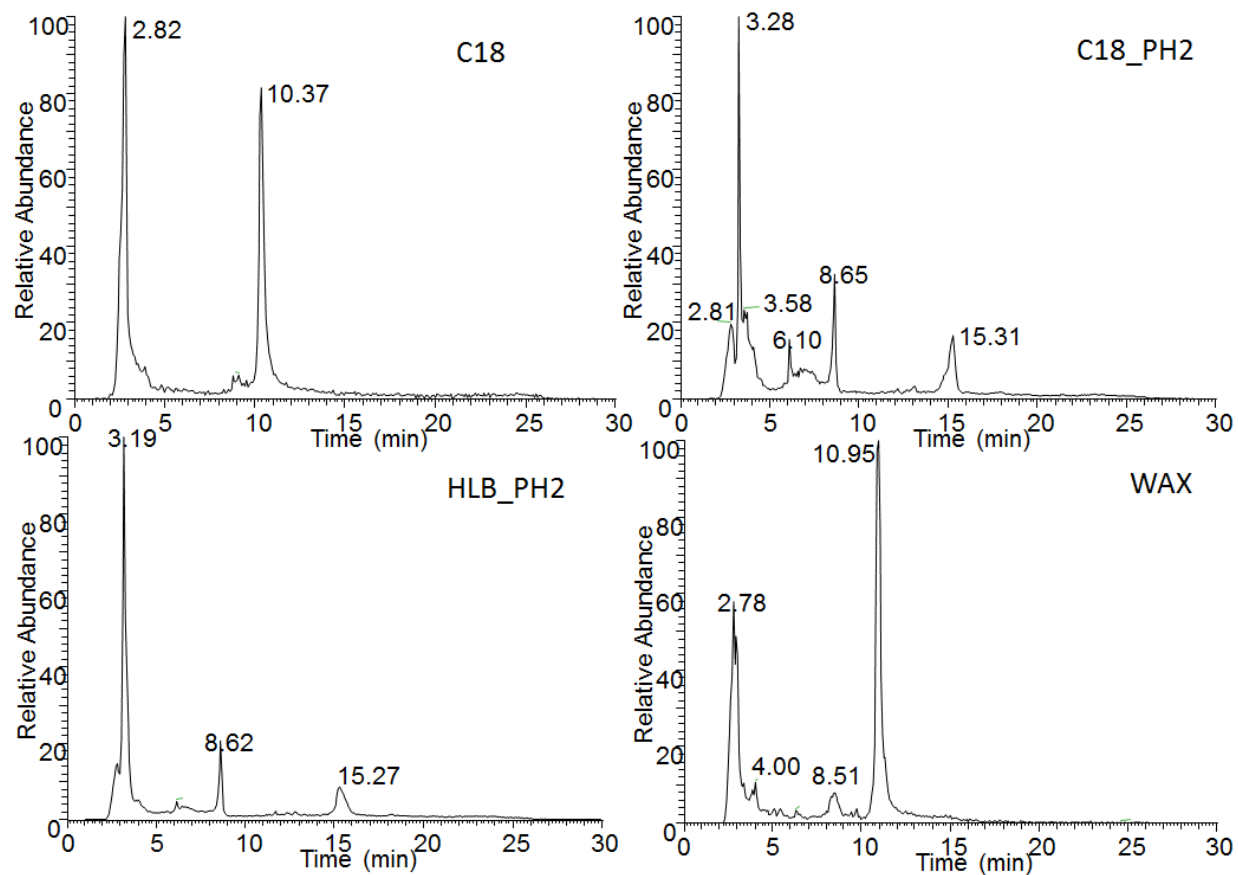


Fig. A.5. Typical chromatograms of Br-DBP peaks (215 ± 2.5 m/z DIA window) using different SPE pretreatment methods. Chromatograms of Br-DBPs using HLB was similar to C18, and thus was not shown here.

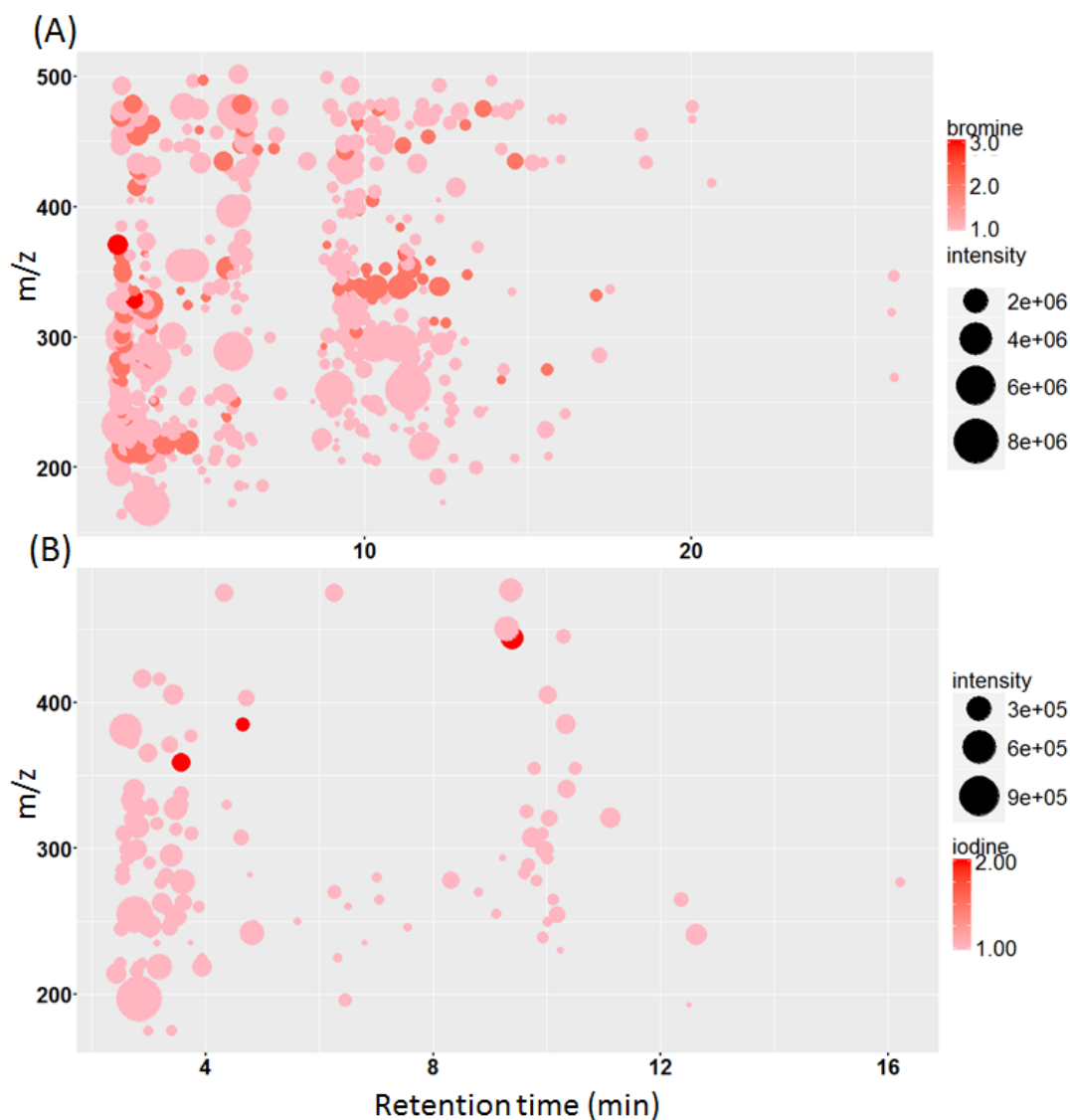


Fig. A.6. Distribution of Br-DBPs and I-DBPs detected in chlorinated raw water and conventionally treated water by retention time (min) and m/z values. (A) Br-DBPs; (B) I-DBPs. Size of the dots is proportional to abundances. Colour of dots represents number of bromine or iodine atoms.

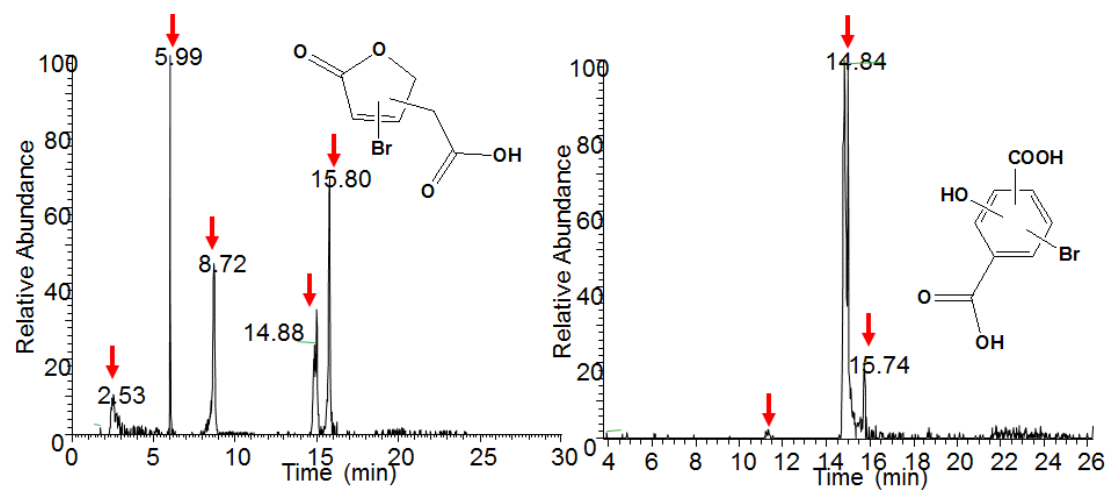


Fig. A.7. Typical chromatogram of isomers of two detected Br-DBPs. Red arrows indicate peaks of isomers. Isomers were determined by exact mass and isotopic peaks.

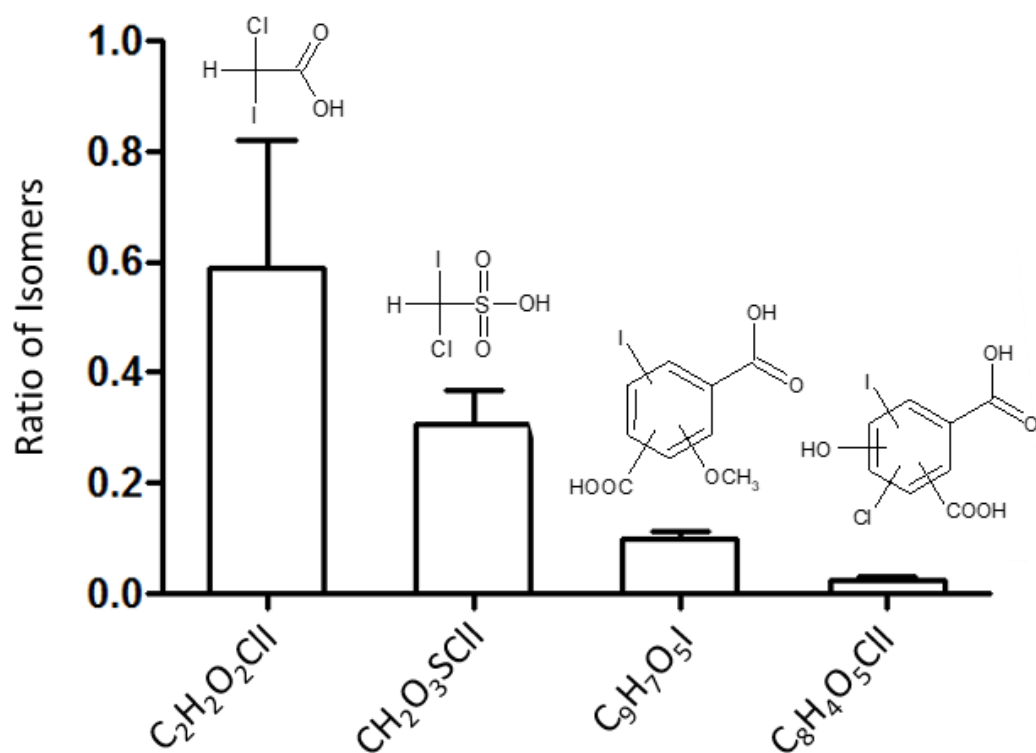


Fig. A.8. Ratios of iodinated DBPs to corresponding brominated DBP analogues. X-axis indicates four different DBPs with predicted compound formulae. Chemical structures are shown for iodinated analogues of each DBPs. Data are expressed as the mean \pm sd (n=3).

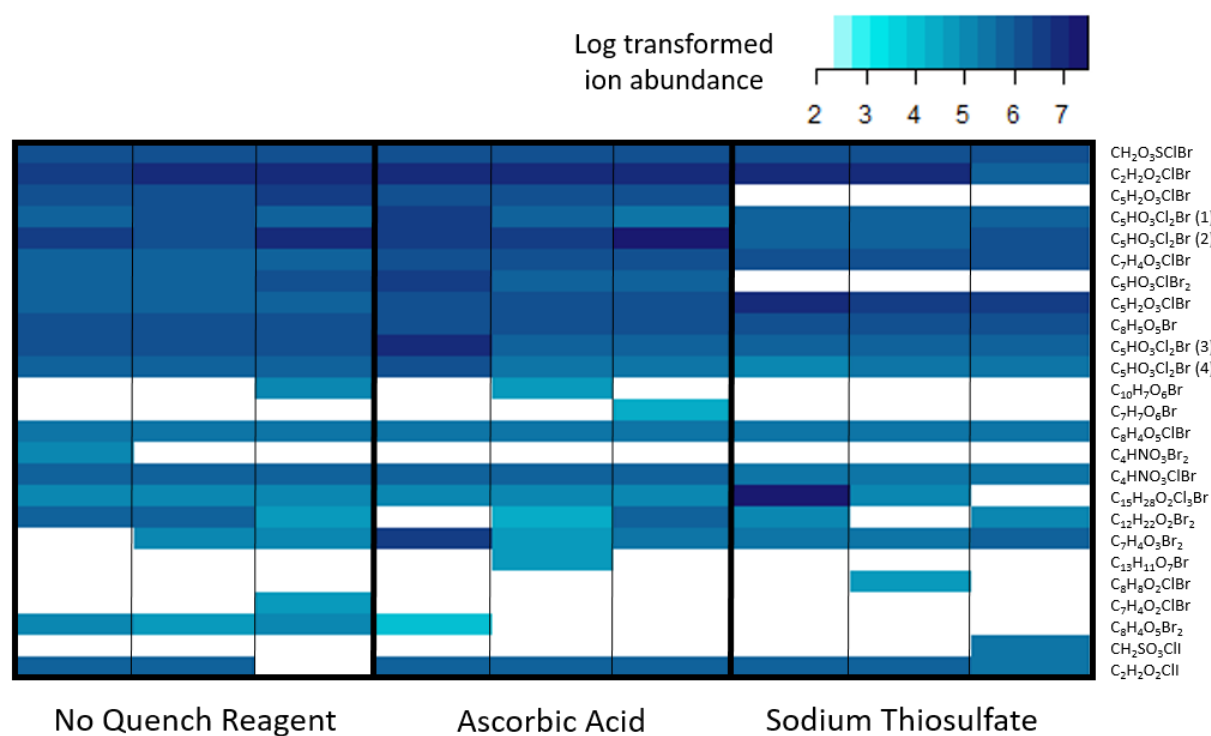


Fig. A.9. Heatmap of 25 Br-DBPs detected in water collected at the preGAC stage of treatment on August 17, 2017. Samples (n=3) were treated with no quenching reagent, an excess of 5 mg/L of ascorbic acid, or an excess of 3.5 mg/L of sodium thiosulfate. Concentrated extracts were analyzed by LC-Q Exactive MS.

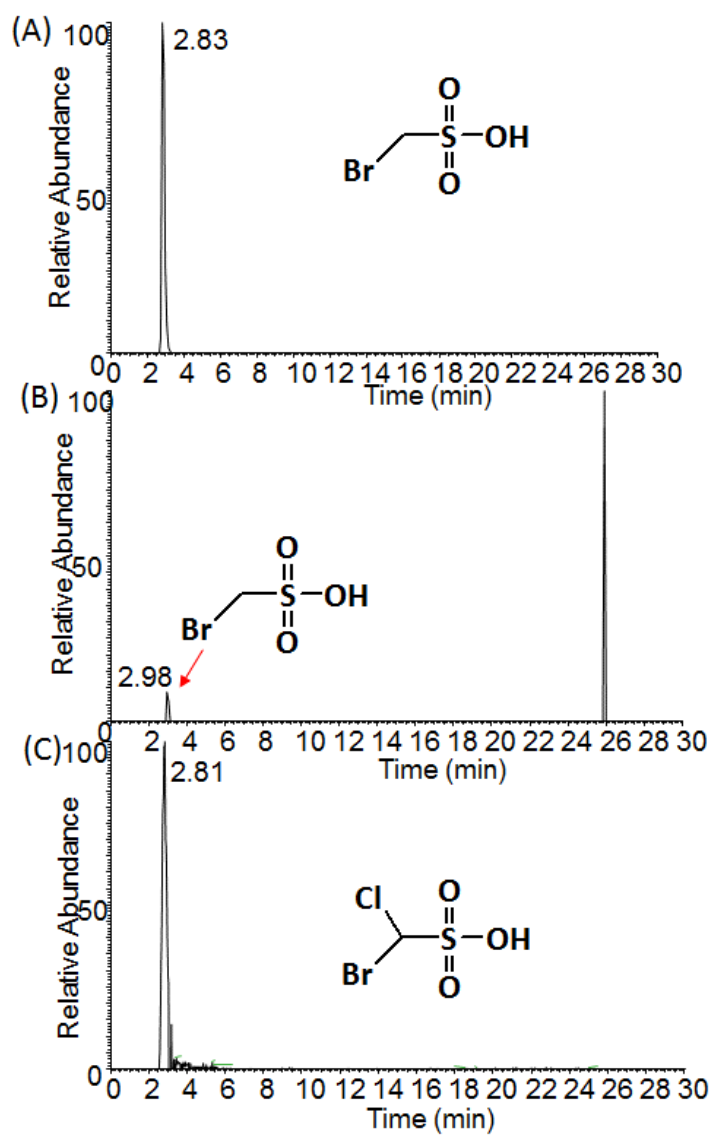


Fig. A.10. Chromatograms of bromomethanesulfonic acid from authentic acid (A), actual drinking water (B) and bromochloromethanesulfonic acid from drinking water (C). Retention times of chlorinated and brominated analogues were similar on an Amide-column.

APPENDIX B

CHAPTER 3 SUPPORTING INFORMATION

This supporting information provides text and figures addressing (1) the water treatment process; (2) quality control and assurance; (3) conditions reported at the water treatment plant on sampling dates; (4) detection frequencies and maximum ion abundances for 54 abundant Br-DBPs; (5) R^2 and p - values for linear models calculated based on detections of sulfur-containing DBPs; (6) ID# and precursor formulae of Br-DBPs in correlation matrices found in Fig. 3.1A and Fig. B.1; (7) correlation matrix of Br-DBPs detected in finished water; (8) linear models for isomers of $C_7H_3O_3ClBr$ and $C_7H_3O_3Br_2$ at the clearwell and finished stages; (9) Br/C and O/C ratios of Br-DBPs compared based on clusters defined in Fig. 3.2A; (10) temporal and spatial trends of NOM; (11) example van Krevelen plots representing relationships between NOM and Br-DBPs; and (12) correlation matrices between raw water parameters and ion abundances of individual Br-DBPs (seven months of data).

Collection of Water Samples

The drinking water treatment plant studied in this project is supplied by the North Saskatchewan River. The treatment process begins with addition of potassium permanganate to oxidize organics as well as seasonal use of powdered activated carbon to control taste and odour in warmer months. This is followed by coagulation with poly-aluminum chloride, flocculation assisted by an additional polymer, a small dosage of chlorine gas (pre-chlorine dose), and silica sand/antracite filtration before the water enters the clear well. After leaving the clear well, UV irradiation is applied and a second, greater dose of chlorine gas is added (post-chlorine dose) as the primary disinfection step before the water travels towards the reservoir.

Quality Control and Assurance

To avoid contamination of samples, all equipment was rinsed regularly with methanol. One procedural blank using ultrapure water was incorporated in the analytical procedure. Background contamination from the blank was subtracted from samples for downstream data analysis, and those DBPs whose abundance was less than 3 times the background abundance in blanks were considered non-detected. Some halogenated compounds were also detected in source water, and thus only those compounds showing >3-fold higher abundance in chlorinated water samples than source water samples were considered to be DBPs produced during chlorination process.

Because most detected DBPs were unregulated compounds for which no authentic standards were available, intensities of peaks were used to semi-quantify their abundances in samples, as has been done previously for organo-bromine compounds (Peng et al., 2016a, 2015). To enhance comparability among samples and avoid potential shifts in sensitivity among compounds during multiple injections, the same set of methods (4 methods in total for each sample, to cover all the mass range) was run at the same time for all samples. Method detection limits (MDLs) could not be calculated for DBPs, but a peak intensity cutoff of 50,000 (Br-DBPs) or 10,000 (I-DBPs) was incorporated into the DIPIC-Frag method as described previously (Peng et al., 2015), and used as the MDL for the DBPs. For the DBPs peaks detected in blanks, 3× the peak abundance were used as MDLs.

Table B.1. Raw water parameters, total bromine determinations, and applied doses of chlorine as reported for the eleven sampling dates of this study (2016-2017).

Date	Raw Water Parameters								Total Bromine as determined by ICP-MS			Chlorine Disinfection	
	Colour (TCU)	River Level (m)	Temperature (°C)	Turbidity (NTU)	UVT (%)	UV ₂₅₄ (m ⁻¹)	TOC (mg/L)	SUVA (L/mg-m)	Raw (µg/L)	Clearwell (µg/L)	Finished (µg/L)	Pre chlorine Dose (mg/L)	Post Chlorine Dose (mg/L)
19-Apr	644	2.11	9	70.85	49.9	NA	NA	NA	17	20	62	0.5	2.0
17-May	101	1.78	15.5	7.95	74.9	NA	NA	NA	30	65	120	0.5	1.8
14-Jun	146.5	1.76	21.5	12.7	56.3	NA	NA	NA	28	45	68	0.74	2.38
12-Jul	148	1.605	20	15.9	74.45	NA	NA	NA	27	49	82	0.50	2.20
29-Sep	140	1.89	14	13.15	60.9	21.45	6.73	3.19	17	32	54	0.4	2.0
25-Oct	153.5	1.975	4	12.55	63.7	22.1	5.53	4	20	20	50	0.33	2.1
18-Nov	90.5	1.68	2	7.04	61.75	25.77	6.75	3.82	24	35	66	0.5	1.8
15-Dec	48	2.355	1	3.115	63.25	24.3	7.38	3.29	38	53	110	0.3	2.04
12-Jan	61.5	2.25	1	5.65	81.05	14.51	3.14	4.62	18	18	40	0.10	2.25
7-Feb	47.5	2.175	1.5	4.225	83.1	13	2.47	5.26	13	20	48	0.6	1.7
8-Mar	50.5	2.22	1.5	4.51	81.25	11.51	2.79	4.13	27	31	60	0.60	1.70

Table B.2. Detection frequencies of Br-DBPs at each stage of treatment, as well as median, minimum, and maximum ion abundances detected at the clearwell and finished stages.

rt (min)	Observed Ion (<i>m/z</i>)	Formula [M-H] ⁻	Detection Frequency			Median Ion Abundance (Min - Max)*	
			Raw Water	Clearwell Water	Finished Water	Clearwell Water	Finished Water
8.59	258.924	C ₈ H ₄ O ₅ Br ⁻	1	11	11	492000 (224000, 3500000)	538000 (110000, 3430000)
2.08	258.924	C ₈ H ₄ O ₅ Br ⁻	0	11	11	201000 (4930, 288000)	279000 (182000, 349000)
2.10	204.916	C ₅ H ₃ N ₂ BrCl ⁻	1	11	11	446000 (11400, 1130000)	2280000 (1060000, 4440000)
2.19	206.851	CHO ₃ SClBr ⁻	0	11	11	211000 (28000, 1010000)	838000 (434000, 2640000)
8.95	206.852	CHO ₃ SClBr ⁻	0	1	3	/ (ND, 11300)	/ (ND, 83500)
8.81	206.896	C ₄ HN ₂ OCIBr ⁻	0	9	11	75200 (ND, 104000)	321000 (224000, 757000)
2.08	231.847	C ₂ NO ₃ SClBr ⁻	0	10	11	91000 (ND, 507000)	3000000 (1640000, 12400000)
2.92	207.880	C ₄ O ₂ NBrCl ⁻	0	7	11	21600 (ND, 122000)	476000 (273000, 1560000)
2.10	221.872	C ₅ HO ₃ ClBr ⁻	0	7	11	52800 (ND, 230000)	/ (ND, 189000)
8.30	221.955	C ₉ H ₅ NOBr ⁻	0	10	6	532000 (ND, 3850000)	115000 (ND, 968000)
2.17	222.879	C ₅ HO ₃ ClBr ⁻	0	11	11	2040000 (342000, 5350000)	796000 (443000, 2120000)
8.73	222.949	C ₈ H ₄ N ₂ OBr ⁻	0	10	0	369000 (ND, 1000000)	/ (ND, ND)
5.14	223.934	C ₈ H ₃ O ₂ NBr ⁻	0	11	10	616000 (194000, 9270000)	463000 (ND, 823000)
2.44	228.878	C ₃ HO ₄ NBrCl ⁻	0	9	11	60300 (ND, 107000)	307000 (83000, 726000)
2.31	228.949	C ₈ H ₆ O ₃ Br ⁻	0	10	9	943000 (ND, 1330000)	280000 (ND, 2160000)
2.30	230.929	C ₇ H ₄ O ₄ Br ⁻	0	4	7	/ (ND, 343000)	392000 (ND, 572000)
2.72	238.867	C ₄ HON ₂ BrClS ⁻	0	6	11	89800 (ND, 575000)	2010000 (305000, 4310000)
10.18	238.867	C ₄ HON ₂ BrClS ⁻	0	1	11	/ (ND, 96500)	241000 (56600, 490000)
5.56	235.911	C ₆ H ₄ O ₂ NBrCl ⁻	0	0	10	/ (ND, ND)	121000 (ND, 271000)
11.79	216.880	C ₂ H ₂ O ₅ BrS ⁻	0	1	11	/ (ND, 67000)	632000 (62800, 899000)
2.21	248.895	C ₇ H ₃ O ₃ ClBr ⁻	0	10	11	230000 (ND, 969000)	1210000 (305000, 10800000)
8.85	248.895	C ₇ H ₃ O ₃ ClBr ⁻	0	6	10	188000 (ND, 893000)	461000 (ND, 955000)
2.10	300.791	C ₅ O ₃ ClBr ₂ ⁻	0	10	4	961000 (ND, 7890000)	/ (ND, 49700)
2.07	256.841	C ₅ O ₃ Cl ₂ Br ⁻	0	11	11	3280000 (10000, 16400000)	600000 (463000, 1020000)
2.14	276.895	C ₅ H ₇ O ₄ BrClS ⁻	0	11	11	149000 (42000, 324000)	357000 (266000, 565000)
8.47	228.950	C ₈ H ₆ O ₃ Br ⁻	0	2	3	/ (ND, 1170000)	/ (ND, 2150000)

8.27	221.955	C ₉ H ₅ NOBr ⁻	0	10	4	532000 (ND, 3850000)	/ (ND, 441000)
2.11	296.841	C ₆ H ₃ O ₄ Br ₂ ⁻	0	10	10	260000 (ND, 365000)	313000 (ND, 700000)
2.10	264.935	C ₇ H ₆ O ₆ Br ⁻	0	11	11	2050000 (110000, 4890000)	533000 (422000, 721000)
8.77	264.935	C ₇ H ₆ O ₆ Br ⁻	0	6	6	99100 (ND, 293000)	166000 (ND, 1590000)
9.31	264.935	C ₇ H ₆ O ₆ Br ⁻	0	11	11	231000 (133000, 364000)	431000 (149000, 3580000)
2.59	238.893	C ₆ H ₃ O ₃ BrCl ⁻	0	11	11	2810000 (305000, 5930000)	198000 (143000, 351000)
2.68	238.846	C ₃ HON ₂ Br ₂ ⁻	0	0	4	/ (ND, ND)	/ (ND, 143000)
2.19	294.843	C ₇ H ₃ O ₃ Br ₂ ⁻	0	4	11	/ (ND, 880000)	254000 (80700, 1530000)
8.86	294.843	C ₇ H ₃ O ₃ Br ₂ ⁻	0	7	11	98800 (ND, 880000)	254000 (80700, 1530000)
2.21	248.895	C ₇ H ₃ O ₃ ClBr ⁻	0	11	11	230000 (71200, 969000)	1210000 (305000, 10800000)
8.85	248.895	C ₇ H ₃ O ₃ ClBr ⁻	0	7	11	198000 (ND, 893000)	461000 (59700, 955000)
2.11	232.944	C ₇ H ₆ O ₄ Br ⁻	0	9	11	400000 (ND, 534000)	1630000 (824000, 2760000)
2.53	251.888	C ₆ H ₂ O ₃ NBrCl ⁻	0	9	8	153000 (ND, 655000)	156000 (ND, 279000)
15.55	228.891	C ₄ H ₃ O ₄ BrCl ⁻	0	4	11	/ (ND, 61700)	141000 (60400, 333000)
11.33	246.873	C ₃ H ₂ O ₆ BrS ⁻	0	8	9	123000 (ND, 386000)	1320000 (ND, 1880000)
3.06	238.867	C ₄ HON ₂ BrClS ⁻	0	6	11	129000 (ND, 575000)	2010000 (305000, 4310000)
8.73	258.855	C ₃ H ₃ O ₂ N ₂ Br ₂ ⁻	0	9	5	134000 (ND, 414000)	/ (ND, 210000)
3.70	170.884	C ₂ HO ₂ ClBr ⁻	0	11	11	715000 (186000, 6040000)	887000 (172000, 10200000)
2.13	197.885	C ₂ HO ₃ NBrS ⁻	0	5	11	/ (ND, 238000)	162000 (85800, 530000)
8.91	192.913	C ₄ H ₂ O ₄ Br ⁻	0	10	10	104000 (ND, 205000)	809000 (ND, 2070000)
9.36	199.935	C ₆ H ₃ O ₂ NBr ⁻	0	5	10	/ (ND, 112000)	366000 (ND, 2400000)
3.63	184.900	C ₃ H ₃ O ₂ ClBr ⁻	0	9	11	55600 (ND, 85800)	270000 (58700, 521000)
5.35	354.990	C ₁₀ H ₁₄ O ₈ NBr ⁻	0	6	7	1170000 (ND, 13600000)	2020000 (ND, 11200000)
5.98	397.000	C ₁₂ H ₁₆ O ₉ NBr ⁻	0	1	2	/ (ND, 694000)	/ (ND, 1300000)
9.39	338.833	C ₈ H ₃ O ₅ Br ₂ ⁻	0	0	5	/ (ND, ND)	/ (ND, 629000)
8.78	352.907	C ₇ H ₁₃ O ₆ Br ₂ ⁻	0	4	11	/ (ND, 450000)	4830000 (1250000, 11600000)
9.39	338.833	C ₅ H ₆ O ₄ NBr ₂ Cl ⁻	0	0	7	/ (ND, ND)	116000 (ND, 629000)
2.10	324.876	C ₈ H ₃ O ₇ BrCl ⁻	0	6	11	207000 (ND, 521000)	331000 (129000, 965000)
Average			0.0	7.2	9.1		
Minimum			0.0	0	0		
Maximum			1	11	11		

* Median reported only if greater than five detections

Table B.3. R^2 and p -values (ANOVA) of linear models calculated based on ion abundances of sulfonated DBPs (found in the red square of Fig. 3.1A) at the clearwell and finished stages of treatment (n=22).

	C₄H₂ON₂BrClS	C₄H₂ON₂BrClS.1	C₂H₂O₃NBrS	CH₂O₃SClBr.1	C₅H₈O₄BrClS	C₄H₂ON₂BrClS.2	C₂HNO₃SClBr
C₄H₂ON₂BrClS	-	$R^2 = 0.99$ $p = < 2.2e-16^*$	$R^2 = 0.11$ $p = 0.14$	$R^2 = 0.12$ $p = 0.12$	$R^2 = 0.31$ $p = 0.01^*$	$R^2 = 0.72$ $p = 5.9e-7^*$	$R^2 = 0.28$ $p = 0.01^*$
C₄H₂ON₂BrClS.1	$R^2 = 0.99$ $p = < 2.2e-16^*$	-	$R^2 = 0.11$ $p = 0.13$	$R^2 = 0.12$ $p = 0.11$	$R^2 = 0.30$ $p = 0.008^*$	$R^2 = 0.72$ $p = 5.8e-7^*$	$R^2 = 0.28$ $p = 0.01^*$
C₂H₂O₃NBrS	$R^2 = 0.11$ $p = 0.14$	$R^2 = 0.11$ $p = 0.13$	-	$R^2 = 0.61$ $p = 2.0e-5$	$R^2 = 0.14$ $p = 0.08$	$R^2 = 0.20$ $p = 0.04^*$	$R^2 = 0.21$ $p = 0.03^*$
CH₂O₃SClBr.1	$R^2 = 0.12$ $p = 0.12$	$R^2 = 0.12$ $p = 0.11$	$R^2 = 0.61$ $p = 2.0e-5$	-	$R^2 = 0.23$ $p = 0.02^*$	$R^2 = 0.29$ $p = 0.01^*$	$R^2 = 0.66$ $p = 4.6e-6^*$
C₅H₈O₄BrClS	$R^2 = 0.31$ $p = 0.007^*$	$R^2 = 0.30$ $p = 0.008^*$	$R^2 = 0.14$ $p = 0.08$	$R^2 = 0.23$ $p = 0.02^*$	-	$R^2 = 0.48$ $p = 3.5e-4^*$	$R^2 = 0.43$ $p = 9.9e-4^*$
C₄H₂ON₂BrClS.2	$R^2 = 0.72$ $p = 5.9e-7^*$	$R^2 = 0.72$ $p = 5.8e-7^*$	$R^2 = 0.20$ $p = 0.04$	$R^2 = 0.29$ $p = 0.01^*$	$R^2 = 0.48$ $p = 3.5e-4^*$	-	$R^2 = 0.62$ $p = 1.3e-7^*$
C₂HNO₃SClBr	$R^2 = 0.28$ $p = 0.01^*$	$R^2 = 0.28$ $p = 0.01^*$	$R^2 = 0.21$ $p = 0.03$	$R^2 = 0.66$ $p = 4.6e-6^*$	$R^2 = 0.43$ $p = 9.9e-4^*$	$R^2 = 0.62$ $p = 1.3e-7^*$	-

* Significant p -value at $\alpha=0.05$ in ANOVA of linear model

Table B.4. ID# and predicted molecular formulae of Br-DBPs in correlation matrix found in Fig. 3.1A.

ID#	Predicted Formula	ID#	Predicted Formula
1	C ₅ HO ₃ ClBr ₂	28	C ₃ H ₃ O ₆ BrS
2	C ₅ HO ₃ Cl ₂ Br	29	C ₇ H ₇ O ₆ Br.3
3	C ₆ H ₄ O ₃ BrCl	30	C ₈ H ₄ O ₇ BrCl
4	C ₈ H ₅ N ₂ OBr	31	C ₇ H ₄ O ₃ ClBr.1
5	C ₇ H ₇ O ₆ Br.1	32	C ₇ H ₄ O ₃ ClBr.2
6	C ₅ H ₂ O ₃ ClBr	33	C ₄ H ₂ ON ₂ BrClS.1
7	C ₈ H ₇ O ₃ Br	34	C ₄ H ₂ ON ₂ BrClS
8	C ₉ H ₆ NOBr	35	C ₂ H ₂ O ₃ NBrS
9	C ₉ H ₆ NOBr.1	36	C ₇ H ₄ O ₃ Br ₂ .1
10	C ₃ H ₄ O ₂ N ₂ Br ₂	37	C ₇ H ₄ O ₃ Br ₂ .2
11	C ₅ H ₂ O ₃ ClBr	38	C ₅ H ₇ O ₄ NBr ₂ Cl
12	C ₈ H ₄ O ₂ NBr	39	CH ₂ O ₃ SClBr.1
13	C ₂ H ₂ O ₂ ClBr	40	C ₆ H ₄ O ₂ NBr
14	C ₈ H ₇ O ₃ Br.1	41	C ₄ H ₃ O ₄ Br
15	C ₇ H ₇ O ₆ Br.2	42	C ₃ H ₄ O ₂ ClBr
16	C ₁₀ H ₁₅ O ₈ NBr	43	C ₅ H ₈ O ₄ BrClS
17	C ₁₂ H ₁₇ O ₉ NBr	44	C ₄ H ₂ N ₂ OClBr
18	CHO ₄ SClBr.2	45	C ₄ HO ₂ NBrCl
19	C ₆ H ₃ O ₃ NBrCl	46	C ₇ H ₁₄ O ₆ Br ₂
20	C ₈ H ₅ O ₅ Br	47	C ₄ H ₂ ON ₂ BrClS.2
21	C ₆ H ₄ O ₄ Br ₂	48	C ₅ H ₄ N ₂ BrCl
22	C ₇ H ₄ O ₃ ClBr.3	49	C ₂ HNO ₃ SClBr
23	C ₇ H ₄ O ₃ ClBr.4	50	C ₇ H ₇ O ₄ Br
24	C ₆ H ₅ O ₂ NBrCl	51	C ₈ H ₅ O ₅ Br.1
25	C ₂ H ₃ O ₅ BrS	52	C ₇ H ₅ O ₄ Br
26	C ₃ HO ₅ NBrCl	53	C ₃ H ₂ ON ₂ Br ₂
27	C ₄ H ₃ O ₅ BrCl	54	C ₈ H ₄ O ₅ Br ₂

Table B.5. ID# and predicted molecular formulae of Br-DBPs in correlation matrix found in Fig. B.1.

ID#	Predicted Formula	ID#	Predicted Formula
1	C ₉ H ₆ NOBr	28	C ₇ H ₄ O ₃ ClBr.4
2	C ₈ H ₇ O ₃ Br.1	29	C ₇ H ₄ O ₃ ClBr.3
3	C ₅ H ₂ O ₃ ClBr	30	C ₇ H ₄ O ₃ ClBr.1
4	C ₉ H ₆ NOBr.1	31	C ₇ H ₄ O ₃ ClBr.2
5	C ₄ H ₂ N ₂ OClBr	32	C ₇ H ₄ O ₃ Br ₂ .1
6	C ₄ HO ₂ NBrCl	33	C ₇ H ₄ O ₃ Br ₂ .2
7	C ₅ HO ₃ Cl ₂ Br	34	C ₆ H ₄ O ₄ Br ₂
8	C ₈ H ₄ O ₂ NBr	35	C ₄ H ₂ ON ₂ BrClS.1
9	C ₆ H ₅ O ₂ NBrCl	36	C ₄ H ₂ ON ₂ BrClS
10	C ₃ H ₂ O ₄ NBrCl	37	C ₇ H ₅ O ₄ Br
11	C ₇ H ₇ O ₆ Br.3	38	C ₇ H ₇ O ₆ Br.2
12	C ₂ H ₂ O ₂ ClBr	39	C ₈ H ₅ O ₅ Br.1
13	C ₃ H ₄ O ₂ ClBr	40	C ₈ H ₇ O ₃ Br
14	C ₆ H ₄ O ₃ BrCl	41	CH ₂ O ₃ SClBr.1
15	C ₄ H ₄ O ₄ BrCl	42	C ₂ HNO ₃ SClBr
16	C ₈ H ₄ O ₇ BrCl	43	C ₇ H ₇ O ₄ Br
17	C ₂ H ₃ O ₅ BrS	44	C ₅ H ₂ O ₃ ClBr
18	C ₃ H ₃ O ₆ BrS	45	C ₇ H ₁₄ O ₆ Br ₂
19	C ₈ H ₅ N ₂ OBr	46	C ₅ H ₄ N ₂ BrCl
20	C ₇ H ₇ O ₆ Br.1	47	C ₁₀ H ₁₅ O ₈ NBr
21	C ₅ H ₈ O ₄ BrClS	48	C ₅ HO ₃ ClBr ₂
22	C ₆ H ₃ O ₃ NBrCl	49	CH ₂ O ₃ SClBr.2
23	C ₁₂ H ₁₇ O ₉ NBr	50	C ₆ H ₄ O ₂ NBr
24	C ₈ H ₅ O ₅ Br	51	C ₂ H ₂ O ₃ NBrS
25	C ₅ H ₇ O ₄ NBr ₂ Cl	52	C ₄ H ₃ O ₄ Br
26	C ₈ H ₄ O ₅ Br ₂	53	C ₃ H ₂ ON ₂ Br ₂
27	C ₄ H ₂ ON ₂ BrClS.2	54	C ₃ H ₄ O ₂ N ₂ Br ₂

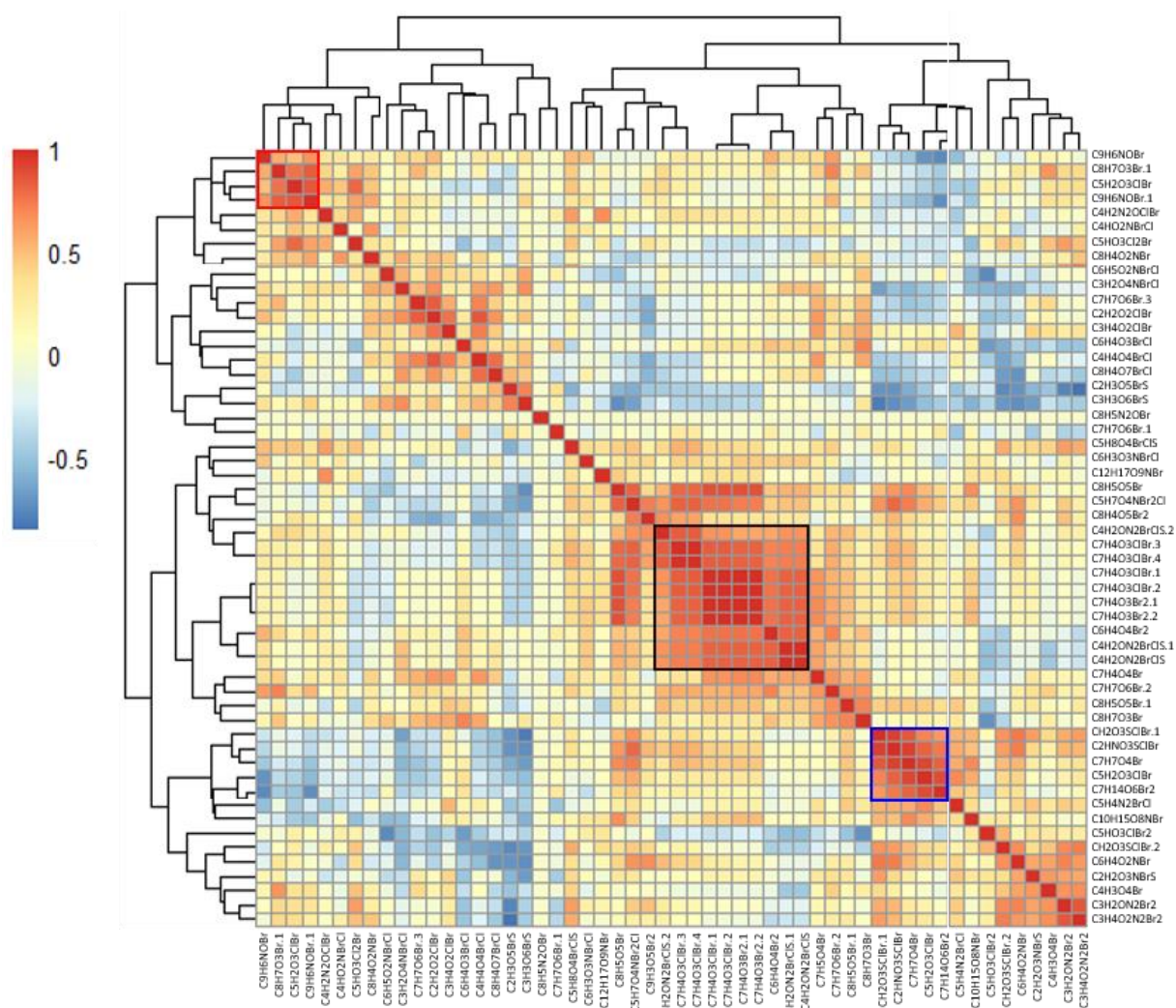


Fig. B.1. Spearman's correlation matrix based on ion abundances of 54 Br-DBPs detected in finished water at 11 monthly time points. Red, black, and blue boxes highlight groups of compounds detected with similar monthly trends. Order of compounds and precursor formulae can be found in Table B.5.

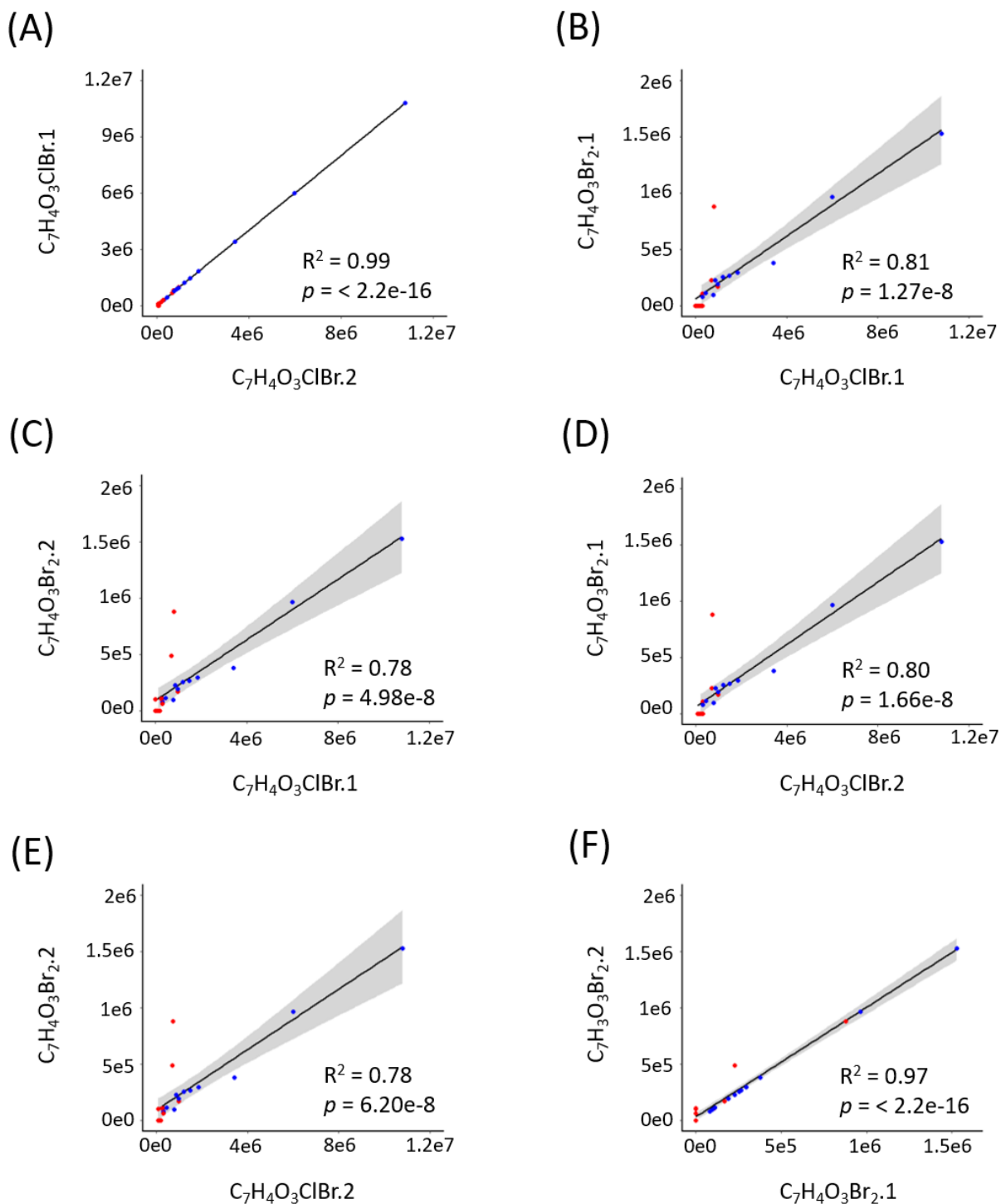


Fig. B.2. Linear models of the strong correlations found between detected ion abundances of isomers of $C_7H_4O_3ClBr$ and $C_7H_4O_3Br_2$ at the clearwell (red) and finished (blue) stages of treatment.

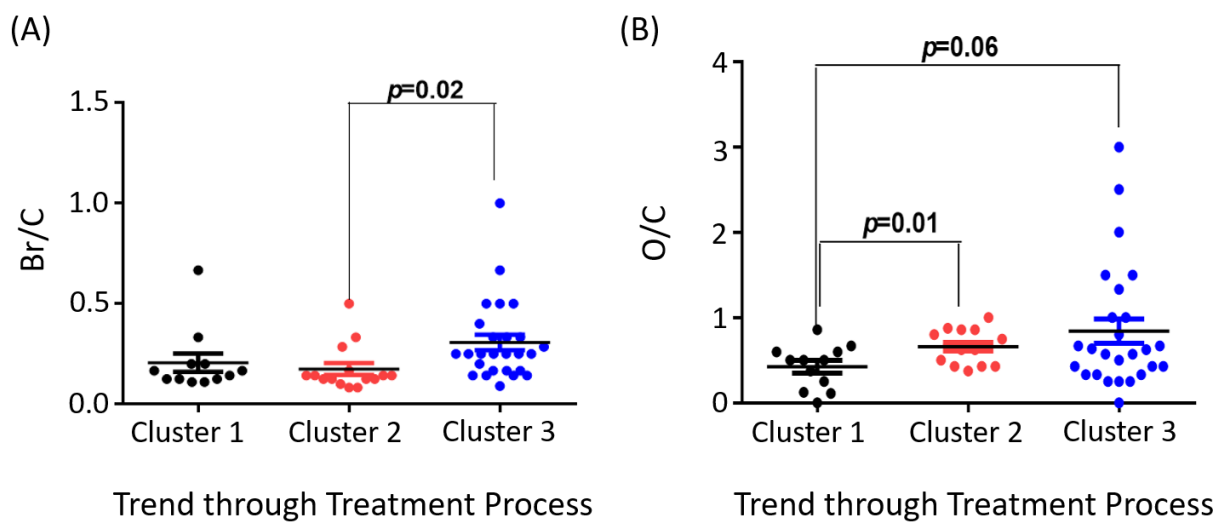
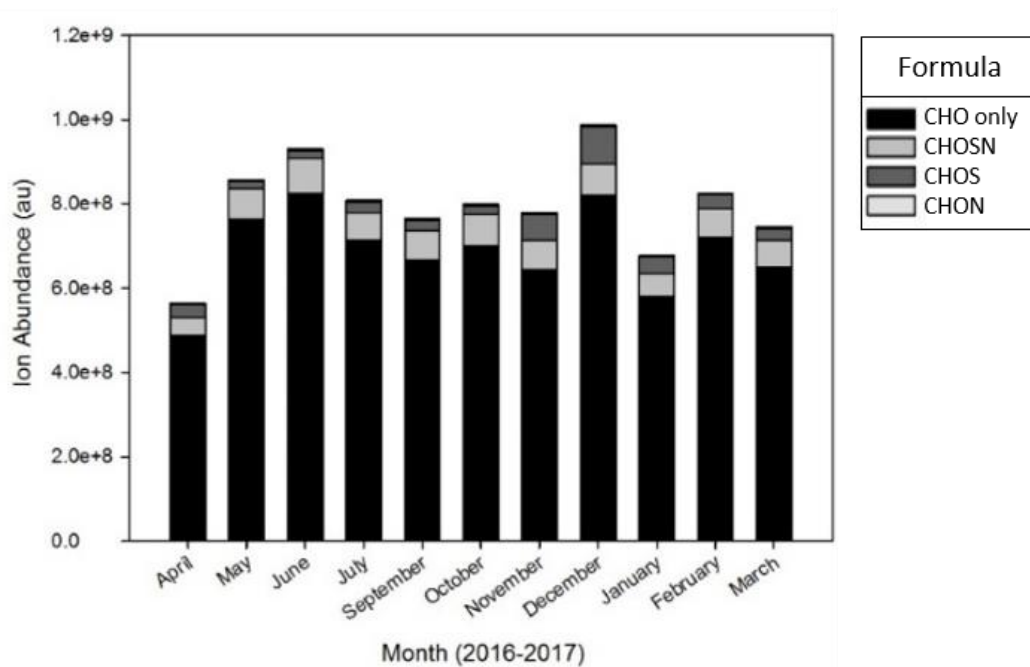


Fig. B.3. (A) Ratio of bromine to carbon (Br/C) and (B) ratio of oxygen to carbon (O/C) in compounds classified by cluster based on their trend through the treatment process (Fig. 3.2A). *P*-values represent results of T-tests.

(A)



(B)

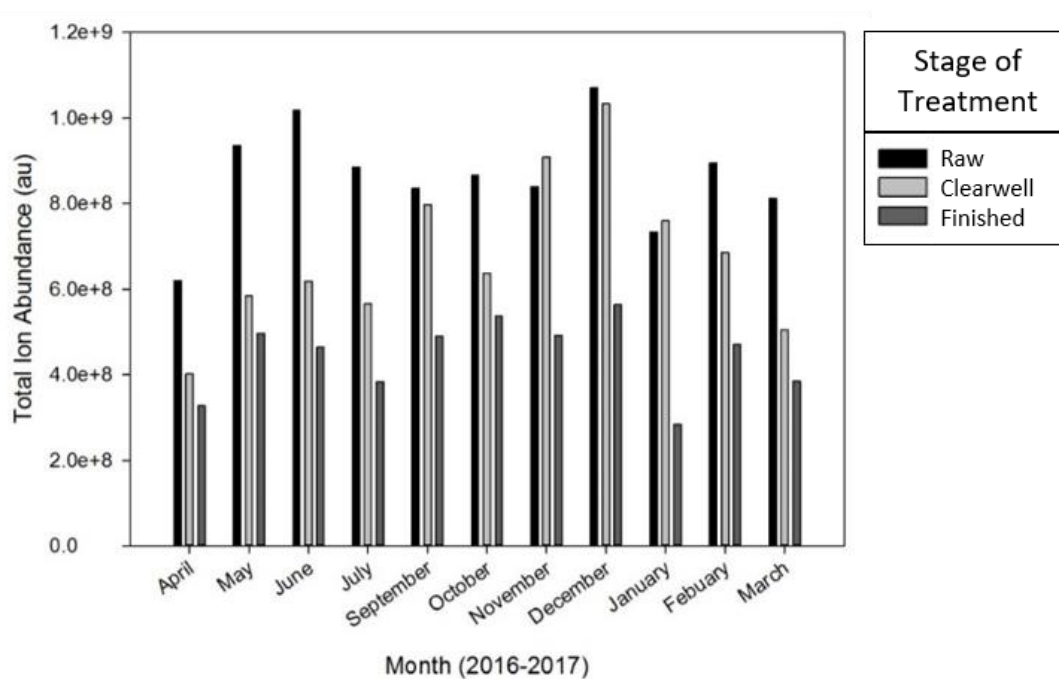


Fig. B.4. (A) Total ion abundance of NOM detected in raw water collected over eleven months, stacked based on composition of chemical formulae. (B) Total ion abundance of NOM detected at raw, clearwell, and finished stages of treatment, collected over eleven months.

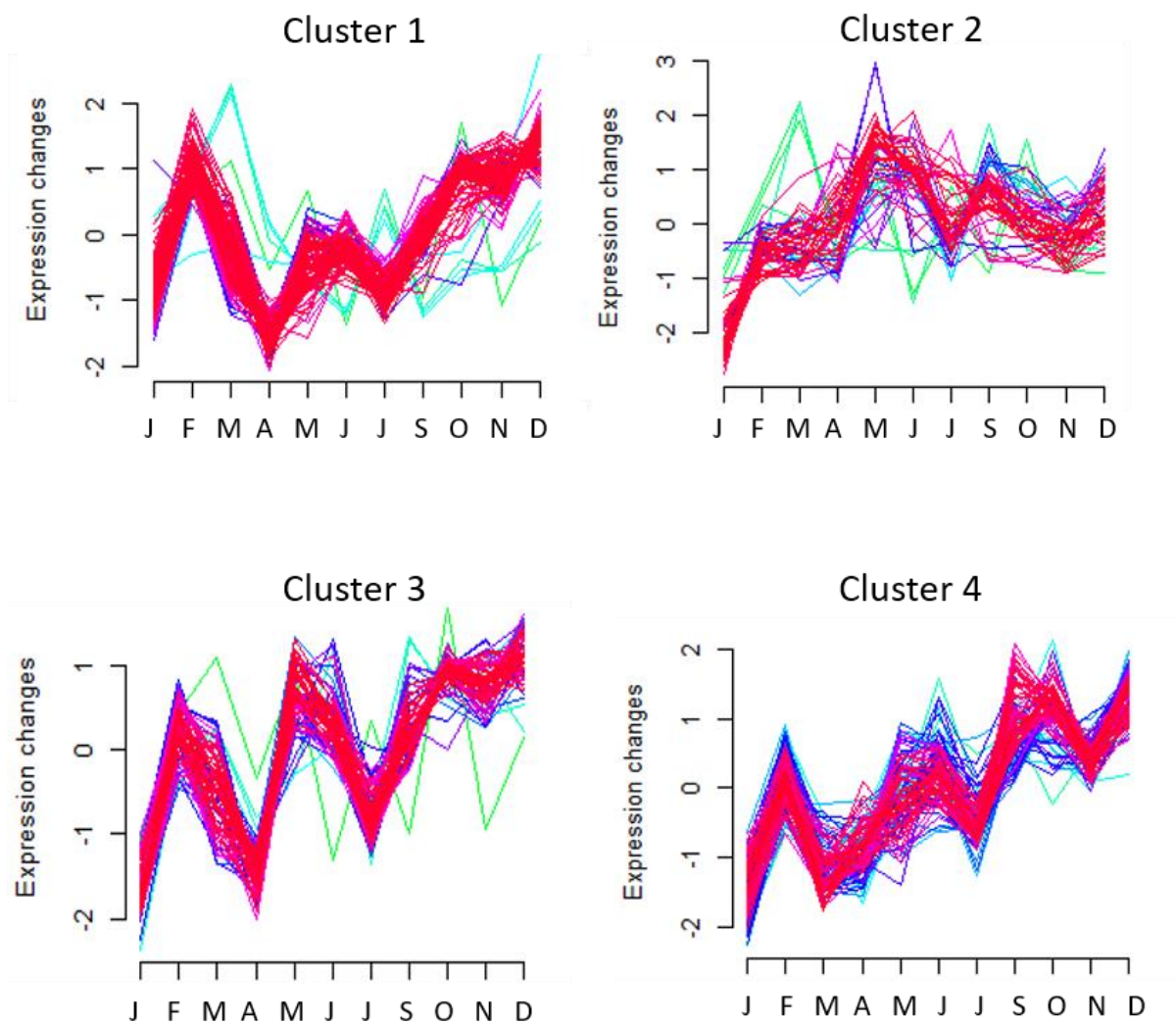


Fig. B.5. Four temporal trends identified by soft clustering analysis for the total ion abundance of NOM detected in raw water.

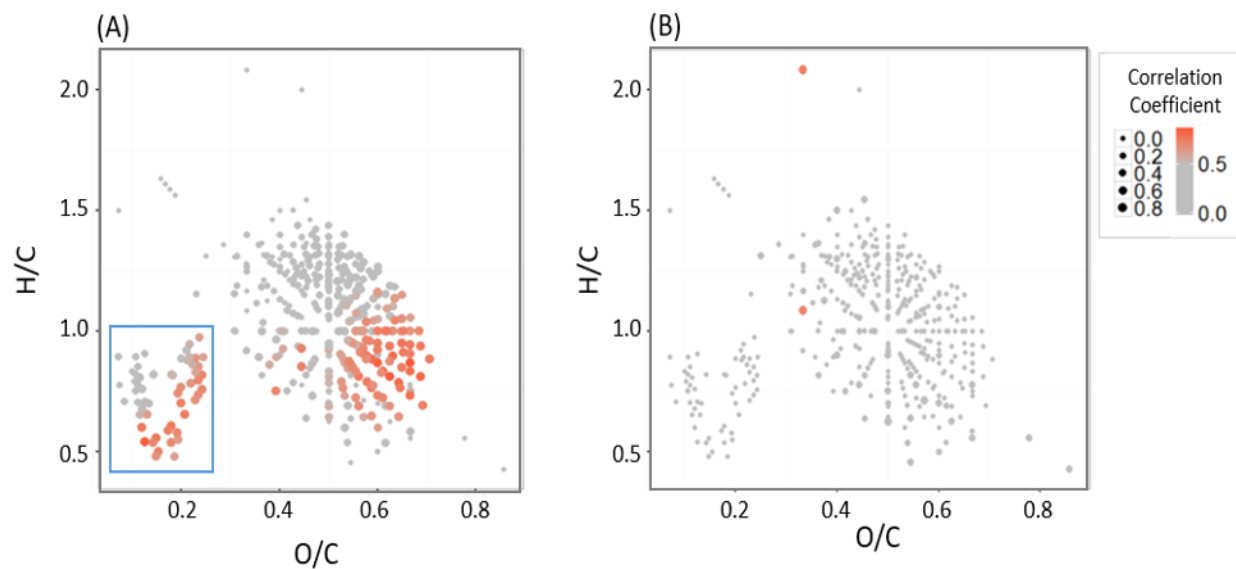


Fig. B.6. Van Krevelen plots of compounds of NOM detected in raw water with correlation to the ion abundances of (A) $C_7H_7O_6Br$ and (B) $C_5HO_3Cl_2Br$ as detected in treated water represented by colour and size. The blue box in (A) indicates compounds of NOM containing CHOSN.

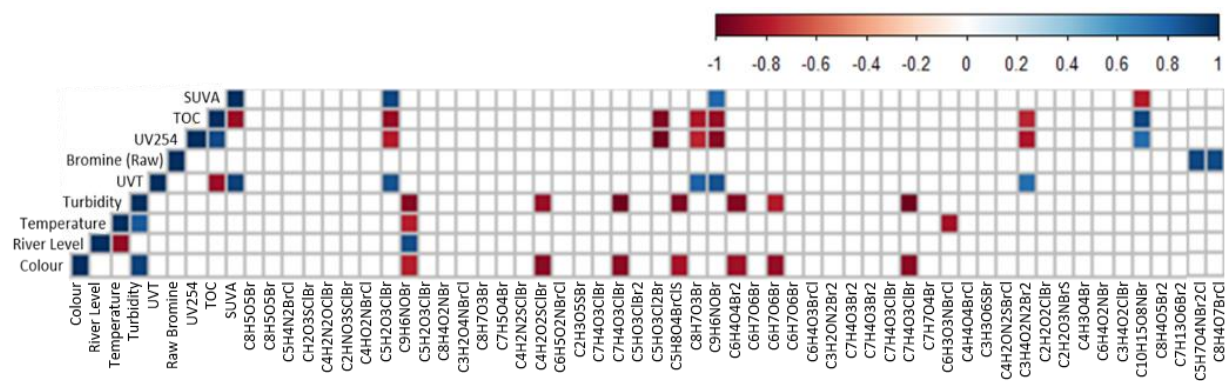


Fig. B.7. Spearman's correlation matrix indicating significant relationships ($\alpha=0.05$) between parameters of raw water and ion abundances of Br-DBPs detected in finished water. Data from seven months included (September 2016 to March 2017).

APPENDIX C

CHAPTER 4 SUPPORTING INFORMATION

This supporting information provides details on (1) chemicals and reagents; (2) conditions for chemical analysis of Br-DBPs; (3) standard curve produced for iodoacetic acid; (4) dose-response curves for concentrated water extracts subjected to the 72 h CHO-K1 cytotoxicity assay; (5) relationships between cytotoxicity of raw and clearwell waters with that of finished water; (6) results from the Nrf2/ARE oxidative stress assay and the MTT cytotoxicity assay conducting in parallel; (7) relationships between oxidative stress of raw and clearwell waters with that of finished water; (8) significant relationships identified to toxicity of finished water; (9) linear models between concentration of total Br and endpoints of toxicity; and (10) correlation between applied doses of chlorine and introduction of Br to the water treatment process.

Chemicals and Reagents

Methanol, acetonitrile, and dichloromethane (omni-solv grade), as well as hydrochloric acid and pH indicator strips (ColorpHast pH 0-6) were purchased from EMD Chemicals (Gibbstown, NJ, USA). Oasis® HLB 6cc (500mg) LP extraction cartridges were purchased from Waters (Milford, MA, USA). Dimethyl sulfoxide (ACS certified), G4 glass fibre filter circles, and phosphate buffered saline (PBS) were purchased from Fisher Scientific (Nepean, ON, Canada). F-12 nutrient mixture (Ham) powder, fetal bovine serum (FBS; qualified one shot), Dulbecco's phosphate buffered saline (DPBS), and Hank's balanced salt solution (HBSS) were purchased from Gibco (Gaithersburg, MD, USA). Dulbecco's modified eagle's medium – high glucose (DMEM), Accustain® crystal violet solution, and sodium bicarbonate were purchased from Sigma (St. Louis, MO, USA). Nrf2/ARE luciferase reporter MCF7 stable cell line was purchased from Signosis Inc. (Santa Clara, CA, USA). CHO-K1 (ATCC® CCL-61™) cell line, the MTT (3-(4,5-dimethylthiazol-2-yl)-2,5-diphenyltetrazolium bromide) cell viability assay kit, and sterile Aeraseal™ sealing film were purchased from Cedarlane (Burlington, ON, Canada), and Steadyliteplus high sensitivity – luminescence reporter gene assay system was purchased from Perkin Elmer (Waltham, MA, USA).

Chemical Analysis for Br-DBPs

Ultrapure water containing 0.1% NH_4OH (A) and acetonitrile containing 0.1% NH_4OH (B) were used as mobile phases. Initially 95% of B was decreased to 90% over 18 min, then decreased to 30% over 8 min, followed by an increase back to 95% of B held for 3 min. Flow rate was 0.40 mL/min and temperatures of the column and sample compartment were maintained at 30 °C and 10 °C, respectively.

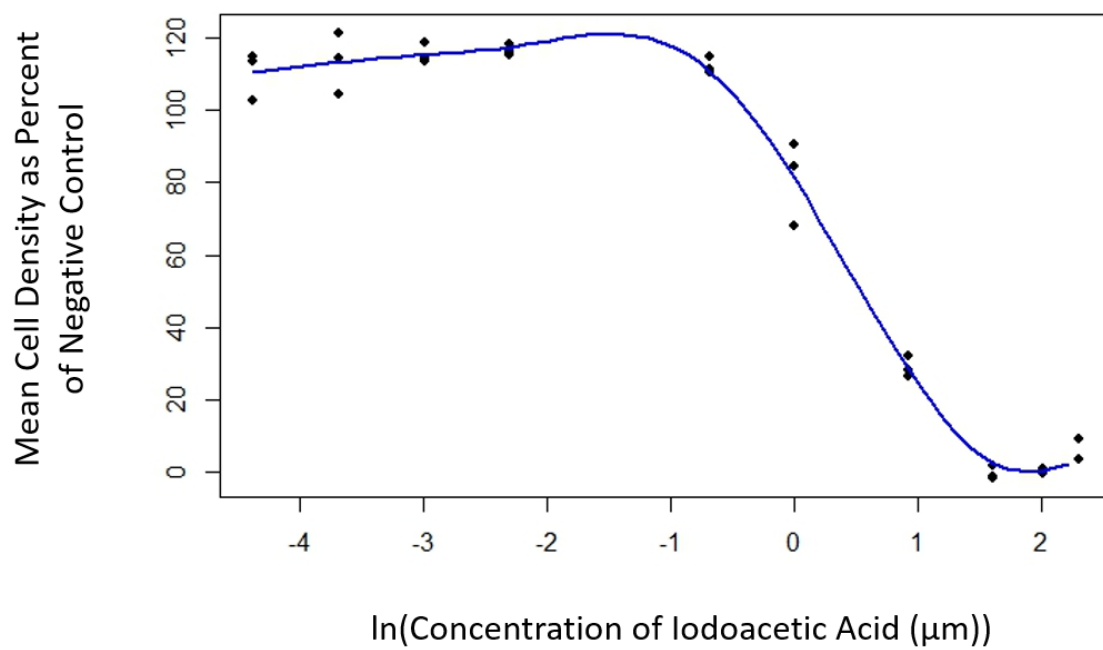


Fig. C.1. Standard dose-response curve of cytotoxicity induced by iodoacetic acid in the 72 h CHO-K1 cytotoxicity assay.

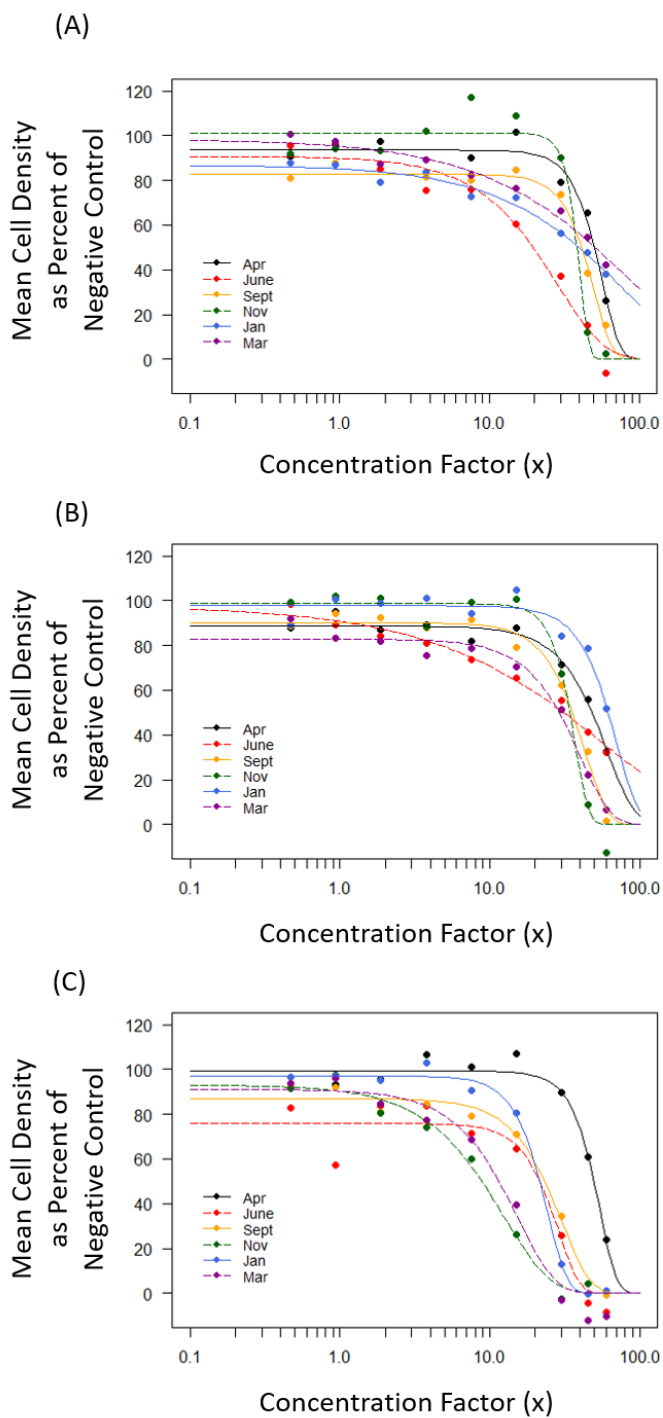


Fig. C.2. 72 h CHO-K1 cytotoxicity of (A) raw, (B) clearwell, and (C) finished water collected at six time points over a year. Average cell density ($n=3$) at nine concentrations plotted as percent of negative control by a Weibull dose-response model with lower limit fixed at zero. Predicted LC_{50} values (concentration factor \pm se) can be found in Table 4.1.

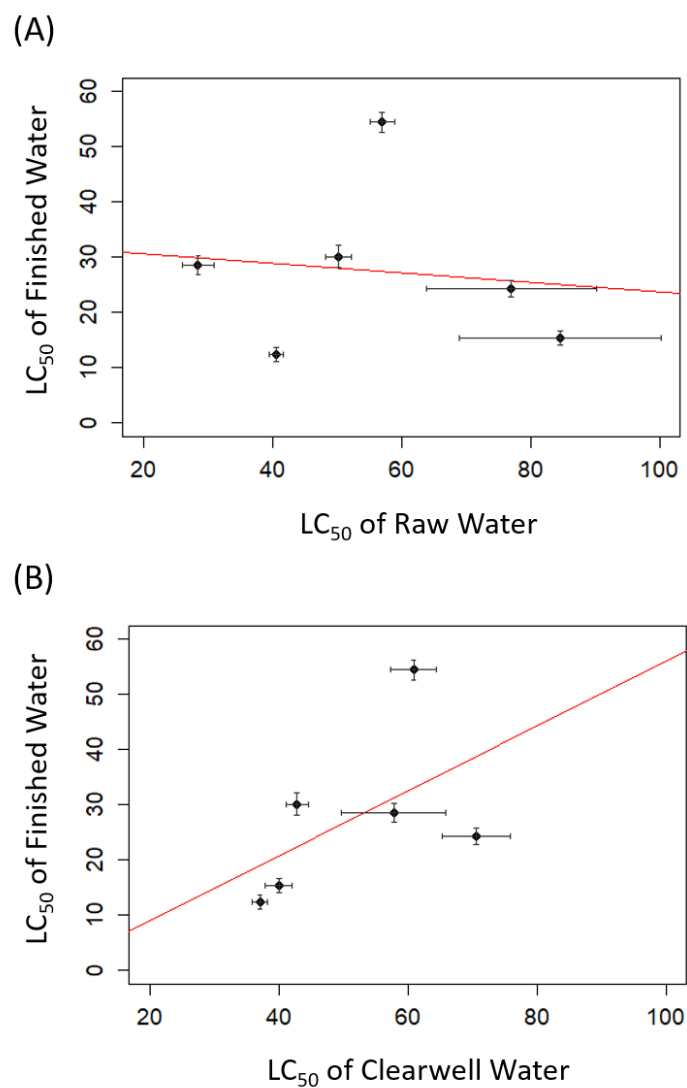


Fig. C.3. Relationships between cytotoxicity of (A) raw and (B) clearwell water with cytotoxicity of finished water. Linear models had (A) $R^2 = 0.015$, $p = 0.82$, and (B) $R^2 = 0.28$, $p = 0.28$.

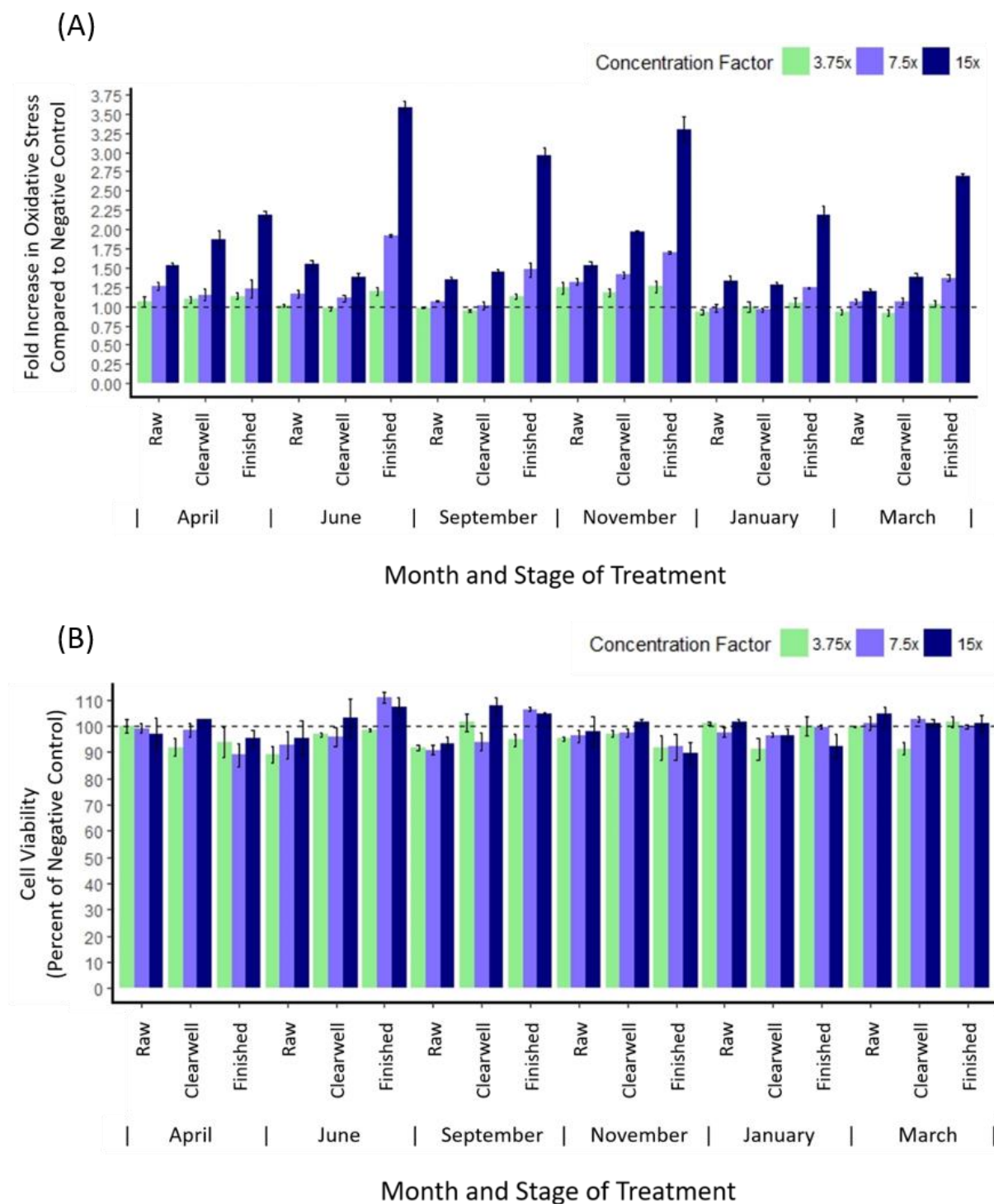


Fig. C.4. (A) Nrf2/ARE oxidative stress assay and (B) MTT cytotoxicity assay of concentrated water extracts collected at three stages of treatment and at six monthly time points. MCF7 cell line was exposed to concentrated extracts for 16 h (n=3).

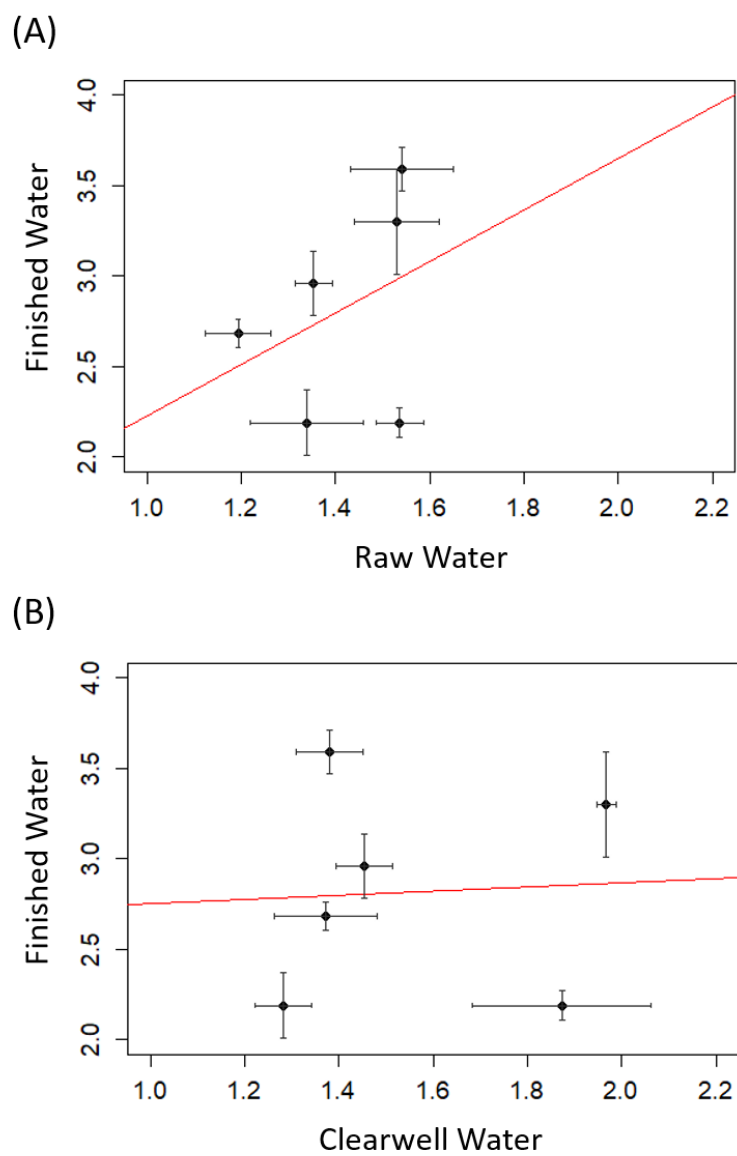


Fig. C.5. Relationships between fold induction of the Nrf2/ARE oxidative stress pathway by (A) raw and (B) clearwell water with that of finished water. Linear models had (A) $R^2 = 0.13$, $p = 0.49$, and (B) $R^2 = 0.64$, $p = 0.91$.

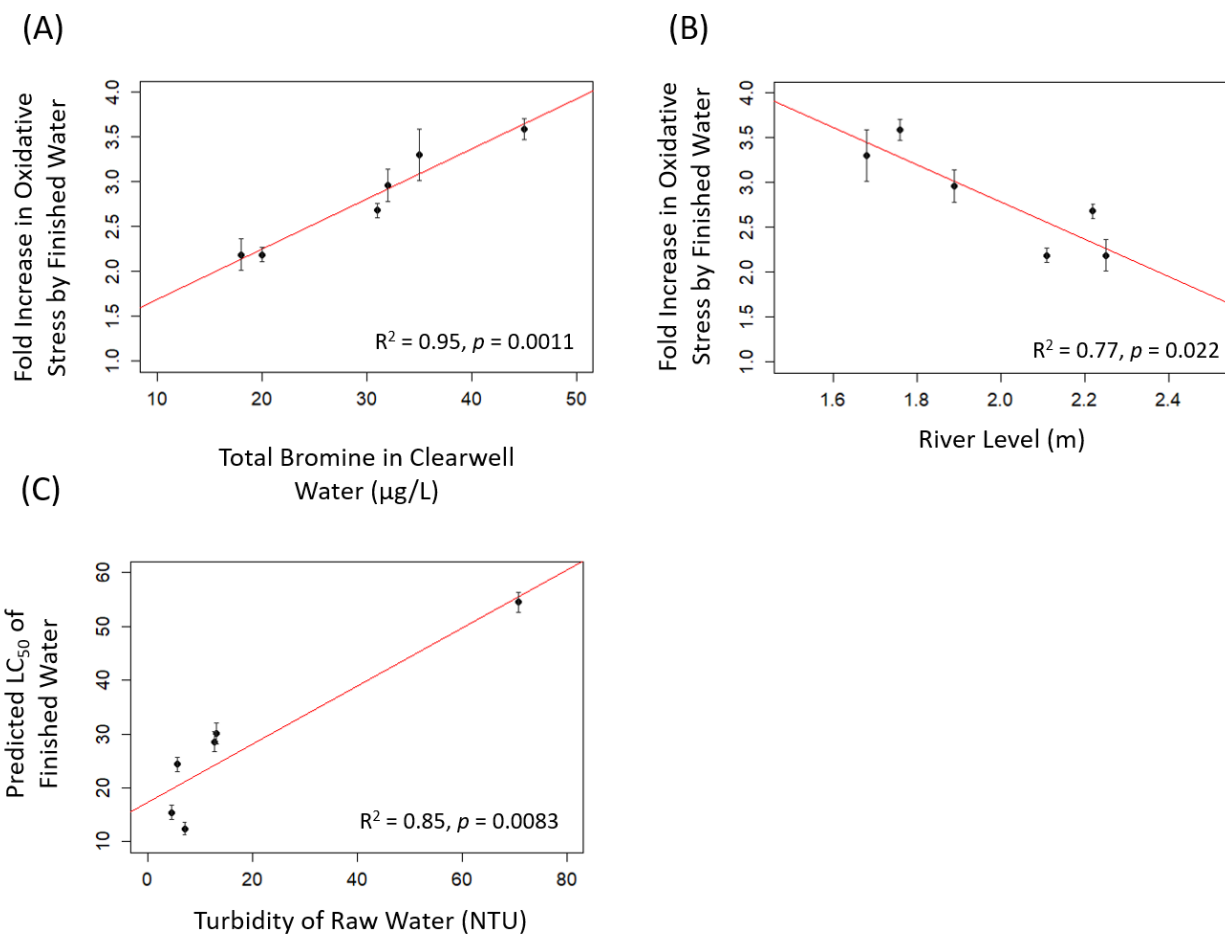
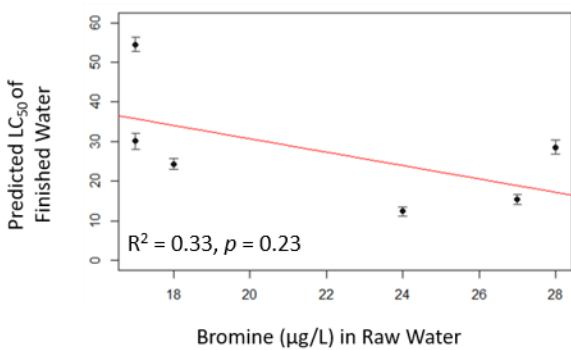
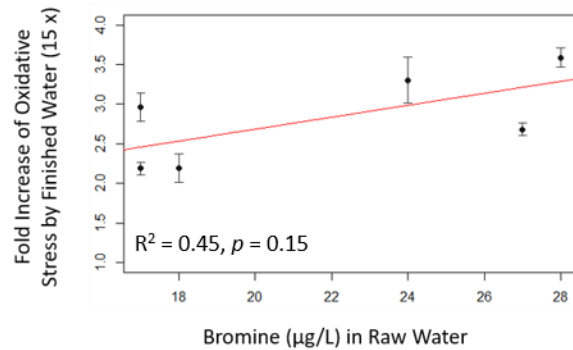


Fig. C.6. Significant ($\alpha = 0.05$) correlations to toxicity of finished water.

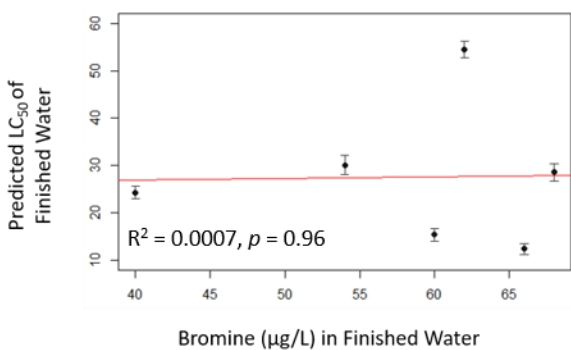
(A)



(B)



(C)



(D)

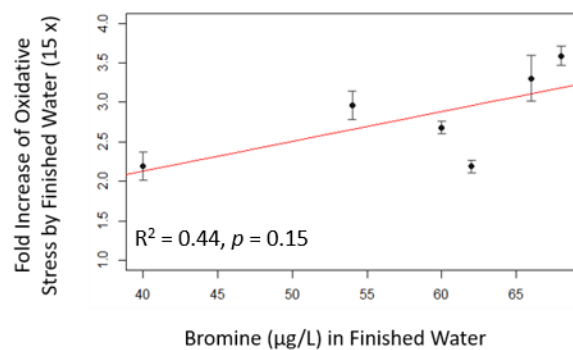


Fig. C.7. Relationships between concentrations of Br in raw water (A and B) or finished water (C and D) to predicted LC_{50} values (A and C) and induction of oxidative stress at 15 x (B and D) for extracts of finished water.

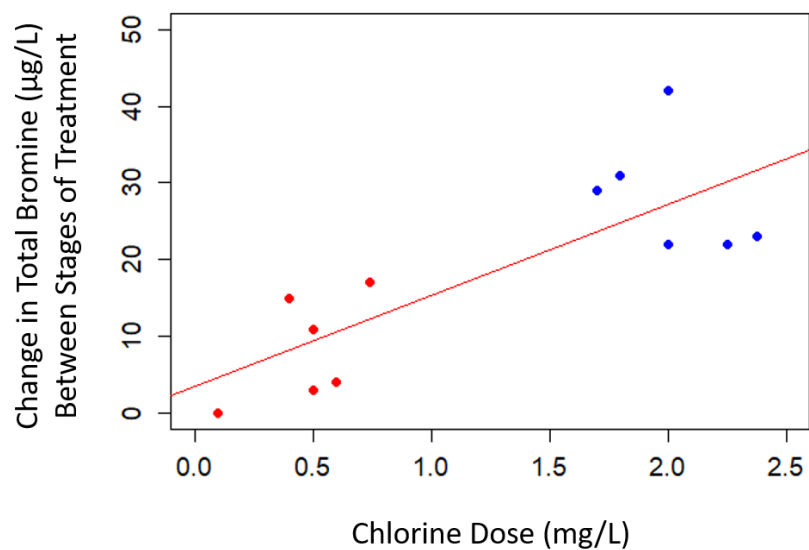


Fig. C.8. Relationship between applied doses of chlorine (pre- and post-chlorine) with the change in Br between related stages of treatment; change from raw to clearwell water (red) and change from clearwell to finished water (blue). Linear model $R^2 = 0.63$, $F_{1,10} = 17.29$, $p = 0.002$.

REFERENCES

- Arbuckle, T.E., Hrudey, S.E., Krasner, S.W., Nuckols, J.R., Richardson, S.D., Singer, P., Mendola, P., Dodds, L., Weisel, C., Ashley, D.L., Froese, K.L., Pegram, R.A., Schultz, I.R., Reif, J., Bachand, A.M., Benoit, F.M., Lynberg, M., Poole, C., Waller, K., 2002. Assessing exposure in epidemiologic studies to disinfection by-products in drinking water: Report from an international workshop. *Environ. Health Perspect.* 110, 53–60.
- Austin, E.W., Parrish, J.M., Kinder, D.H., Bull, R.J., 1996. Lipid peroxidation and formation of 8-hydroxydeoxyguanosine from acute doses of halogenated acetic acids. *Fundam. Appl. Toxicol.* 31, 77–82.
- Bechard, M.J., Rayburn, W.R., 1979. Volatile organic sulfites from freshwater algae. *J. Phycol.* 15, 379–383.
- Bellar, T.A., Lichtenberg, J.J., Kroner, R.C., 1974. The occurrence of organohalides in chlorinated drinking waters. *Am. Water Work. Assoc.* 66, 703–706.
- Bentley, R., Chasteen, T.G., 2004. Environmental VOSCs--formation and degradation of dimethyl sulfide, methanethiol and related materials. *Chemosphere* 55, 291–317.
- Boal, A.K., Patsalis, F.I., 2017. Peer reviewed use of sodium thiosulfate to quench hypochlorite solutions prior to chlorate analysis. *Am. Water Work. Assoc.* 109, 410–415.
- Bond, T., Templeton, M.R., Rifai, O., Ali, H., Graham, N.J.D., 2014. Chlorinated and nitrogenous disinfection by-product formation from ozonation and post-chlorination of natural organic matter surrogates. *Chemosphere* 111, 218–224.
- Buffalo Pound Water Board of Directors, 2016. 2016 Annual Report.
- Bull, R.J., Reckhow, D.A., Li, X., Humpage, A.R., Joll, C., Hrudey, S.E., 2011. Potential carcinogenic hazards of non-regulated disinfection by-products: Haloquinones, halocyclopentene and cyclohexene derivatives, N-halamines, halonitriles, and heterocyclic amines. *Toxicology* 286, 1–19.
- Cantor, K.P., Lynch, C.F., Hildesheim, M.E., Dosemeci, M., Lubin, J., Alavanja, M., Craun, G., 1998. Drinking water source and chlorination byproducts. I. Risk of bladder cancer. *Epidemiology* 9, 21–28.
- Cemeli, E., Wagner, E.D., Anderson, D., Richardson, S.D., Plewa, M.J., 2006. Modulation of the cytotoxicity and genotoxicity of the drinking water disinfection byproduct iodoacetic acid by suppressors of oxidative stress. *Environ. Sci. Technol.* 40, 1878–1883.
- Centers for Disease Control and Prevention, 2014. Disinfection by-products and the safe water system [WWW Document]. URL http://www.cdc.gov/safewater/publications_pages/thm.pdf

- Chellam, S., Krasner, S.W., 2001. Disinfection byproduct relationships and speciation in chlorinated nanofiltered waters. *Environ. Sci. Technol.* 35, 3988–3999.
- Chen, B., Westerhoff, P., 2010. Predicting disinfection by-product formation potential in water. *Water Res.* 44, 3755–3762.
- Chen, C., Zhang, X.J., Zhu, L.X., Liu, J., He, W.J., Han, H. Da, 2008. Disinfection by-products and their precursors in a water treatment plant in North China: Seasonal changes and fraction analysis. *Sci. Total Environ.* 397, 140–147.
- Conrad, D., 2017. Personal communication. Buffalo Pound Water Treat. Corp.
- Costet, N., Garlantézec, R., Monfort, C., Rouget, F., Gagnière, B., Chevrier, C., Cordier, S., 2012. Environmental and urinary markers of prenatal exposure to drinking water disinfection by-products, fetal growth, and duration of gestation in the PELAGIE birth cohort (Brittany, France, 2002–2006). *Am. J. Epidemiol.* 175, 263–275.
- Cowman, G.A., Singer, P.C., 1996. Effect of bromide ion on haloacetic acid speciation resulting from chlorination and chloramination of aquatic humic substances. *Environ. Sci. Technol.* 30, 16–24.
- Dad, A., Jeong, C.H., Pals, J.A., Wagner, E.D., Plewa, M.J., 2013. Pyruvate remediation of cell stress and genotoxicity induced by haloacetic acid drinking water disinfection by-products. *Environ. Mol. Mutagen.* 54, 629–637.
- De Nora Water Technologies, 2015. Impurities In Sodium Hypochlorite Solutions.
- Ding, G., Zhang, X., 2009. A picture of polar iodinated disinfection byproducts in drinking water by (UPLC/ESI-tqMS). *Environ. Sci. Technol.* 43, 9287–9293.
- Ding, G., Zhang, X., Yang, M., Pan, Y., 2013. Formation of new brominated disinfection byproducts during chlorination of saline sewage effluents. *Water Res.* 47, 2710–2718.
- Domínguez-Tello, A., Arias-Borrego, A., García-Barrera, T., Gómez-Ariza, J.L., 2015. Seasonal and spatial evolution of trihalomethanes in a drinking water distribution system according to the treatment process. *Environ. Monit. Assess.* 187.
- Escher, B.I., Dutt, M., Maylin, E., Tang, J.Y.M., Toze, S., Wolf, C.R., Lang, M., 2012. Water quality assessment using the AREc32 reporter gene assay indicative of the oxidative stress response pathway. *J. Environ. Monit.* 14, 2877.
- Fan, Z., Hu, J., An, W., Yang, M., 2013. Detection and occurrence of chlorinated byproducts of bisphenol a, nonylphenol, and estrogens in drinking water of China: Comparison to the parent compounds. *Environ. Sci. Technol.* 47, 10841–10850.
- Farré, M., Kantiani, L., Petrovic, M., Pérez, S., Barceló, D., 2012. Achievements and future trends in the analysis of emerging organic contaminants in environmental samples by mass spectrometry and bioanalytical techniques. *J. Chromatogr. A.*

<https://doi.org/10.1016/j.chroma.2012.07.024>

- Farré, M.J., Day, S., Neale, P.A., Stalter, D., Tang, J.Y.M., Escher, B.I., 2013. Bioanalytical and chemical assessment of the disinfection by-product formation potential : Role of organic matter. *Water Res.* 47, 5409–5421.
- Francis, R.A., Vanbriesen, J.M., Small, M.J., 2010. Bayesian statistical modeling of disinfection byproduct (DBP) bromine incorporation in the ICR database. *Environ. Sci. Technol.* 44, 1232–1239.
- Gao, P., Thornton-Manning, J.R., Pegram, R.A., 1996. Protective effects of glutathione on bromodichloromethane in vivo toxicity and in vitro macromolecular binding in Fischer 344 rats. *J. Toxicol. Environ. Health* 49, 145–159.
- Giller, S., Le Curieux, F., Erb, F., Marzin, D., 1997. Comparative genotoxicity of halogenated acetic acids found in drinking water. *Mutagenesis* 12, 321–328.
- Gong, T., Zhang, X., 2015. Detection, identification and formation of new iodinated disinfection byproducts in chlorinated saline wastewater effluents. *Water Res.* 68, 77–86.
- Gonsior, M., Schmitt-Kopplin, P., Stavklint, H., Richardson, S.D., Hertkorn, N., Bastviken, D., 2014. Changes in dissolved organic matter during the treatment processes of a drinking water plant in sweden and formation of previously unknown disinfection byproducts. *Environ. Sci. Technol.* 48, 12714–12722.
- Government of Newfoundland and Labrador, 2009. Best management practices for the control of disinfection by-products in drinking water systems in Newfoundland and Labrador.
- Government of Saskatchewan, 2016. Husky Incident.
- Gribble, G.W., 2000. The natural production of organobromine compounds. *Environ. Sci. Pollut. Res. Int.* 7, 37–47.
- Haag, W.R., Hoigné, J., 1983. Ozonation of bromide-containing waters: Kinetics of formation of hypobromous acid and bromate. *Environ. Sci. Technol.* 17, 261–267.
- Health Canada. Water and Air Quality Bureau Healthy Environments and Consumer Safety Branch, 2014. Guidelines for canadian drinking water quality - Summary table.
- Hua, G., Kim, J., Reckhow, D.A., 2014. Disinfection byproduct formation from lignin precursors. *Water Res.* 63, 285–295.
- Hua, G., Reckhow, D.A., Kim, J., 2006. Effect of bromide and iodide ions on the formation and speciation of disinfection byproducts during chlorination. *Environ. Sci. Technol.* 40, 3050–3056.
- Itoh, K., Wakabayashi, N., Katoh, Y., Ishii, T., Igarashi, K., Engel, J.D., Yamamoto, M., 1999. Keap1 represses nuclear activation of antioxidant responsive elements by Nrf2 through

- binding to the amino-terminal Neh2 domain. *Genes Dev.* 13, 76–86.
- Jeong, C.H., Postigo, C., Richardson, S.D., Simmons, J.E., Kimura, S.Y., Mariñas, B.J., Barcelo, D., Liang, P., Wagner, E.D., Plewa, M.J., 2015. Occurrence and comparative toxicity of haloacetaldehyde disinfection byproducts in drinking water. *Environ. Sci. Technol.* 13749–13759.
- Jeong, C.H., Wagner, E.D., Siebert, V.R., Anduri, S., Richardson, S.D., Daiber, E.J., McKague, A.B., Kogevinas, M., Villanueva, C.M., Goslan, E.H., Luo, W., Isabelle, L.M., Pankow, J.F., Grazuleviciene, R., Cordier, S., Edwards, S.C., Righi, E., Nieuwenhuijsen, M.J., Plewa, M.J., 2012. Occurrence and toxicity of disinfection byproducts in European drinking waters in relation with the HIWATE epidemiology study. *Environ. Sci. Technol.* 46, 12120–12128.
- Junot, C., Madalinski, G., Tabet, J.C., Ezan, E., 2010. Fourier transform mass spectrometry for metabolome analysis. *Analyst* 135, 2203–2219.
- Kansanen, E., Kuosmanen, S.M., Leinonen, H., Levonen, A.-L., 2013. The Keap1-Nrf2 pathway: Mechanisms of activation and dysregulation in cancer. *Redox Biol.* 1, 45–9.
- Kawamoto, T., Makihata, N., 2004. Distribution of bromine/chlorine-containing disinfection by-products in tap water from different water sources in the hyogo prefecture. *J. Heal. Sci.* 50, 235–247.
- Kim, H.C., Yu, M.J., 2005. Characterization of natural organic matter in conventional water treatment processes for selection of treatment processes focused on DBPs control. *Water Res.* 39, 4779–4789.
- Kim, J., 2009. Fate of THMs and HAAs in low TOC surface water. *Environ. Res.* 109, 158–165.
- Kind, T., Fiehn, O., 2007. Seven golden rules for heuristic filtering of molecular formulas obtained by accurate mass spectrometry. *BMC Bioinformatics* 8.
- Koch, B.P., Dittmar, T., Witt, M., Kattner, G., 2007. Fundamentals of molecular formula assignment to ultrahigh resolution mass data of natural organic matter. *Anal. Chem.* 79, 1758–1763.
- Krasner, S.W., 2009. The formation and control of emerging disinfection by-products of health concern. *Philos. Trans. A. Math. Phys. Eng. Sci.* 367, 4077–4095.
- Krasner, S.W., Lee, T.C.F., Westerhoff, P., Fischer, N., Hanigan, D., Karanfil, T., Beita-Sandí, W., Taylor-Edmonds, L., Andrews, R.C., 2016. Granular activated carbon treatment may result in higher predicted genotoxicity in the presence of bromide. *Environ. Sci. Technol.* 50, 9583–9591.
- Kristiana, I., Lethorn, A., Joll, C., Heitz, A., 2014. To add or not to add: The use of quenching agents for the analysis of disinfection by-products in water samples. *Water Res.* 59, 90–98.

- Kundu, B., Richardson, S.D., Granville, C.A., Shaughnessy, D.T., Hanley, N.M., Swartz, P.D., Richard, A.M., DeMarini, D.M., 2004. Comparative mutagenicity of halomethanes and halonitromethanes in *Salmonella* TA100: structure-activity analysis and mutation spectra. *Mutat. Res.* 554, 335–50.
- Lavonen, E.E., Gonsior, M., Tranvik, L.J., Schmitt-Kopplin, P., Köhler, S.J., 2013. Selective chlorination of natural organic matter: Identification of previously unknown disinfection byproducts. *Environ. Sci. Technol.* 47, 2264–2271.
- Li, J., Moe, B., Vemula, S., Wang, W., Li, X.F., 2016. Emerging disinfection byproducts, halobenzoquinones: Effects of isomeric structure and halogen substitution on cytotoxicity, formation of reactive oxygen species, and genotoxicity. *Environ. Sci. Technol.* 50, 6744–6752.
- Li, X.-F., Mitch, W.A., 2018. Drinking water disinfection byproducts (DBPs) and human health effects: Multidisciplinary challenges and opportunities. *Environ. Sci. Technol.* 52, 1681–1689.
- Lilly, P.D., Ross, T.M., Pegram, R.A., 1997. Trihalomethane comparative toxicity: Acute renal and hepatic toxicity of chloroform and bromodichloromethane following aqueous gavage. *Fundam. Appl. Toxicol.* 40, 101–10.
- Lomans, B.P., Leijdekkers, P., Wesselink, J.J., Bakkes, P., Pol, A., Van Der Drift, C., Op Den Camp, H.J.M., 2001. Obligate sulfide-dependent degradation of methoxylated aromatic compounds and formation of methanethiol and dimethyl sulfide by a freshwater sediment isolate, *Parasporobacterium paucivorans* gen. nov., sp. nov. *Appl. Environ. Microbiol.* 67, 4017–4023.
- MacPhee, M.J., Cornwell, D.A., Brown, R., American Water Works Association, 2002. Trace contaminants in drinking water chemicals. AWWA Research Foundation and American Water Works Association.
- Matilainen, A., Vepsäläinen, M., Sillanpää, M., 2010. Natural organic matter removal by coagulation during drinking water treatment: A review. *Adv. Colloid Interface Sci.* 159, 189–197.
- Mercier Shanks, C., Sérodes, J.-B., Rodriguez, M.J., 2013. Spatio-temporal variability of non-regulated disinfection by-products within a drinking water distribution network. *Water Res.* 47, 3231–43.
- Muellner, M.G., Wagner, E.D., McCalla, K., Richardson, S.D., Woo, Y.T., Plewa, M.J., 2007. Haloacetonitriles vs. regulated haloacetic acids: Are nitrogen-containing DBPs more toxic? *Environ. Sci. Technol.* 41, 645–651.
- Munch, D., Hautman, D., 1995. Method 551.1: Determination of chlorination disinfection byproducts, chlorinated solvents, and halogenated pesticides/ herbicides in drinking water by liquid-liquid extraction and gas chromatography with electron-capture detection.

- Nathanson, J.A., 2015. Water supply system. *Encycl. Br.*
- National Cancer Institute, 1976. Report on carcinogenicity bioassay of chloroform. CAS No 67-66-3.
- Neale, P.A., Antony, A., Bartkow, M.E., Farré, M.J., Heitz, A., Kristiana, I., Tang, J.Y.M., Escher, B.I., 2012. Bioanalytical assessment of the formation of disinfection byproducts in a drinking water treatment plant. *Environ. Sci. Technol.* 46, 10317–10325.
- Nguyen, T., Nioi, P., Pickett, C.B., 2009. The Nrf2-antioxidant response element signaling pathway and its activation by oxidative stress. *J. Biol. Chem.* 284, 13291–5.
- Nieuwenhuijsen, M.J., Martinez, D., Grellier, J., Bennett, J., Best, N., Iszatt, N., Vrijheid, M., Toledano, M.B., 2009a. Chlorination disinfection by-products in drinking water and congenital anomalies: Review and meta-analyses. *Environ. Health Perspect.* 117, 1486–1493.
- Nieuwenhuijsen, M.J., Smith, R., Golfinopoulos, S., Best, N., Bennett, J., Aggazzotti, G., Righi, E., Fantuzzi, G., Bucchini, L., Cordier, S., Villanueva, C.M., Moreno, V., La Vecchia, C., Bosetti, C., Vartiainen, T., Rautiu, R., Toledano, M., Iszatt, N., Grazuleviciene, R., Kogevinas, M., 2009b. Health impacts of long-term exposure to disinfection by-products in drinking water in Europe: HIWATE. *J. Water Health* 7, 185–207.
- Obolensky, A., Singer, P.C., 2008. Development and interpretation of disinfection byproduct formation models using the Information Collection Rule database. *Environ. Sci. Technol.* 42, 5654.
- Pals, J.A., Attene-Ramos, M.S., Xia, M., Wagner, E.D., Plewa, M.J., 2013. Human cell toxicogenomic analysis linking reactive oxygen species to the toxicity of monohaloacetic acid drinking water disinfection byproducts. *Environ. Sci. Technol.* 47, 12514–23.
- Pan, Y., Li, W., Li, A., Zhou, Q., Shi, P., Wang, Y., 2016a. A new group of disinfection byproducts in drinking water: Trihalo-hydroxy-cyclopentene-diones. *Environ. Sci. Technol.* 50, 7344–7352.
- Pan, Y., Wang, Y., Li, A., Xu, B., Xian, Q., Shuang, C., Shi, P., Zhou, Q., 2017. Detection, formation and occurrence of 13 new polar phenolic chlorinated and brominated disinfection byproducts in drinking water. *Water Res.* 112, 129–136.
- Pan, Y., Zhang, X., 2013. Four groups of new aromatic halogenated disinfection byproducts: Effect of bromide concentration on their formation and speciation in chlorinated drinking water. *Environ. Sci. Technol.* 47, 1265–1273.
- Pan, Y., Zhang, X., Li, Y., 2016b. Identification, toxicity and control of iodinated disinfection byproducts in cooking with simulated chlor(am)inated tap water and iodized table salt. *Water Res.* 88, 60–68.
- Peng, H., Chen, C., Cantin, J., Saunders, D.M.V., Sun, J., Tang, S., Codling, G.P., Hecker, M.,

- Wiseman, S., Jones, P.D., Li, A., Rockne, K.J., Sturchio, N.C., Giesy, J.P., 2016a. Untargeted screening and distribution of organo-bromine compounds in sediments of Lake Michigan. *Environ. Sci. Technol.* 15, 321–330.
- Peng, H., Chen, C., Cantin, J., Saunders, D.M. V., Sun, J., Tang, S., Codling, G., Hecker, M., Wiseman, S., Jones, P.D., Li, A., Rockne, K.J., Sturchio, N.C., Cai, M., Giesy, J.P., 2016b. Untargeted screening and distribution of organo-iodine compounds in sediments from Lake Michigan and the Arctic Ocean. *Environ. Sci. Technol.* 50, 10097–10105.
- Peng, H., Chen, C., Saunders, D.M. V., Sun, J., Tang, S., Codling, G., Hecker, M., Wiseman, S., Jones, P.D., Li, A., Rockne, K.J., Giesy, J.P., 2015. Untargeted identification of organo-bromine compounds in lake sediments by ultrahigh-resolution mass spectrometry with the data-independent precursor isolation and characteristic fragment method. *Anal. Chem.* 87, 10237–10246.
- Peng, H., Saunders, D.M. V., Jones, P.D., Giesy, J.P., 2016c. Mutagenic azo dyes, rather than flame retardants, are the predominant brominated compounds in house dust. *Environ. Sci. Technol.* 50, 12669–12677.
- Platikanov, S., Tauler, R., Rodrigues, P.M.S.M., Antunes, M.C.G., Pereira, D., Esteves da Silva, J.C.G., 2010. Factorial analysis of the trihalomethane formation in the reaction of colloidal, hydrophobic, and transphilic fractions of DOM with free chlorine. *Environ. Sci. Pollut. Res.* 17, 1389–1400.
- Plewa, M.J., Muellner, M.G., Richardson, S.D., Fasano, F., Buettner, K.M., Woo, Y.T., McKague, a. B., Wagner, E.D., 2008. Occurrence, synthesis, and mammalian cell cytotoxicity and genotoxicity of haloacetamides: An emerging class of nitrogenous drinking water disinfection byproducts. *Environ. Sci. Technol.* 42, 955–961.
- Plewa, M.J., Wagner, E.D., 2009. Mammalian cell cytotoxicity and genotoxicity of disinfection by-products.
- Plewa, M.J., Wagner, E.D., Jazwierska, P., Richardson, S.D., Chen, P.H., McKague, a B., 2004. Halonitromethane drinking water disinfection byproducts: Chemical characterization and mammalian cell cytotoxicity and genotoxicity. *Environ. Sci. Technol.* 38, 62–68.
- Plewa, M.J., Wagner, E.D., Richardson, S.D., Thruston, A.D., Woo, Y.-T., McKague, a B., 2004. Chemical and biological characterization of newly discovered iodoacid drinking water disinfection byproducts. *Environ. Sci. Technol.* 38, 4713–4722.
- Postigo, C., Cojocariu, C.I., Richardson, S.D., Silcock, P.J., Barcelo, D., 2016. Characterization of iodinated disinfection by-products in chlorinated and chloraminated waters using Orbitrap based gas chromatography-mass spectrometry. *Anal. Bioanal. Chem.* 408, 3401–3411.
- Rahal, A., Kumar, A., Singh, V., Yadav, B., Tiwari, R., Chakraborty, S., Dhama, K., 2014. Oxidative stress, prooxidants, and antioxidants: The interplay. *Biomed Res. Int.*

- Reemtsma, T., 2009. Determination of molecular formulas of natural organic matter molecules by (ultra-) high-resolution mass spectrometry. Status and needs. *J. Chromatogr. A* 1216, 3687–3701.
- Regli, S., Chen, J., Messner, M., Elovitz, M.S., Letkiewicz, F., Pegram, R., Pepping, T., Richardson, S., Wright, J.M., 2015. Estimating potential increased bladder cancer risk due to increased bromide concentrations in sources of disinfected drinking waters. *Environ. Sci. Technol.* 13094–13102.
- Richardson, S.D., 2002. The role of GC-MS and LC-MS in the discovery of drinking water disinfection by-products. *J. Environ. Monit.* 4, 1–9.
- Richardson, S.D., Fasano, F., Ellington, J.J., Crumley, F.G., Buettner, K.M., Evans, J.J., Blount, B.C., Silva, L.K., Waite, T.J., Luther, G.W., Mckague, a. B., Miltner, R.J., Wagner, E.D., Plewa, M.J., 2008. Occurrence and mammalian cell toxicity of iodinated disinfection byproducts in drinking water. *Environ. Sci. Technol.* 42, 8330–8338.
- Richardson, S.D., Plewa, M.J., Wagner, E.D., Schoeny, R., DeMarini, D.M., 2007. Occurrence, genotoxicity, and carcinogenicity of regulated and emerging disinfection by-products in drinking water: A review and roadmap for research. *Mutat. Res. - Rev. Mutat. Res.* 636, 178–242.
- Richardson, S.D., Thruston, A.D., Caughran, T. V., Chen, P.H., Collette, T.W., Floyd, T.L., Schenck, K.M., Lykins, B.W., Sun, G.R., Majetich, G., 1999. Identification of new drinking water disinfection byproducts formed in the presence of bromide. *Environ. Sci. Technol.* 33, 3378–3383.
- Richardson, S.D., Thruston, A.D., Rav-Acha, C., Groisman, L., Popilevsky, I., Juraev, O., Glezer, V., McKague, A.B., Plewa, M.J., Wagner, E.D., 2003. Tribromopyrrole, brominated acids, and other disinfection byproducts produced by disinfection of drinking water rich in bromide. *Environ. Sci. Technol.* 37, 3782–3793.
- Ritz, C., Baty, F., Streibig, J.C., Gerhard, D., 2015. Dose-Response Analysis using R. *PLoS One* 10, e0146021.
- Rodriguez, M.J., Sérodes, J.B., 2001. Spatial and temporal evolution of trihalomethanes in three water distribution systems. *Water Res.* 35, 1572–1586.
- Sawade, E., Fabris, R., Humpage, A., Drikas, M., 2016. Effect of increasing bromide concentration on toxicity in treated drinking water. *J. Water Health* 14, 183–191.
- Serrano, M., Montesinos, I., Cardador, M.J., Silva, M., Gallego, M., 2015. Seasonal evaluation of the presence of 46 disinfection by-products throughout a drinking water treatment plant. *Sci. Total Environ.* 517, 246–258.
- Shah, A.D., Mitch, W.A., 2012. Halonitroalkanes, halonitriles, haloamides, and N-nitrosamines: A critical review of nitrogenous disinfection byproduct formation pathways. *Environ. Sci. Technol.* 46, 119–131.

- Sharma, V.K., Zboril, R., McDonald, T.J., 2014. Formation and toxicity of brominated disinfection byproducts during chlorination and chloramination of water: A review. *J. Environ. Sci. Health. B.* 49, 212–28.
- Singer, P.C., 1999. Humic substances as precursors for potentially harmful disinfection by-products. *Water Sci. Technol.* 40, 25–30.
- Smith, C.A., Want, E.J., O'Maille, G., Abagyan, R., Siuzdak, G., 2006. XCMS: Processing mass spectrometry data for metabolite profiling using nonlinear peak alignment, matching, and identification. *Anal. Chem.* 78, 779–787.
- Sohn, J., Amy, G., Yoon, Y., 2006. Bromide ion incorporation into brominated disinfection by-products. *Water. Air. Soil Pollut.* 174, 265–277.
- Stalter, D., Malley, E.O., Gunten, U. Von, Escher, B.I., 2016. Fingerprinting the reactive toxicity pathways of 50 drinking water disinfection by-products. *Water Res.* 91, 19–30.
- The NSF Joint Committee on Drinking Treatment Chemicals, 2013. Drinking water treatment chemicals - Health effects. Ann Arbor, Michigan.
- Tikkanen, M., Schroeter, J.H., Leong, L.Y.C., Ganesh, R., 2001. Guidance manual for the disposal of chlorinated water. Denver, CO.
- Tindall, K.R., Stankowski Jr, L.F., 1989. Molecular analysis of spontaneous mutations at the gpt locus in Chinese hamster ovary (AS52) cells. *Mutat. Res. - Rev. Genet. Toxicol.* 220, 241–253.
- Toledano, M.B., Nieuwenhuijsen, M.J., Best, N., Whitaker, H., Hambly, P., de Hoogh, C., Fawell, J., Jarup, L., Elliott, P., 2005. Relation of trihalomethane concentrations in public water supplies to stillbirth and birth weight in three water regions in England. *Environ. Health Perspect.* 113, 225–232.
- Tsugawa, H., Cajka, T., Kind, T., Ma, Y., Higgins, B., Ikeda, K., Kanazawa, M., Vandergheynst, J., Fiehn, O., Arita, M., 2015. MS-DIAL: Data-independent MS/MS deconvolution for comprehensive metabolome analysis. *Nat. Methods* 12, 523–526.
- United States Environmental Protection Agency, 2008. Stage 2 disinfectants and disinfection byproducts rule: Operational evaluation guidance manual. Denver, CO.
- Uyak, V., Ozdemir, K., Toroz, I., 2008. Seasonal variations of disinfection by-product precursors profile and their removal through surface water treatment plants. *Sci. Total Environ.* 390, 417–424.
- Uyak, V., Toroz, I., 2007. Investigation of bromide ion effects on disinfection by-products formation and speciation in an Istanbul water supply. *J. Hazard. Mater.* 149, 445–451.
- VanBriesen, J.M., n.d. Potential drinking water effects of bromide discharges from coal-fired electric power plants.

- Villanueva, C.M., Fernández, F., Malats, N., Grimalt, J.O., Kogevinas, M., 2003. Meta-analysis of studies on individual consumption of chlorinated drinking water and bladder cancer. *J. Epidemiol. Community Heal.* 57, 166–173.
- Wagner, E.D., Plewa, M.J., 2017. CHO cell cytotoxicity and genotoxicity analyses of disinfection by-products: An updated review. *J. Environ. Sci.* 58, 64–76.
- Wang, X., Zhang, H., Zhang, Y., Shi, Q., Wang, J., Yu, J., Yang, M., 2017. New insights into trihalomethane and haloacetic acid formation potentials : Correlation with the molecular composition of natural organic matter in source water. *Environ. Sci. Technol.* 51, 2015–2021.
- Water Quality and Health Council, 2015. A public health giant step: Chlorination of U.S. drinking water [WWW Document]. URL http://www.waterandhealth.org/drinkingwater/chlorination_history.html (accessed 11.29.15).
- Water Resources Management Division, Department of Environment and Labour, 2000. Trihalomethane levels in public water supplies of Newfoundland and Labrador [WWW Document]. URL <http://www.env.gov.nl.ca/env/waterres/reports/thm/chapter2thm.pdf>
- Watson, K., Farré, M.J., Birt, J., McGree, J., Knight, N., 2014. Predictive models for water sources with high susceptibility for bromine-containing disinfection by-product formation: Implications for water treatment. *Environ. Sci. Pollut. Res.* 22, 1963–1978.
- Wei, T., Simko, V., Levy, M., Xie, Y., Jin, Y., Zemla, J., 2017. Package “corrplot.”
- Weinberg, H.S., 2009. Modern approaches to the analysis of disinfection by-products in drinking water. *Philos. Trans. A. Math. Phys. Eng. Sci.* 267, 4097–4118.
- Westerhoff, P., Chao, P., Mash, H., 2004. Reactivity of natural organic matter with aqueous chlorine and bromine. *Water Res.* 38, 1502–1513.
- Westerhoff, P., Song, R., Amy, G., Minear, R., 1998. NOM’s role in bromine and bromate formation during ozonation. *J. / Am. Water Work. Assoc.* 90, 82–94.
- World Health Organization, 2000. EHC 216: Disinfectants and disinfection by-products. Toxicology of disinfection by-products [WWW Document]. URL http://www.who.int/ipcs/publications/ehc/216_disinfectants_part_3.pdf
- Xie, S.-H., Liu, A.-L., Chen, Y.-Y., Zhang, L., Zhang, H.-J., Jin, B.-X., Lu, W.-H., Li, X.-Y., Lu, W.-Q., 2010. DNA damage and oxidative stress in human liver cell L-02 caused by surface water extracts during drinking water treatment in a waterworks in China. *Environ. Mol. Mutagen.* 51, 229–235.
- Yang, M., Zhang, X., 2016. Current trends in the analysis and identification of emerging disinfection byproducts. *Trends Environ. Anal. Chem.* 10, 24–34.

- Yang, M., Zhang, X., 2013. Comparative developmental toxicity of new aromatic halogenated DBPs in a chlorinated saline sewage effluent to the marine polychaete *platynereis dumerilii*. *Environ. Sci. Technol.* 47, 10868–10876.
- Yang, X., Shang, C., Westerhoff, P., 2007. Factors affecting formation of haloacetonitriles, haloketones, chloropicrin and cyanogen halides during chloramination. *Water Res.* 41, 1193–1200.
- Yang, Y., Komaki, Y., Kimura, S.Y., Hu, H.-Y., Wagner, E.D., Mariñas, B.J., Plewa, M.J., 2014. Toxic impact of bromide and iodide on drinking water disinfected with chlorine or chloramines. *Environ. Sci. Technol.* 48, 12362–9.
- Ye, B., Wang, W., Yang, L., Wei, J., 2009. Factors influencing disinfection by-products formation in drinking water of six cities in China. *J. Hazard. Mater.* 171, 147–152.
- Yoch, D.C., 2002. Dimethylsulfoniopropionate: Its sources, role in the marine food web, and biological degradation to dimethylsulfide. *Appl. Environ. Microbiol.* 68, 5804–5815.
- Zahn, D., Frömel, T., Knepper, T.P., 2016. Halogenated methanesulfonic acids: A new class of organic micropollutants in the water cycle. *Water Res.* 101, 292–299.
- Zhai, H., Zhang, X., 2011. Formation and decomposition of new and unknown polar brominated disinfection byproducts during chlorination. *Environ. Sci. Technol.* 45, 2194–2201.
- Zhai, H., Zhang, X., 2009. A new method for differentiating adducts of common drinking water DBPs from higher molecular weight DBPs in electrospray ionization-mass spectrometry analysis. *Water Res.* 43, 2093–2100.
- Zhai, H., Zhang, X., Zhu, X., Liu, J., Ji, M., 2014. Formation of brominated disinfection byproducts during chloramination of drinking water: New polar species and overall kinetics. *Environ. Sci. Technol.* 48, 2579–2588.
- Zhang, H., Zhang, Y., Shi, Q., Hu, J., Chu, M., Yu, J., Yang, M., 2012a. Study on transformation of natural organic matter in source water during chlorination and its chlorinated products using ultrahigh resolution mass spectrometry. *Environ. Sci. Technol.* 46, 4396–4402.
- Zhang, H., Zhang, Y., Shi, Q., Ren, S., Yu, J., Ji, F., Luo, W., Yang, M., 2012b. Characterization of low molecular weight dissolved natural organic matter along the treatment trail of a waterworks using Fourier transform ion cyclotron resonance mass spectrometry. *Water Res.* 46, 5197–204.
- Zhang, H., Zhang, Y., Shi, Q., Zheng, H., Yang, M., 2014. Characterization of unknown brominated disinfection byproducts during chlorination using ultrahigh resolution mass spectrometry. *Environ. Sci. Technol.* 48, 3112–3119.
- Zhang, S.H., Miao, D.Y., Liu, A.L., Zhang, L., Wei, W., Xie, H., Lu, W.Q., 2010. Assessment of the cytotoxicity and genotoxicity of haloacetic acids using microplate-based cytotoxicity test and CHO/HGPRT gene mutation assay. *Mutat. Res. - Genet. Toxicol. Environ.*

Mutagen. 703, 174–179.

Zhang, X., Echigo, S., Lei, H., Smith, M.E., Minear, R.A., Talley, J.W., 2005. Effects of temperature and chemical addition on the formation of bromoorganic DBPs during ozonation. *Water Res.* 39, 423–35.

Zhang, X., Echigo, S., Minear, R. a, Plewa, M.J., 2000. Characterization and comparison of disinfection by-products of four major disinfectants. *Am. Chem. Soc.* 299–314.

Zhang, X., Talley, J.W., Boggess, B., Ding, G., Birdsell, D., 2008. Fast selective detection of polar brominated disinfection byproducts in drinking water using precursor ion scans. *Environ. Sci. Technol.* 42, 6598–6603.

Zhu, X., Zhang, X., 2016. Modeling the formation of TOCl, TOBr and TOI during chlor(am)ination of drinking water. *Water Res.* 96, 166–176.

Zwiener, C., Richardson, S.D., 2005. Analysis of disinfection by-products in drinking water by LC-MS and related MS techniques. *Trends Anal. Chem.* 24, 613–621.